

Differential sympathetic activity to adipose tissue
Implications in energy homeostasis and weight loss

Laura Marie Sipe
Mount Airy, Maryland

Bachelors of Arts, St. Mary's College of Maryland, 2011

A Dissertation presented to the Graduate Faculty of the
University of Virginia in Candidacy for the
Degree of Doctor of Philosophy

Department of Biology
University of Virginia
April 2018

Abstract

In order to provide precise control of energy homeostasis, the sympathetic nervous system (SNS) activity is differentially regulated to specific adipose depots. Throughout calorie restriction, the SNS activity toward each adipose depot is unique in timing, pattern of activation, and habituation with the most dramatic contrast between the visceral and subcutaneous adipose depots. Sympathetic drive toward visceral gonadal adipose is more than doubled early in weight loss and then suppressed later in the diet when weight loss has plateaued. Coincident with the decline in SNS activity toward visceral adipose is an increase in activity toward subcutaneous depots indicating a switch in lipolytic sources. The SNS activity was necessary for adipose loss, as a pharmacological blockage of sympathetic activity on adipose tissue suppressed loss of visceral adipose tissue. This pattern of sympathetic activation is required for energy liberation and loss of adipose tissue in response to a calorie restricted diet.

Although, SNS activity to adipose depots is differentially regulated in response to calorie restriction, the importance of this observation is unknown. To determine the consequence of disrupting the preferential sympathetic drive to adipose depots, we analyzed the p75 Neurotrophin Receptor (p75NTR) deficient mice. p75NTR deficient mice are resistant to body weight loss during calorie restriction independent of changes in starting body weight or food intake. p75NTR deficient mice lost significantly less visceral adipose mass following calorie restriction. The sympathetic drive to adipose tissue is essential for adipose tissue loss and p75NTR deficient mice exhibited decreased sympathetic drive to white adipose tissue following calorie restriction. One mechanism behind the decrease in sympathetic drive could be the increase in synapses during

development at the sympathetic ganglia, which would lead to altered differential sympathetic outflow to adipose tissue. We have begun to elucidate the cell autonomous role of p75NTR in the SNS and cement the importance of differential sympathetic activity to adipose tissue throughout calorie restriction.

We established that differential sympathetic drive is essential for adipose loss from calorie restriction. Future work will address how differential sympathetic drive to adipose tissue regulated, which will lead to advances in metabolic health and the understanding of energy homeostasis.

Acknowledgments

I would like to thank my mentor, Christopher Deppmann, for his continuous support during my PhD training. Chris has always provided me with encouragement in my research, in my career goals, and most importantly in the daily challenges that science brings. Thank you for your mentorship and providing an environment that I could be a successful scientist. I am thankful for everyone I worked with in the Deppmann laboratory for their support, technical advice, and productive conversations. Thank you to Pamela Neff for keeping the laboratory functioning and her relentless kindness. I would like to thank the intelligent and enthusiastic undergraduates I have worked with, Chris Yang, Joseph Ephrem, T. Parks Remcho, and Dove Anna Johnson. They were invaluable to the experiments presented in this thesis and for enriching my career as a scientist.

I would like to thank my committee members Ignacio Provencio, Ali Guler, Susanna Keller, and Eyleen O'Rourke for creating an enthusiastic learning environment with insightful comments and probing questions. Thank you to Susanna Keller for teaching me every metabolic technique I know and for help designing experiments.

Next I would like to thank my parents for their constant support. My mother encouraged compassion and hard work. My father encouraged my curious nature and my sarcastic sense of humor. My sister is always there for me and even helped proof read. I would not be in graduate school nor have made it through graduate school without my family.

Finally I would like to thank my friends in Charlottesville who made my time here one of the greatest times of my life. We shared countless adventures that enriched my life and made lasting memories.

Table of Contents

Chapter 1. Introduction	1
The role of the sympathetic nervous system in energy homeostasis	1
Effects of norepinephrine on adipocytes	1
Change in sympathetic input to specific adipose tissue depots	4
Visceral versus subcutaneous adipose tissue	7
Central regulation of sympathetic activity	11
Other neuronal innervation of adipose tissue	13
Methods to measure sympathetic outflow	14
Calorie restriction	17
Consequences of obesity on the sympathetic nervous system	17
Potential mechanisms for change in sympathetic tone in obesity	20
p75 Neurotrophin receptor	22
p75 neurotrophin receptor in the sympathetic nervous system	23
p75 neurotrophin receptor in metabolism	26
p75 neurotrophin receptor expression fluctuates in a circadian manner	29
Conclusions	30
Chapter 2. Differential sympathetic outflow to adipose depots is required for visceral fat loss in response to calorie restriction	31
Abstract	31
Introduction	32
Results	34
Adipose loss in response to calorie restriction occurs preferentially from visceral depots	34
Dynamic sympathetic outflow to adipose depots in response to calorie restriction	36
Antagonizing sympathetic activity on adipose depots prevents diet induced adipose loss	38
Figures	41
Discussion	51

Chapter 3. Mice deficient in p75 Neurotrophin Receptor are resistant to diet induced weight loss	55
Introduction	55
Results	56
Mice deficient in p75NTR are resistant to diet induced body weight loss and adipose mass loss	56
Mice deficient in p75NTR have altered sympathetic drive to adipose tissue during calorie restriction	58
<i>p75NTR</i> ^{-/-} mice display no changes in food intake over time on diet	60
<i>p75NTR</i> ^{-/-} mice do not compensate for the energy deficient state of calorie restriction	61
Calorie Restriction produces intermittent fasting-like changes in RER	63
p75NTR expression in the sympathetic nervous system is necessary for reduction in adipose mass following calorie restriction	64
p75NTR expression in sympathetic nervous system does not alter activity levels following calorie restriction	65
Figures	66
Discussion	76
Chapter 4. Discussion and Future directions	84
Chapter 5. Methods	90
Appendix 1. Differential sympathetic drive to adipose does not regulate energy storage	94
References	102

Abbreviations

AgRP	Agouti Related Peptide
AL	Ad Libitum
AMPT	Alpha-Methyl-p-Tyrosine
AR	Adrenergic Receptor
BDNF	Brain Derived Neurotrophic Factor
CNS	Central Nervous System
CR	Calorie Restriction
GLUT4	Glucose Transporter 4
HSL	Hormone Sensitive Lipase
NE	Norepinephrine
NETO	Norepinephrine Turnover
NGF	Nerve Growth Factor
p75NTR	p75 Neurotrophin Receptor
PKA	Protein Kinase A
POMC	Pro-opiomelanocortin
RER	Respiratory Exchange Ratio
RMR	Resting Metabolic Rate
SNS	Sympathetic Nervous System
TH	Tyrosine Hydroxylase
UCP1	Uncoupled Protein 1

Chapter 1. Introduction

The role of the sympathetic nervous system in energy homeostasis

The sympathetic nervous system (SNS) is a component of the autonomic nervous system, which controls unconscious behavior. The SNS is often described as mediating the “fight or flight response” because it primes the body for action (Bartness and Song, 2007). For example, the SNS acts to increase heart rate and shuttle blood to the skeletal muscle to allow for physical activity (Davy and Orr, 2009). Beyond the “fight or flight response”, the SNS regulates a wide variety of energy homeostatic processes. A simplified interpretation of the role the SNS plays in energy homeostasis is that the SNS responds to increased energy intake with increased energy expenditure and the SNS responds to decreased energy intake with decreased energy expenditure (Landsberg, 1986). The sympathetic activity towards adipose tissue is directly proportional to energy liberation from adipose tissue, as neurotransmitters from sympathetic terminals causes lipolysis and stimulates thermogenesis (Bartness et al., 2010a, 2010b). This thesis will have implications for understanding both whole body energy homeostasis and the pathology of obesity.

Effects of norepinephrine on adipocytes

Adrenergic receptors expressed on adipocytes

The β adrenergic receptors (AR) bind norepinephrine (NE) from sympathetic nerve terminals. Of the three β -AR's, β 3-AR is of particular interest; unlike β 1-AR and β 2-AR, β 3-AR is highly expressed in murine white and brown adipose tissue and its

expression is relatively specific to the adipose tissues (Bartness et al., 2010b). The $\alpha 2$ -AR are also expressed on adipocytes and have greater affinity to epinephrine, released from the adrenal medulla in circulation, compared to NE, released predominantly from sympathetic terminals. These two adrenergic receptors classes have opposing effects on lipolysis and adipocyte proliferation due to differential G protein coupling; activation of $\beta 3$ -AR stimulates cAMP production via coupling to $G_{\alpha s}$ proteins whereas $\alpha 2$ -AR inhibit cAMP production via coupling to $G_{\alpha i}$ (Langin, 2006). Therefore, a balance between lipolysis-promoting β AR activation and lipolysis inhibiting $\alpha 2$ -AR activation dictates the degree of lipolysis (Bartness et al., 2010b). Interestingly, the visceral adipose tissue has decreased levels of $\alpha 2$ -AR compared to subcutaneous depots (Lefebvre et al., 1998). Consequently, visceral adipose tissue has a higher capacity for sympathetic induced lipolysis. The variances among adipose depots are of great interest and will be discussed in further sections of this thesis.

Lipolysis

Lipolysis is the process by which adipocytes break down triglyceride stores into fatty acids and glycerol. The free fatty acids are released into the blood stream to be used for energy by other organs. The process of lipolysis will decrease the lipid stores in the adipocyte and lead to smaller adipocytes. NE binding β -AR initiates the $G_{\alpha s}$ signaling pathway. $G_{\alpha s}$ triggers cAMP production by adenylyl cyclase that in turn activates protein kinase A (PKA). PKA then phosphorylates the proteins involved in lipolysis: hormone sensitive lipase (HSL) and perilipin A (Bartness et al., 2014). The phosphorylation of perilipin A provides access to the lipid droplets which store triglycerides (Langin, 2006).

Triglycerides are then broken down by a series of lipases to cleave fatty acids off the glycerol backbone; adipose triglyceride lipase cleaves triglycerides, phosphorylated HSL cleaves diacylglycerides, and monoacylglyceride lipase cleaves monoacylglycerides (Bartness et al., 2014). The resulting free fatty acids and glycerol backbone are then released from the adipocyte into circulation. Whether these byproducts also signal to sympathetic and sensory nerves is an open question.

Adipocyte proliferation

Increases in adipocyte cell number correlates with obesity (Bartness et al., 2005). NE inhibits proliferation of adipocyte precursor cells in vitro and can be blocked by a general β -AR antagonist (Foster and Bartness, 2006; Jones et al., 1992). In vivo, the denervation of subcutaneous adipose tissue increases adipocyte proliferation, measured by BrDU staining (Jones et al., 1992). Therefore sympathetic activity inhibits white adipocyte proliferation and ultimately leads to fewer adipocytes and a smaller adipose depot.

Browning and thermogenesis

Brown adipocytes produce heat in a process termed non-shivering thermogenesis. The expression of uncoupling protein 1 (UCP-1) uncouples the electron transport chain so that electrons are not used to produce ATP and are instead dissipated as heat (Weyer et al., 1999). This inefficient use of energy has become a target in the treatment of obesity, as extra energy intake from overeating is lost. The β 3-AR is the predominant receptor in brown adipocytes, but they also express β 1-AR and α 2-AR (Bartness et al., 2010a).

Similar to the effect on white adipocyte, NE signals on β_3 AR to increase cAMP and activate PKA. PKA then phosphorylates the transcription factor cAMP response element binding protein, which induces UCP-1 expression (Bartness et al., 2010a). Brown adipocytes also undergo lipolysis and the liberated fatty acids are available as an energy source in thermogenesis. Initiating thermogenesis is a major mechanism by which the SNS increases energy expenditure when confronted with excess energy intake.

Release of norepinephrine does not always lead to a functional response

Since NE causes increased lipolysis and decreased adipocyte proliferation, an increase in sympathetic tone should decrease white adipose tissue mass. However, this relationship is not always observed. In one example, a Siberian hamster treated with leptin had increased sympathetic outflow to white adipose tissue, but adipose mass did not change (Penn et al., 2006). This could be due to a lack of sensitivity to NE because of down-regulation of adrenergic receptors or downstream signaling. Another possibility is that the adipose mass may not significantly change if lipolysis is only moderately increased (Bartness and Song, 2007). After analyzing changes in sympathetic outflow to adipose tissue the efficacy is best assessed by AR expression and the downstream signals resulting in lipolysis, adipocyte proliferation, and thermogenesis.

Change in sympathetic input to specific adipose tissue depots

Cold exposure increases sympathetic tone to both brown and white adipose

Exposure to cold temperature stimulates SNS activity to brown adipose tissue. Brown adipocytes then increase expression of UCP-1 and produce heat. In acute

exposure to 4°C, the subcutaneous brown adipose depot in rats showed an increase in NE turnover 12-fold compared with ambient temperature controls (Young et al., 1982). Bartness and colleagues expanded on this finding and measured the NE turnover in white and brown adipose depots after cold exposure. Subcutaneous white adipose tissue and two visceral white adipose tissue depots (gonadal and retroperitoneal) also had increases in NE turnover in response to cold exposure; however, the largest increase in NE turnover was observed in the brown adipose (Brito et al., 2008a). The lipolysis stimulated in white adipose tissue and the resulting free fatty acids can be used by the brown adipose tissue as energy to be converted to heat (Bartness et al., 2010a). In fact a recent finding showed activated brown adipocytes receive the majority of the energy source from lipolysis in white adipose (Shin et al., 2017). The response to cold exposure demonstrates that sympathetic outflow can differ between adipose tissues in magnitude.

Fasting increases sympathetic tone to white but not brown adipose tissue

Fasting leads to a decrease in sympathetic activity to the heart and vasculature to reduce energy expenditure by lowering heart rate and blood pressure (Landsberg and Young, 1978). In times of fasting, the adipose tissue must mobilize lipid stores as an alternative fuel source for the body and this is triggered by the increased sympathetic outflow. After a 16 hour fast, the NE turnover was increased in only the subcutaneous adipose tissue and gonadal adipose tissue, while brown adipose tissue is unchanged (Brito et al., 2008a). In a separate paper, the NE turnover in brown adipose tissue was decreased after two days of fasting (Young et al., 1982). This behavior indicates that the sympathetic outflow differs between adipose depots in direction as well. In the case of

fasting, energy must be conserved; therefore it would be counterproductive for the brown adipose tissue to have increased sympathetic activity. This homeostatic conservation of energy reserves provides an important clue as to why diets become ineffective over time.

Overfeeding and calorie composition has only been measured in brown adipose tissue

The Landsberg laboratory carried out a series of overfeeding experiments that analyzed the changes in sympathetic tone to the heart, pancreas, and brown adipose tissue. Both feeding mice a sucrose solution and a high fat diet were considered models of overfeeding and increased NE turnover in brown adipose to the same degree, 92% and 113% respectively (Schwartz et al., 1983; Young and Landsberg, 1977; Young et al., 1982). Landsberg and Young then analyzed how calorie composition affects sympathetic outflow. The overfeeding experiments suggested an increase in carbohydrates, and a diet of half fat from lard, showed an increase in NE turnover to brown adipose tissue to the same degree (Landsberg and Young, 1978; Schwartz et al., 1983; Young and Landsberg, 1977). When the chow diet was supplemented with protein there was a minimal increase in NE turnover to brown adipose tissue, especially compared to the lard and sucrose supplements (Kaufman et al., 1986). Overall it indicates that both dietary carbohydrates and fats increase brown adipose sympathetic tone and dietary protein has no effect. The effect of diet composition on the sympathetic drive to white adipose tissue has not been measured.

Visceral versus subcutaneous adipose tissue

The type of adipocytes, sympathetic innervation, lipolytic activity, and response to hormones all differ between subcutaneous adipose tissue and visceral adipose tissue (Ibrahim, 2010). Abdominal visceral adipose is more highly associated with metabolic risk factors such as cardiovascular disease, diabetes, metabolic syndrome, and non-alcoholic fatty liver disease (Fox et al., 2007).

In rodents, the inguinal subcutaneous adipose depot is the primary subcutaneous depot. There is some incongruity in defining rodent visceral adipose tissue, as the gonadal, or epididymal, adipose is the largest depot within the visceral cavity however it does not drain to the portal vein, a hallmark of visceral adipose depots (Tchkonia et al., 2013; Catalano et al., 2010). If the definition of a visceral adipose depot is that it drains to the hepatic portal vein, the only true rodent visceral depot is the mesenteric depot, a small depot along the intestine. The gonadal and retroperitoneal depots drain to the inferior vena cava and can be labeled intra-abdominal depots (Tchkonia et al., 2013; Catalano et al., 2010). Furthermore, the gonadal depot does not exist in humans. While this discrepancy between rodent and human adipose tissue may lead to incorrect assumptions or translations into human adipose biology, it is broadly assumed that the gonadal adipose depot behaves as a human visceral adipose depot in terms of adipocyte type, sympathetic innervation, lipolysis, and beiging (Tchkonia et al., 2013).

Sympathetic innervation and lipolysis

Visceral adipocytes are more metabolically active and have a greater lipolytic activity than subcutaneous adipocytes. This is due to increased β AR expression on

visceral adipose compared to subcutaneous. In addition, anti-lipolytic signals such as α ARs and insulin receptors are expressed in lower levels on visceral adipose tissue. Therefore, visceral adipose maintains a higher susceptibility for catecholamine induced lipolysis (Bouchard et al., 1993). However the lipolytic machinery, such as HSL, is expressed in equal amounts between visceral adipose and subcutaneous (Lefebvre et al., 1998).

Youngstrom and Bartness first saw the relationship between differential sympathetic drive and lipolysis in 1995. They noted that during short winter-like days, Siberian hamsters had increased SNS activity to visceral adipose tissue that lead to preferential adipose mass loss and increased lipolysis (Youngstrom and Bartness, 1995). One can note, that due to the increased propensity for lipolysis seen in the visceral adipose, a little increase in SNS activity can lead to large effects in lipolysis.

Propensity for beiging

Brown adipocytes are characterized by expression of uncoupling protein 1, increases in mitochondria, and small multilocular lipid droplets. The beiging of white adipose tissue is defined as the appearance of brown-like adipocytes within white adipose depots and is primarily seen in subcutaneous adipose depots (Harms and Seale, 2013). Subcutaneous adipose tissue express higher levels of PRDM16, which is necessary for inducing the brown-like gene program. When PRDM16 is deleted, subcutaneous adipose takes on properties of visceral adipose such as large adipocytes and increased inflammation (Cohen et al., 2014). Under basal conditions and when stimulated by cold or exercise, UCP1 is more highly expressed in subcutaneous than visceral (Bouchard et

al., 1993; Harms and Seale, 2013). The inducible nature of beiging, classically achieved through sympathetic activation, is now of great interest to treat obesity.

Loss of visceral adipose after calorie restriction

Visceral adipose tissue is more sensitive to weight reduction than subcutaneous adipose because it is more metabolically active and sensitive to lipolysis (Wajchenberg, 2000). Not only does visceral adipose express higher basal levels of β 3-AR, the expression of β 3AR, HSL, and PPAR γ increases in response to fasting specifically in visceral adipose (Li et al., 2003). In humans, all forms of weight loss, including calorie restriction, exercise, pharmacologic therapy, or gastrointestinal surgery, cause greater percent visceral adipose loss than subcutaneous adipose (Doucet et al., 2002; Smith and Zachwieja, 1999). The propensity to lose visceral adipose is higher for patients starting with higher visceral adipose mass (Smith and Zachwieja, 1999). While visceral adipose is lost early in weight loss, the loss of subcutaneous adipose was seen in instances of high total weight loss or extended time on low calorie diets. Interestingly, very low calorie diets provided exceptional short-term preferential visceral adipose loss (Chaston and Dixon, 2008a).

Pathogenic visceral adipose tissue

Abdominal visceral adipose is more highly associated with metabolic risk factors such as cardiovascular disease, diabetes, metabolic syndrome, and non-alcoholic fatty liver disease (Fox et al., 2007). The gender difference in visceral adipose tissue is an important factor in explaining the gender differences in cardiovascular risk profile. Men

have about twice the amount of visceral adipose compared to premenopausal women (Wajchenberg, 2000). One link between visceral adiposity and cardiovascular risk is elevated sympathetic tone to organs like skeletal muscle and blood vessels. The levels of muscle SNS activity are positively correlated with lower abdominal visceral adipose tissue mass, as measured in humans by computed tomography (Alvarez, 2002). Those with larger visceral adipose mass had 40% higher levels of muscle SNS activity (Alvarez, 2002). This correlation was seen in both obese and non-obese men and was independent of total adipose mass, subcutaneous adipose mass, or age (Alvarez, 2002; Alvarez et al., 2004). Elevated sympathetic tone is a determining factor for cardiovascular disease.

The hepatic-portal theory is a second link between visceral adiposity and pathological consequences. The portal draining of visceral adipose free fatty acids, adipokines, and inflammatory cytokines through the liver may be a mechanism for linking obesity and liver insulin resistance. Free fatty acids are known to impact liver metabolism through increased glucose production and reduced hepatic clearance of insulin, which in turn lead to hyperinsulemia. Subcutaneous adipose tissue drains through systemic veins and therefore the free fatty acids, adipokines, and inflammatory cytokines secreted by subcutaneous adipose have a less direct effect on internal organ functions (Ibrahim, 2010; Tchernof et al., 2013).

Another hypothesis to link visceral adiposity to insulin resistance hinges on the obese visceral adipose secretion of proinflammatory cytokines, such as IL-6, that contribute to insulin resistance (Li et al., 2003). In addition, adipocytes from visceral adipose tissue are more insulin resistant than subcutaneous adipocytes. Large adipocytes become more insulin resistant and adipocytes from visceral adipose grow larger than

subcutaneous adipocytes during obesity. Therefore, the amount of visceral adipose is associated with variations in insulin sensitivity and progression of diabetes (Wajchenberg, 2000; Ibrahim, 2010).

Central regulation of sympathetic activity

Central regions that connect to sympathetic innervations of adipose

The first paper to definitively establish the presence of sympathetic nerves innervating white adipose tissue was by Youngstrom and Bartness working on Siberian hamsters (Youngstrom and Bartness, 1995). They used single neuron tract tracers to reveal direct sympathetic innervation of brown and white adipose tissue. In subsequent studies, they used retrograde transsynaptic viral tract tracers to identify the origin of sympathetic outflow to the adipose tissue within the CNS. After injections into epididymal (gonadal) and subcutaneous adipose depots, neurons infected with pseudorabies virus were found in the spinal cord, brain stem (medulla, nucleus of the solitary tract, caudal raphe nucleus, C1 and A5 regions), midbrain (central gray) and several areas of the forebrain (Bamshad et al., 1998; Bartness et al., 2010b). In rats, pseudorabies virus injected into the retroperitoneal and subcutaneous adipose depots found third order neurons that synapse onto the preganglionic neurons in the medulla and hypothalamus (parvocellular paraventricular nucleus, lateral hypothalamic area, and retrochiasmatic area, and medial preoptic area). Fourth order virally labeled neurons are present in the hypothalamus within the lateral hypothalamus, suprachiasmatic nucleus, and arcuate nucleus. Also likely to be fourth order are neurons in regions of the medulla and midbrain including the nucleus of the solitary tract, area postrema, locus coeruleus,

parabrachial nuclei, and in the periaqueductal gray (Adler et al., 2012; Stefanidis et al., 2014).

In the original experiments by Bartness and colleagues, the central nervous system (CNS) labeling between gonadal and subcutaneous adipose depots was more similar than different (Bamshad et al., 1998). More recently, Bartness and colleagues injected the mesenteric visceral adipose and the subcutaneous adipose depot and found less overlap between brain projection regions and overall less projections to mesenteric adipose (Nguyen et al., 2014). CNS projections to separate adipose depots follow a rostrocaudal separation and the differences in projections could be based on location in the body. Regardless, the presence of independent direct connections to specific adipose depots may provide a mechanism for differential sympathetic regulation. Alternatively, differential sympathetic activity to adipose depots could be regulated by neuronal cell type within a brain region. Within the hypothalamus, projections from the arcuate nucleus to the subcutaneous depots were predominantly from pro-opiomelanocortin (POMC) cells, with a notable lack of projections from agouti-related protein (AgRP)-expressing neurons (Adler et al., 2012; Stefanidis et al., 2014). The melanocortin-4 receptor, the receptor for the POMC product α -melanocyte stimulating hormone and responsible for downstream effects in energy balance and lipid mobilization, is expressed in white adipose projecting neurons (Song et al., 2005). Further research has connected POMC neuronal activity to functional changes in SNS activity to adipose tissue (Dodd et al., 2015).

Leptin acts in the hypothalamus to induce sympathetic nerve activity

Leptin is expressed and secreted by adipocytes in proportion to adipose mass and acts as a negative feedback to combat excess adipose mass. Specifically, leptin actions on leptin receptors in the hypothalamus drive suppression of food intake and increased energy expenditure. One mechanism by which leptin increases energy expenditure is through increased SNS activity to brown adipose tissue, increasing brown adipose tissue UCP-1 expression and thermogenesis (Morrison et al., 2014). In addition, leptin acts via sympathetic neurons to induce phosphorylation of hormone sensitive lipase and lipolysis in white adipose tissue (Zeng et al., 2015). Increased leptin sensitivity in POMC neurons promoted browning of subcutaneous adipose tissue through increased sympathetic drive. The leptin induced beiging and brown adipose thermogenesis increases energy expenditure and reduced body weight (Dodd et al., 2015).

Other Neuronal innervation of adipose tissue

Adipose tissue is devoid of parasympathetic innervation

While it is typical for the SNS and parasympathetic nervous system to innervate and exert antagonistic effects on endocrine and exocrine organs, adipose tissue does not show evidence of parasympathetic innervation. Across various rodent models and adipose depots (gonadal, subcutaneous, and retroperitoneal) none show the presence of known parasympathetic markers including vesicular acetylcholine transporter vasoactive intestinal peptide, and neuronal oxide synthase (Giordano et al., 2006). Therefore, within the adipose tissue, the SNS acts unopposed by the parasympathetic nervous system in the regulation of lipid mobilization and energy homeostasis, although it is possible that another signal may exist to balance the sympathetic outflow to the adipose tissue.

Sensory innervation could provide feedback and regulation

The first evidence for sensory innervation in adipose tissue was identified by using the neuroanatomical tracer *true blue* to track axons from adipose tissue to sensory neurons of the dorsal root ganglia (Fishman and Dark, 1987). The current hypothesis for the role of sensory neurons in the adipose tissue is to sense lipid stores and leptin levels (Bartness and Song, 2007). There is a subset of leptin sensitive sensory nerves that express the leptin receptor and fire after intra-adipose leptin injection (Murphy et al., 2013). Another possible signal to the sensory nerves is free fatty acids, which are a product of lipolysis. Indeed, some sensory nerves are known to express free fatty acid receptors such as GPR40 and GPR120 (Matsumara et al., 2007). A point of communication between the efferent sympathetic nerves and the afferent sensory nerves of the adipose tissue is currently unidentified. However, a circuit whereby sensory afferents directly or indirectly feedback onto sympathetic outflow is an attractive model for how adipose tissue may tune homeostatic energy liberation (Esler et al., 2006a).

Methods to measure sympathetic outflow

Sympathetic activity can only be assessed directly either by electrophysiology or by NE turnover. Absolute levels of NE in the tissue do not indicate release because the synthesis and the degradation of NE allow for two variables that can alter the concentration of NE (Landsberg and Young, 1978). As such, the absolute levels of NE in adipose tissue are more likely a reflection of innervation density (i.e. unreleased NE resides in presynaptic terminals). Therefore it is critical to measure sympathetic activity

either by direct nerve activity or by a dynamic measurement of NE levels. *Microneurography* uses fine electrodes inserted into superficial nerves to record bursts of activity (Parati and Esler, 2012). This method allows for precise measures of nerve activity; however it is invasive and can only measure one nerve at a time. Another common measurement in humans is regional *NE spillover*, a measure comparable to NE turnover. Tritiated NE is infused and incorporated into the endogenous NE pools (Parati and Esler, 2012). After release, NE is either degraded by monoamine oxygenase, transported back to the nerve terminal by amine transporters, or diffused into the blood stream (Esler et al., 2006b). The release of NE from an organ can be measured by the isotope dilution in the plasma of the regional veins (Parati and Esler, 2012). This technique can be done without radioactive NE, however this is less precise. Since the adipose tissue does not have superficial access for an electrode, examining NE spillover is the only way to determine sympathetic activity to adipose tissue in humans.

In rodents both electrophysiology and NE turnover are used as well. Electrophysiology is technically complicated especially in the sparsely innervated adipose tissue (Foster and Bartness, 2006). *NE turnover* is the preferred method to measure sympathetic activity in adipose tissue. NE is synthesized by tyrosine hydroxylase (TH) at the nerve terminal and packaged into vesicles for release. The overall NE turnover reflects the continuous loss by metabolism and replenishment by synthesis. NE is metabolized either extraneuronally, through diffusion or non-neuronal uptake, and intraneuronally, through reuptake and degradation by MAO or passive leakage from the storage vesicles. Loss of extraneuronal NE after release accounts for 18% of NE turnover (Eisenhofer et al., 2004). The bulk of NE turnover is through passive

leakage of NE from intracellular vesicles. Measurement of NE turnover employs alpha-methyl-p-tyrosine (AMPT), a competitive inhibitor of TH, to block synthesis of NE (Bartness et al., 2014; Vaughan et al., 2014). By inhibiting NE synthesis, the only variable affecting the amount of NE is metabolism either extraneuronally or intraneuronally, both which occur actively only after release (Eisenhofer et al., 2004). Therefore we can assume NE metabolism is dependent on NE release. NE turnover measures the decline of NE concentrations over time as an indication of NE release, and therefore overall sympathetic activity (Bartness et al., 2014; Landsberg and Young, 1978; Vaughan et al., 2014).

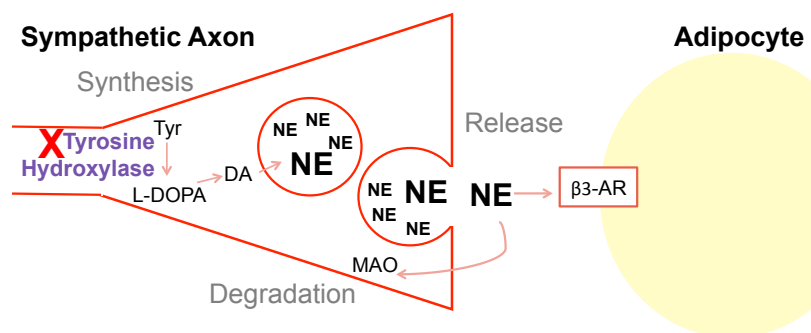


Figure 1.1

Schematic of Norepinephrine (NE) synthesis by tyrosine hydroxylase, release from the sympathetic neuron, NE signaling through the β_3 adrenergic receptor (β_3 AR) on adipocytes, and degradation by monoamine oxidase (MAO). NE turnover is assayed by inhibiting tyrosine hydroxylase, represented by the red "X".

Calorie Restriction

Calorie restriction diets are demonstrably effective for weight loss in both rodents and humans. Calorie restriction results in improved insulin sensitivity, lowered cancer risks, and elongated life span (Denny et al., 2006; Mahoney et al., 2006). Calorie restriction lowers serum insulin levels, lowers serum triglycerides, and improves glucose tolerance, all of which reduce the risk of atherosclerosis, diabetes, and obesity (Verdery and Walford, 1998).

The individual responses to calorie restriction vary due to genetic and physiological differences. For example, animals and humans with higher resting metabolic rate before diet, exhibit increased weight loss from caloric restriction (Vaanholt et al., 2015). Regardless, following weight loss, animals and humans decrease the resting metabolic rate to maintain energy homeostasis (Rosenbaum and Leibel, 2014). In addition, animals with a compensatory decrease in activity levels lose less weight following calorie restriction (Vaanholt et al., 2015). Difficulty in maintaining weight loss can be attributed in large part to these compensatory changes in energy expenditure and activity.

Consequences of obesity on the sympathetic nervous system

Overfeeding leads to increased sympathetic tone

Obesity in the simplest terms is a result of more energy intake than energy output. Rodent models of obesity are typically generated by feeding a high fat diet. Landsberg and Young performed many experiments to show that short term overfeeding readily increased sympathetic activity to heart, pancreas and brown adipose in rats (Landsberg

and Young, 1978). Recent work using telemetry to measure sympathetic activity has shown that after three weeks on a high fat diet rabbits had increased renal SNS activity and rats had increased lumbar SNS activity (Armitage et al., 2012; Muntzel et al., 2012). The short term overfeeding experiments show that the increased sympathetic activity observed in obesity is likely a response to increased energy intake. Following his findings, Landsberg hypothesized that overeating initiates diet-induced thermogenesis by stimulation of the SNS. The diet-induced thermogenesis would act to stabilize body weight. However, the eventual consequence would be the heightened regional sympathetic activation seen in obesity that leads to diseases such as hypertension. Taken together, increased regionally specific sympathetic outflow is an adaptive response to overeating (Landsberg, 1986).

Specificity of sympathetic outflow

Most of the work done to link obesity to the SNS has examined relatively few tissues, such as the heart and kidney. However, SNS outflow to one region may not reflect the outflow to another (Morrison, 2001). As discussed earlier, there are instances where SNS activity not only differs across tissues but within a type of tissue such as white vs. brown adipose tissue. The analysis of sympathetic activity in humans is typically measured by NE spillover or muscle SNS activity, focusing on heart, kidney, and vasculature. In obese patients the sympathetic tone to kidneys and vasculature of the skeletal muscle is elevated, while the adrenal medullary secretion of epinephrine is normal (Esler et al., 2006a). Both human and rodent models of obesity neglect the sympathetic tone to adipose tissue. In one study of obese women, the NE spillover from

white adipose tissue was decreased compared to lean patients (Coppack et al., 1998). While Landsberg showed brown adipose tissue has elevated sympathetic tone after short term overfeeding, the white adipose tissue was not analyzed. The brown and white adipose tissue would likely have different responses to obesity due to their uncoordinated roles in energy expenditure.

Obesity-related diseases have sympathetic nervous system components

Obesity related diseases such as hypertension, cardiovascular disease, sleep apnea, and renal dysfunction all have sympathetic components and are often treated with adrenergic receptor antagonists (Lambert et al., 2010; Rahmouni et al., 2005). Perhaps the best link established is that of obesity-associated hypertension. It is estimated that obesity contributes to hypertension in over 60% of men and women (Garrison et al., 1987). Although studies in patients do not always produce consistent results, the consensus is that obese patients have heightened activation of the SNS in regionally specific areas (van Baak, 2001; Davy and Orr, 2009). The heightened sympathetic activity is viewed as the cause of obesity-related hypertension, and is ultimately the target for its treatment. It is important to note that the increased SNS activity is regionally specific, particularly to the kidney and legs. Interestingly, treatment of hypertension with β -AR antagonists is associated with weight gain in patients (Rössner et al., 1990).

Treatment of obesity with β 3 adrenergic receptor agonists

The promise β 3-AR agonists came from treatment of rodent models of obesity. Agonist treatment increased insulin sensitivity, lowered plasma glucose levels, and

lowered leptin levels. β 3-AR agonists stimulated expression of the uncoupling proteins in white adipose tissue (Weyer et al., 1999). Overall, the treatment of mice with β 3-AR agonists successfully decreased obesity. However, it is important to note, β 3-AR agonists in humans are not identical to their rodent counterpart. In humans, β 2-AR, rather than β 3-AR, is the dominant receptor regulating lipolysis and thermogenesis as it is in rodents (Arch and Wilson, 1996). Therefore, while the use of β 3-AR agonists in mice is a useful tool to specifically target adipose tissue, they are not directly translatable for human treatment.

Potential mechanisms for change in sympathetic tone in obesity

There is good evidence that sympathetic tone increases in obesity in a regionally specific way, however the mechanism for this is unknown. There are various hypotheses for the mechanism that span from the response to short term overfeeding to more pathological changes. Several reviews delve into all of the potential mechanisms, however this discussion focuses primarily on the mechanisms relevant to the proposed aims (Esler et al., 2006a).

Visceral adipose tissue

The levels of muscle sympathetic activity are positively correlated with lower abdominal visceral adipose tissue mass, as measured in humans by computed tomography (Alvarez, 2002). Those with larger visceral adipose mass had 40% higher levels of muscle SNS activity (Alvarez, 2002). This correlation was seen in both obese and non-obese men and was independent of total adipose mass, subcutaneous adipose mass, or age

(Alvarez, 2002; Alvarez et al., 2004). This evidence leads to the hypothesis that the increase in sympathetic tone, at least to the muscle, is due to a factor released in proportion to the amount of visceral adipose tissue.

Leptin

Leptin is a hormone released from adipose tissue in amounts proportional to the adipose tissue in the body and circulating concentrations are elevated in obesity. Leptin acts on hypothalamic neuronal targets to suppress appetite, reduce energy intake, and increase energy expenditure (Russell et al., 1998). When rats are infused with leptin there is an increase in sympathetic outflow to kidney, hind limb vasculature, and to the adrenal medulla. Leptin expression and secretion is lower in visceral compared to subcutaneous adipose tissue, therefore the hypothesis of leptin as a potential mechanism for the increase in sympathetic tone in obesity is incongruent with the observation of the quantitative link between sympathetic outflow and visceral adipose (Russell et al., 1998). Furthermore, muscle sympathetic activity was unchanged compared to men with three-fold higher leptin concentrations (Alvarez et al., 2004). Taken together, these findings indicate that leptin is a regulator of the SNS, but is not necessarily the mechanism underlying diet induced changes to weight.

Insulin

Obesity, particularly visceral obesity, is typically accompanied by hyperinsulinemia. Experiments in humans demonstrate that infusion of insulin produces an increase in sympathetic outflow to the skeletal muscle vasculature as measured by

microneurography (Esler et al., 2006a; Vollenweider et al., 1993). This increase in SNS was thought to be the link between obesity and elevated sympathetic tone. However, a confounding experiment, in which insulin was administered intranasally to act on the CNS, showed no change in muscle sympathetic activity even though insulin affects the SNS through the CNS (Benedict et al., 2005). Hyperinsulinemia is a component of Landsberg's central hypothesis for sympathetic activation; he hypothesized that insulin was the signal that relates dietary intake to SNS activity.

The sympathetic nervous system is a major regulator of energy homeostasis through the control of energy expenditure by brown adipose tissue and energy liberation by white adipose tissue. The ability of the sympathetic nervous system to target individual adipose depots is essential for its roles in energy homeostasis. This thesis will explore the differential sympathetic drive to individual adipose depots following an extended energy deficit. Is sympathetic activation necessary for loss of adipose mass on a weight loss diet? Furthermore, the regulation of discrete sympathetic drive by the CNS, the sensory nervous system, or by the individual adipose depots remains a fascinating open question.

p75 Neurotrophin Receptor

Neurotrophins regulate neuronal survival and differentiation during the development of the nervous system. Neurotrophins bind to specific receptors; for example, Neuron Growth Factor (NGF) binds to TrkA. Additionally, all neurotrophins

bind to p75 Neurotrophin Receptor (p75NTR), a member of the Tumor Necrosis Factor (TNF) superfamily (Kaplan and Miller, 2000). Like all TNF family members, p75NTR contains a death domain in its intercellular region. When TrkA and p75NTR are co-expressed, the two receptors form a high affinity binding complex, which enhances the pro-survival effects of neurotrophins (Barker, 2004). In the absence of TrkA receptors, neurotrophin binding to p75NTR can activate apoptotic pathways (Kaplan and Miller, 2000). In addition to binding to all neurotrophins, p75NTR can bind pro-neurotrophins, with the co-receptor sortilin. Pro-neurotrophin binding to p75NTR can induce cell death, again opposing the effects of mature neurotrophins on TrkA (Barker, 2004).

p75NTR in the sympathetic nervous system

During mammalian development, neurons are overproduced in hopes of reaching a final target. Neurons that do not reach a final target or that reach an incorrect target undergo programmed cell death. Developing sympathetic neurons express high levels of TrkA and p75NTR and have an absolute requirement of NGF for survival. During the first two postnatal weeks, sympathetic neurons compete for limited amounts of target-derived NGF. NGF binds to TrkA to send a retrograde survival signal. When there is a lack of TrkA-NGF signal, p75NTR signaling induces apoptosis. Independent of TrkA, p75NTR can also signal apoptosis through other neurotrophin binding events, such as Brain Derived Neurotrophic Factor (BDNF) and Neurotrophin 3, which are excreted by target matched neurons to promote apoptosis in neighboring neurons (Bamji et al., 1998; Deppmann et al., 2008). TrkA is the dominant signal meaning any activation of TrkA by NGF negates the cell death signal from p75NTR through suppressing c-jun kinase

activity (Yoon et al., 1998). Therefore, developmental neuronal death occurs when p75NTR is activated and TrkA-NGF survival signals are low.

p75NTR null mice exhibit delayed developmental neuronal death. In normal mice, sympathetic neurons numbers decreased by 42% from birth to p23, however in p75NTR null mice, sympathetic neuron numbers increased between birth and p23, but interestingly returned to normal levels by adulthood (Bamji et al., 1998). In addition to increased number of neurons during development in the SCG, p75NTR null mice also exhibit increased pre- and post-synaptic specializations at postnatal day 10 (Sharma et al., 2010). It is currently unknown the level of synapses in adult p75NTR deficient mice. However, at adulthood the mutation of p75NTR did not change the size of sympathetic ganglia or the density of sympathetic innervation of the iris or salivary gland (Lee et al., 1992). Interestingly, the sympathetic innervation of pineal glands and sweat glands of the footpad was absent in adult p75NTR null mice. This absence was due to a failure of neurons to reach the target tissues. Many of the adult tissues including heart, lung, spleen, and kidney had normal sympathetic innervation (Lee et al., 1994). In contrast to the SNS, the sensory nervous system remained perturbed in adult p75NTR null mice. p75NTR null mice at adulthood show decreased sensory innervation of the footpad, leading to loss of heat and touch sensitivity, and indicating an opposing role of p75NTR in the sensory nervous system (Lee et al., 1992).

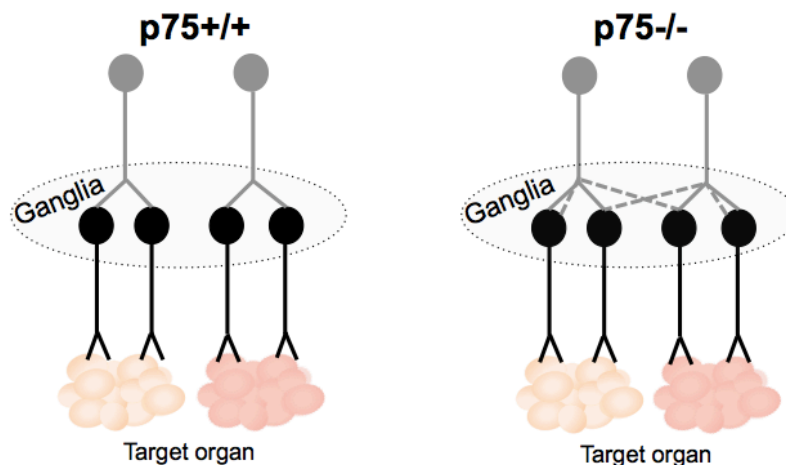


Figure 1.2

Schematic representation of the hypothesis that increased synapses at the sympathetic ganglia would lead to diffused signal from the preganglionic neurons (gray) onto the postganglionic neurons (black) or incorrect matching of preganglionic signal to the target organs.

While the sympathetic neuron number, ganglion size, and final target innervation was normal in *p75NTR* deficient adult mice, it is currently unknown if synapse formation remains different in adult mice. These changes during sympathetic development in neuron number, axon outgrowth, and especially synapse formation, could have lasting impacts on adult sympathetic function. This thesis presents the hypothesis that the increased synapse formation during development seen in *p75NTR^{-/-}* mice could cause incorrect target matching and diffusion of the preganglionic signal (Figure 1.2). It is imperative in the SNS to match the CNS inputs to the innervating neuron of the correct target organ. We know there is differential sympathetic drive between adipose depots in

cases such as fasting and cold exposure (Brito et al., 2008b). If the increased synapses in p75NTR deficient mice lead to incorrect target matching, then the differential sympathetic drive to adipose tissue could be disrupted. Accordingly, the increased synapses in p75NTR deficient mice, can lead to diffusion of preganglionic signals onto postganglionic neurons. The diffusion of this preganglionic signal would ultimately reduce sympathetic activity. Therefore, within the adult SNS, p75NTR could influence sympathetic activity through incorrect target matching and decreased sympathetic drive.

While essential for proper regulation of the developing nervous system, p75NTR expression and functions were thought to decrease into adulthood. p75NTR expression in the central and peripheral nervous system declines in adulthood however can be reactivated upon injury and degeneration (Ibáñez and Simi, 2012). This has led to new avenues of research into p75NTR functions in Alzheimer's and other degenerative diseases (Ibáñez and Simi, 2012).

p75NTR in metabolism

p75NTR is expressed outside of the nervous system and functions in adult homeostasis. p75NTR is widely expressed outside of the nervous system, interestingly in insulin sensitive and metabolically active tissues such as liver, muscle, white adipose, and brown adipose (Baeza-Raja et al., 2012; Lomen-Hoerth and Shooter, 1995; Nisoli et al., 1996a; Peeraully et al., 2004). In muscle and liver, p75NTR has been shown to influence proliferation and differentiation through RhoA inhibition, therefore p75NTR is an important factor in muscle and liver repair (De Ponti et al., 2009; Passino et al., 2007).

Despite the roles of p75NTR in differentiation in liver and muscle, there have been no implications for roles in adipogenesis (Baeza-Raja et al., 2012; Bernat et al., 2016).

p75NTR insulin sensitivity

In myocytes and adipocytes, deletion of p75NTR enhances the insulin-stimulated glucose uptake and trafficking of Glucose Transporter 4 (GLUT4) to the plasma membrane. In adipocytes, the death domain of p75NTR directly inhibits the GTPases, Rab 5 and Rab 31, which regulate GLUT4 translocation. The increased cellular insulin sensitization makes the p75NTR null mouse more insulin sensitive on a standard diet, even without changes in body weight, as measured by glucose and insulin tolerance tests and the euglycemic clamp (Baeza-Raja et al., 2012).

Outside of direct interaction with Rab 5 and Rab 31, Sortilin, co-receptors for p75NTR, is a major component of GLUT4 vesicles in adipocytes (Morris et al., 1998). Sortilin acts as a co-receptor with p75NTR to bind pro-neurotrophins and mediate apoptosis (Barker, 2004). This opens up the possibility of pro-neurotrophins having p75NTR and sortilin dependent effects on adipocytes and insulin sensitivity.

Notably, the inhibitory effects of the p75NTR death domain on Rab 5 and Rab 31 occur independently of a neurotrophin ligand. Neither stimulation with NGF, BDNF, or neurotrophin inhibition through antibodies had an effect on the inhibition of glucose uptake by p75NTR (Baeza-Raja et al., 2012). It is difficult to entirely conclude these effects are ligand-independent as not all of the possible p75NTR ligands were tested. Studies with exogenous expression of the intracellular death domain of p75NTR, which directly interacted with Rab 5 and Rab 31, do not rule out ligand-dependency in vivo. It is

possible there is a ligand-dependent association of the death domain to Rab5 or a ligand dependent cleavage event, as both options have been reported in the literature (Schachtrup et al., 2015).

p75NTR also intersects in glucose homeostasis in the pancreas, as high glucose concentrations increase expression of p75NTR in islets (Raile et al., 2006). Interestingly, some studies suggest a role in beta cell apoptosis (Gezginci-Oktayoglu and Bolkent, 2011; Pierucci et al., 2001). It is currently unknown how p75NTR expression in pancreatic islets impact overall insulin sensitivity.

Adipocytes themselves express and secrete NGF. Expression of NGF is increased by TNF α exposure (Peeraully et al., 2004). NGF expression decreases during prolonged cold exposure and NE treatment in brown adipocytes, meaning sympathetic activation decreases brown adipose NGF expression. After obesity, NGF expression was increased in brown adipose tissue, but still decreased expression in response to cold (Nisoli et al., 1996a).

p75NTR regulates energy expenditure

p75NTR deficient mice are resistant to diet induced obesity. Following eight weeks on a high-fat diet, mice deficient in p75NTR had significantly less adipose mass and liver triglycerides. *p75NTR*^{-/-} mice maintained insulin sensitivity after high fat diet. p75NTR deficient mice were protected from obesity due to increases in energy expenditure and oxygen consumption resulting from over active PKA signaling. Bernat and colleagues determined p75NTR directly binds to the regulatory and catalytic subunits of PKA to inhibit PKA signaling. In the absence of inhibition by p75NTR, active PKA

leads to an increase in lipolysis, fat oxidation, and UCP-1 expression (Bernat et al., 2016). p75NTR was previously shown to dampen the cAMP signaling pathway in fibroblasts by interacting with phosphodiesterase 4A to enhance cAMP degradation. In both instances, p75NTR dampens the cAMP signaling cascade (Sachs et al., 2007).

Importantly, the changes in energy expenditure and oxygen consumption after a high fat diet were isolated to the role of p75NTR in adipocytes rather than hepatocytes or myocytes. p75NTR specifically deleted in adipocytes recapitulates the increase in oxygen consumption, lipolysis, fat oxidations, and UCP1 expression. Since PKA was relieved of inhibition by p75NTR, PKA phosphorylation of HSL increased, which then stimulated lipolysis (Bernat et al., 2016). Overall, p75NTR expression in adipocytes is required for diet induced obesity.

p75NTR expression fluctuates in a circadian manner

p75NTR is an oscillating gene regulated by the master circadian clock regulators CLOCK and BMAL1 through E-box enhancers. p75NTR gene expression specifically oscillates in the suprachiasmatic nucleus, the central regulator of circadian rhythmicity, as well as the liver, a regulator of glucose homeostasis. Expression of p75NTR in the suprachiasmatic nucleus and liver is higher during the light period. The oscillation of p75NTR remains even in constant dark conditions, indicating that p75NTR expression is driven by E-box dependent and not light-dependent transcription. Not only is p75NTR expression circadian, p75NTR is necessary for expression of other clock genes. p75NTR deletion alters the oscillation of the clock genes, *Period1* and *Period2*, and glucose homeostatic genes in the liver such as *PEPCK* and *GLUT4*. Mice deficient in global

p75NTR maintain locomotor activity rhythms in constant darkness although with elevated activity levels (Baeza-Raja et al., 2013).

Conclusion

In this thesis, I will examine the differential sympathetic activation to adipose tissue during calorie restriction. Does the SNS drive energy liberation in discrete adipose depots in a hierarchical manner? Following the elucidation of differential sympathetic drive during calorie restriction, I will ask what occurs if sympathetic drive is disrupted. To attack this question, I will examine mice deficient in p75NTR. Mice deficient in p75NTR have impaired development of the SNS. Overall, I will elucidate the impact of differential sympathetic drive on adipose loss during calorie restriction.

Chapter 2. Differential sympathetic outflow to adipose depots is required for visceral fat loss in response to calorie restriction

LM Sipe, C Yang, J Ephrem, E Garren, J Hirsh and CD Deppmann

Nutrition & Diabetes (2017) 7, e260; doi:10.1038/nutd.2017.13

ABSTRACT

The sympathetic nervous system (SNS) regulates energy homeostasis in part by governing fatty acid liberation from adipose tissue. We first examined whether SNS activity toward discrete adipose depots changes in response to a weight loss diet in mice. We found that SNS activity toward each adipose depot is unique in timing, pattern of activation, and habituation with the most dramatic contrast between visceral and subcutaneous adipose depots. Sympathetic drive toward visceral gonadal adipose is more than doubled early in weight loss and then suppressed later in the diet when weight loss plateaued. Coincident with the decline in SNS activity toward visceral adipose is an increase in activity toward subcutaneous depots indicating a switch in lipolytic sources. In response to calorie restriction, SNS activity toward retroperitoneal and brown adipose depots is unaffected. Finally, pharmacological blockage of sympathetic activity on adipose tissue using the β 3-AR antagonist, SR59230a, suppressed loss of visceral adipose mass in response to diet. These findings indicate that SNS activity toward discrete adipose depots is dynamic and potentially hierarchical. This pattern of sympathetic activation is required for energy liberation and loss of adipose tissue in response to calorie restricted diet.

INTRODUCTION

Obesity has reached epidemic proportions in modern society. Pharmaceuticals have been developed that target endocrine pathways including leptin, ghrelin, and insulin (Bell-Anderson and Bryson, 2004; Levri et al., 2005; Patterson et al., 2011). Unfortunately, these drugs have proven largely ineffectual or unsafe in weight loss. The safest treatment for obesity remains dietary intervention or increased exercise. Although diet is the preferred method of remediation, there remains much that we don't know including: 1. What is the primary driver of adipose loss after dietary intervention? 2. Is adipose tissue lost evenly across the body in response to dietary intervention? Here we seek to address these questions by examining an understudied element governing energy liberation: the sympathetic nervous system (SNS).

While obesity is characterized as an overall increase in adipose mass and fat droplet storage, accumulation of only specific fat depots are directly associated with adverse health risks. In particular the deposition of adipose mass in visceral depots correlates with pathologies such as type II diabetes, cardiovascular diseases and some cancers (Misra and Vikram, 2003; Reaven, 2011; Tchernof et al., 2013). The reasons for this association remain obscure. It has been suggested that proximity of these depots to internal organs and drainage of excess free fatty acids and inflammatory cytokines into the portal vein may contribute to such comorbidities (Cancello et al., 2006; Gasteyger and Tremblay, 2002; Ibrahim, 2010). The alarming negative associations of visceral adipose tissue make this depot an attractive therapeutic target.

The SNS is a key regulator of energy homeostasis through its control of heart rate, blood pressure, and energy expenditure (Esler et al., 2006b; Messina et al., 2013; Young

et al., 2011). Sympathetic nerve fibers innervate brown and white adipose depots to signal thermogenesis and energy liberation, respectively (Zeng et al., 2015). Norepinephrine (NE) from sympathetic axon terminals binds the β_3 adrenergic receptor (AR) on rodent white and brown adipose depots to induce lipase activation, which breaks down triglyceride stores (Bartness et al., 2014). Free fatty acids and glycerol are then released into the bloodstream to be used as energy by other organs (Bartness et al., 2014; Bowers et al., 2004). Lipolysis over long periods results in smaller adipocytes and decreased adipose mass (Bartness and Song, 2007; Bartness et al., 2014).

Clues about SNS dynamics in energy homeostasis come from Bartness and colleagues, who challenged animals with fasting or cold exposure. When hamsters are fasted for 16 hours, sympathetic outflow is increased dramatically to the subcutaneous depot and to a lesser extent to the visceral gonadal depot and not at all to the visceral retroperitoneal depot (Brito et al., 2008a; Nguyen et al., 2014). Likewise, hamsters and mice exposed to cold (5°C) for 16 hours display increased sympathetic drive to both brown and white adipose depots resulting in free fatty acids that can be converted to heat (Brito et al., 2008a; Young et al., 1982). Taken together, these findings indicate that sympathetic outflow can differ between adipose depots in response to a particular environmental challenge. These seminal studies indicate that not only does sympathetic outflow change in response to environmental challenge but it also appears to do so non-uniformly across adipose depots. Instead, depending on the environmental challenge, discrete fat pads preferentially receive increased sympathetic outflow. Although paradigm shifting, interpretation from these studies were somewhat limited due to the relatively short window of environmental challenge (16 hours) examined. These studies

were unable to ascertain whether discrete fat pads are preferentially and perhaps hierarchically used as lipolytic sources over sustained periods. Therefore, how SNS outflow to discrete fat pads controls prolonged diet induced weight loss, remains a critical open question. Such a longitudinal analysis would be particularly relevant to weight loss in humans.

Here we examine SNS activation toward discrete adipose depots in response to an acute calorie restrictive diet over 12 days. We report a unique pattern of sympathetic activity to adipose depots throughout weight loss that dictates loss of discrete adipose depot mass. For example, sympathetic drive to visceral gonadal adipose is elevated early in weight loss and suppressed later in the diet. Coincident with the decline in sympathetic activity toward gonadal adipose, we observe an increase in sympathetic activity toward subcutaneous depots indicating a switch in lipolytic sources after extended time on the diet. Using a β 3-AR antagonist, we found that the sympathetic drive to adipose tissue is necessary for the loss of visceral adipose mass during calorie restriction. Taken together this indicates that the SNS drives energy liberation from discrete adipose depots in a potentially hierarchical manner to manage overall energy homeostasis.

RESULTS

Adipose loss in response to calorie restriction occurs preferentially from visceral depots

We employed a calorie restriction (CR) model for dietary weight loss in mice over the course of 12 days. C57BL/6 adult male mice were limited to 75 percent of their

individual standard chow intake. Mice on the calorie-restricted diet lose weight rapidly over the first 5 days, losing 13.0 ± 2.4 percent of their starting body weight and by day 12 mice reach a loss of 16.9 ± 2.8 percent (Figure 2.1A). Control mice that were fed *ad libitum* (AL) maintained their weight over this 12 day period (Figure 2.1A). In this model of calorie restriction we chose 3 and 12 days for subsequent analysis to reflect a period of early and late phase weight loss. Mice have significantly different body weights between the initial weight loss at day 3 and day 12 of calorie restriction.

We focused on the loss of adipose mass during calorie restriction. We first examined the summed mass of four adipose depots: gonadal, retroperitoneal, subcutaneous, and brown. This total mass was not significantly reduced by day 3 compared to AL controls (Figure 2.1B). Instead, the loss of adipose mass is more gradual, with only significant loss of summed adipose mass observed after 12 days of calorie restriction (Figure 2.1B). The non-adipose loss that occurs by three days can be attributed to decreases in food intake and loss of bound water to glycogen stores as has been reported in rodent, primate, and human studies (Lane et al., 1999; Oscai and Holloszy, 1969; Yang and Van Itallie, 1976).

We next sought to determine how individual adipose pads (*i.e.* visceral or subcutaneous) lose mass as a function of time after calorie restriction. The only depot that displayed significant change by day 3 was gonadal adipose tissue, suggesting that this is an early source for lipolysis (Figure 2.1C, D). By day 12 of diet, both visceral depots (gonadal and retroperitoneal) examined decreased by half of their original weight. Gonadal adipose and retroperitoneal adipose mass reduced by 52.9 ± 18.6 percent and 66.9 ± 11.2 , respectively compared to *ad libitum* controls (Figure 2.1C-F). The

subcutaneous adipose tissue displays a modest but significant decrease of 28.7 ± 11.5 percent (Figure 2.1G, H). Intrascapular brown adipose displays no significant change in mass after 12 days on diet (Figure 2.1I, J).

Dynamic sympathetic outflow to adipose depots in response to calorie restriction

We next examined whether changes in sympathetic outflow to particular adipose depots correspond with the loss of mass reported in Figure 1. Simply measuring the concentration of NE in a tissue is likely more reflective of innervation density rather than release onto the tissue (Youngstrom and Bartness, 1995). Therefore, we turned to a classic method to measure sympathetic activity, the NE turnover (NETO) assay (Brownstein and Axelrod, 1974; De Champlain et al., 1969; Schwartz et al., 1983; Vaughan et al., 2014). The amount of NE in a tissue is a balance between synthesis in the axon, release and degradation in the tissue. NE is degraded rapidly after it is released onto tissue, therefore, as suggested by Axelrod and colleagues, NE degradation is roughly equivalent to NE release (Axelrod, 1971; Cooper et al., 2003). We are able to assess NE turnover by isolating the rate of NE release and subsequent degradation using a chemical inhibitor of NE synthesis, alpha-methyl-*p*-tyrosine (AMPT) (Vaughan et al., 2014). The rate of NE degradation over four hours is multiplied by the total NE content of the adipose depot to obtain a final value of NETO to reflect the overall sympathetic drive toward each tissue.

We predicted that the timing of adipose mass loss of discrete depots would be matched by an elevation in sympathetic activity. Importantly, with enough time and sympathetic activity, we speculated that adipose depots would become depleted

necessitating that sympathetic outflow to several of the tissues would be depressed at later time points. Indeed, the largest fat pad examined, the visceral gonadal adipose depot, displays a roughly 2.3-fold increase in NE turnover after three days of calorie restriction, which is consistent with the early loss of mass that we observe for this depot (Figure 2.2A, Figure 2.1E, F). This initial increase in NE turnover to gonadal adipose is decreased to baseline by day 12 of calorie restriction (Fig. 2A).

Importantly, we found that not all adipose depots followed the same pattern of NE turnover rate as the gonadal depot. The retroperitoneal adipose depot did not display a significant change in NE turnover rate in response to calorie restriction at either time point examined (Figure 2.2B). Despite this, retroperitoneal adipose still decreases in mass after calorie restriction (Figure 2.1E, F). While this is the smallest of the white adipose depots examined, it suggests a mechanism for adipose mass loss that may be independent of changes to SNS outflow.

Unlike the gonadal adipose where we observed initial increases in NE turnover, the subcutaneous adipose showed no change in NE turnover after 3 days (Figure 2.2C). Instead, increase in NE turnover to this depot occurred after 12 days of calorie restriction (Figure 2.2C). This delayed increase in SNS activity toward subcutaneous adipose corresponds to the modest reduction in adipose mass by 12 days (Figure 2.1G, H). Because University of Virginia Animal Care and Use Committee regulations require that we remove animals from calorie restriction once animals have lost 20 percent of their body weight, we were unable to assess whether outflow to subcutaneous adipose would return to baseline with time.

In contrast to the dynamic sympathetic activity toward white adipose depots, brown adipose tissue does not show significant changes in sympathetic outflow or adipose mass (Figure 2.2D, Figure 2.1I, J).

Antagonizing sympathetic activity on adipose depots prevents diet induced adipose loss

To determine the contribution of sympathetic activity to adipose tissue in dietary weight loss, we inhibited adipose specific adrenergic signaling using the β 3-AR antagonist SR59230a (Bexis and Docherty, 2009; Mizuno et al., 2002; Nisoli et al., 1996b; Ootsuka et al., 2011). The β 3-AR is specifically expressed in both brown and white adipose tissue and is the primary receptor for NE on adipocytes in mice (Collins et al., 2004). Mice treated daily with intraperitoneal injections of SR59230a (1mg/kg) lost significantly less body weight on calorie restriction, evident by day 8 and through day 12, a time in which the majority of weight loss is from fat (Figure 2.3A, Figure 2.1B). Mice fed *ad libitum* had no change in body weight with daily treatment of SR59230a (Figure 2.3A). SR59230a treatment caused no change in *ad libitum* food intake or consumption of the entire allotment of chow during calorie restriction (Figure 2.3B). Daily treatment with SR59230a inhibits calorie restriction induced lipolysis (Figure 2.3C). Importantly, SR59230a treated mice still lose non-adipose weight in the early phase of weight loss in the same manner as untreated mice. Measurement of liver mass was not significantly changed between groups (Figure 2.3D). Therefore, we conclude that the extent of weight loss that was inhibited can be primarily attributed to suppressed loss of adipose mass.

We next sought to test the effect of SR52930a on adipose mass by examining summed adipose loss as described in Figure 1B. Consistent with observations in Figure 1, mice treated with saline had decreased total adipose mass after 12 days on calorie restriction (Figure 2.4A). However when treated with SR59230a, mice no longer lost significant total adipose mass after calorie restriction (Figure 2.4A). SR59230a treated mice fed *ad libitum* displayed no significant change in total adipose mass (Figure 2.4A).

We next sought to examine the effect of SR59230a within specific adipose depots. Treatment with SR59230a has the most dramatic impact on visceral adipose depots. Consistent with observations in Figure 1, gonadal adipose under saline treatment displayed a 49.2 ± 5.0 percent reduction in mass after 12 days of calorie restriction (Figure 2.4B, C). Interestingly, gonadal adipose mass from calorie restricted SR59230a treated mice decreased by only 16.0 ± 11.8 percent, which is statistically insignificant compared to saline treated *ad libitum* fed mice (Figure 2.4B, C).

Unlike the gonadal tissue, SR59230a affected the retroperitoneal adipose mass in *ad libitum* and calorie-restricted conditions. *Ad libitum* fed mice treated with SR59230a displayed a roughly 40 percent increase in retroperitoneal adipose mass (Figure 2.4D, E). Under calorie restriction, SR59230a treated mice only lost 15 percent of retroperitoneal adipose mass compared to the 60 percent under saline treatment (Figure 2.4D, E). In this experiment, subcutaneous adipose mass still decreased by 30 percent, but did not reach the significance observed in Figure 1. This relatively small change (compared to 60-80 percent in visceral depots) as well as the additional statistical stringency added by the two way ANOVA could account for the discrepancy in statistical significance between Figure 2.1G and Figure 2.4F. Additionally, when represented as percent change and analyzed

with Dunnett's multiple comparisons there is a significant decline in adipose mass after calorie restriction. Nevertheless, the subcutaneous depot did not show significant weight loss after antagonist treatment, due to the role of sympathetic drive in weight loss (Figure 4F,G). Brown adipose mass displayed no change after calorie restriction and likewise SR59230a treatment had no effect on their mass (Figure 2.4 H,I). Taken together these data suggest that the visceral depots are uniquely sensitive to sympathetic activity both with respect to energy storage and liberation.

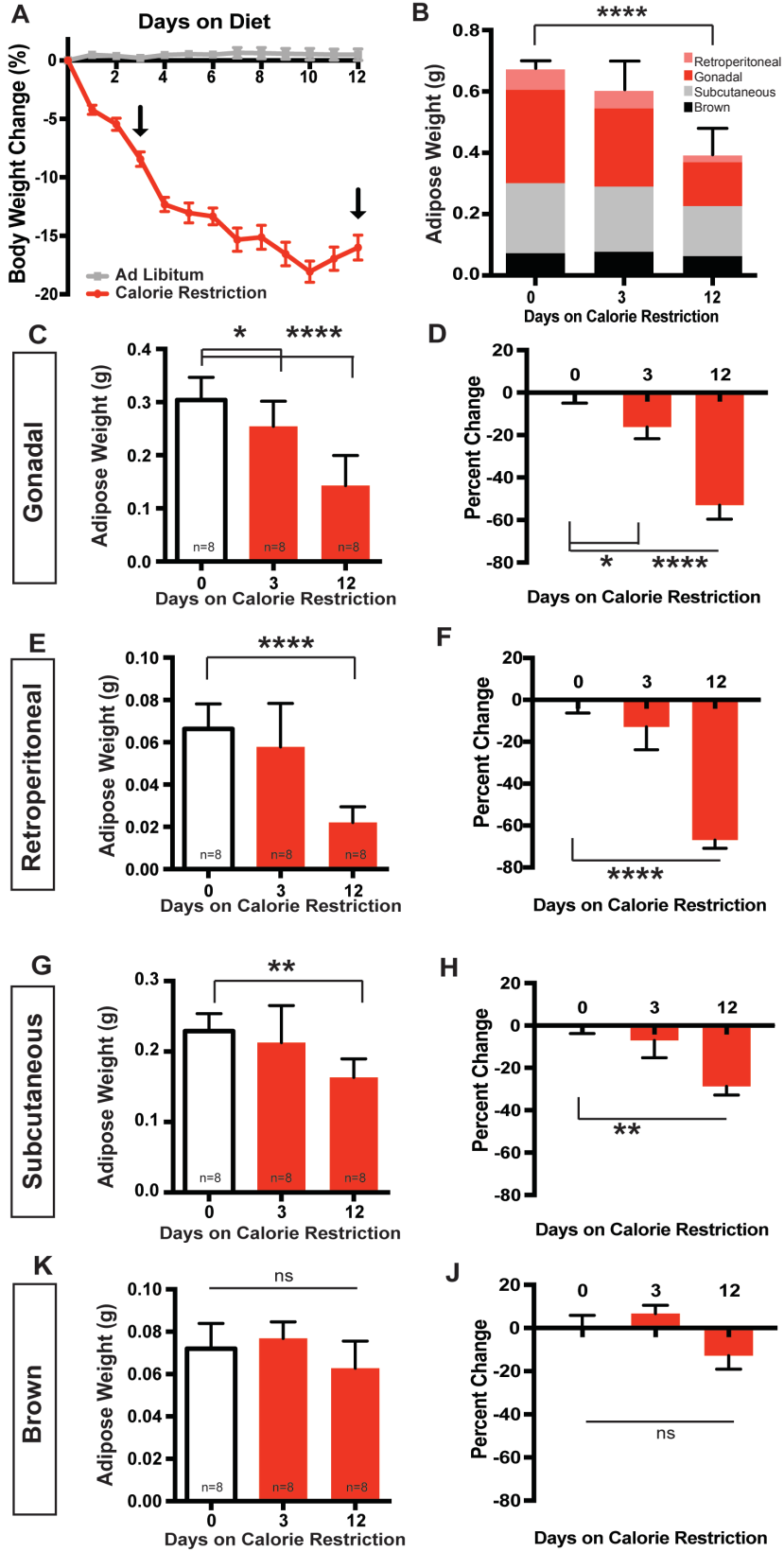


Figure 2.1 Selective loss of adipose mass in response to calorie restriction.

- A. C57BL/6 male mice at least 12 weeks of age and 25 grams were either fed *ad libitum* or 75 percent of the average daily standard chow intake. Mice were weighed daily and percent body weight change from starting body mass was calculated. Arrows mark early and late phases of weight loss (days 3 and 12) that are used in subsequent experiments. * $p < 0.0001$ day 0 compared to day 3 on calorie restriction, * $p < 0.0001$ day 3 compared to day 12 on calorie restriction. Two way ANOVA, Tukey's multiple comparisons
- B. Total adipose weight of dissected adipose depots following 0, 3, or 12 days of calorie restriction. The contribution of individual depots to the total dissected adipose mass is shown. Pink=Retroperitoneal, Red= Gonadal, Gray=Subcutaneous, and Black= Intrascapular brown. $P < 0.0001$ day 0 compared to day 12.
- C. Dissected gonadal adipose mass after 0, 3, or 12 days of calorie restriction. * $p = 0.05$ day 0 compared to day 3, **** $p < 0.0001$ day 0 compared to day 12
- D. Percent change in gonadal adipose mass compared to the average of calorie restriction day 0. * $p = 0.05$ day 0 compared to day 3 , **** $p < 0.0001$ day 0 compared to day 12
- E. Dissected retroperitoneal adipose mass after 0, 3, or 12 days of calorie restriction. *** $p = 0.0001$ day 0 compared to day 12
- F. Percent change in retroperitoneal adipose mass compared to the average of calorie restriction day 0. **** $p < 0.0001$ day 0 compared to day 12

- G. Dissected subcutaneous adipose mass after 0, 3, or 12 days of calorie restriction
**p=0.0048 day 0 compared to day 12
- H. Percent change in subcutaneous adipose mass compared to the average of calorie restriction day 0. **p=0.0034 Day 0 compared to day 12
- I. Dissected intrascapular brown adipose mass after 0, 3, or 12 days of calorie restriction no significant differences
- J. Percent change in intrascapular brown adipose mass compared to the average of calorie restriction no significant differences

B,C,E,G,I- One way ANOVA with Tukey's multiple comparisons D,F,H,J- One way ANOVA with Dunnett's multiple comparisons against the control (ad libitum) Data shown as \pm SEM

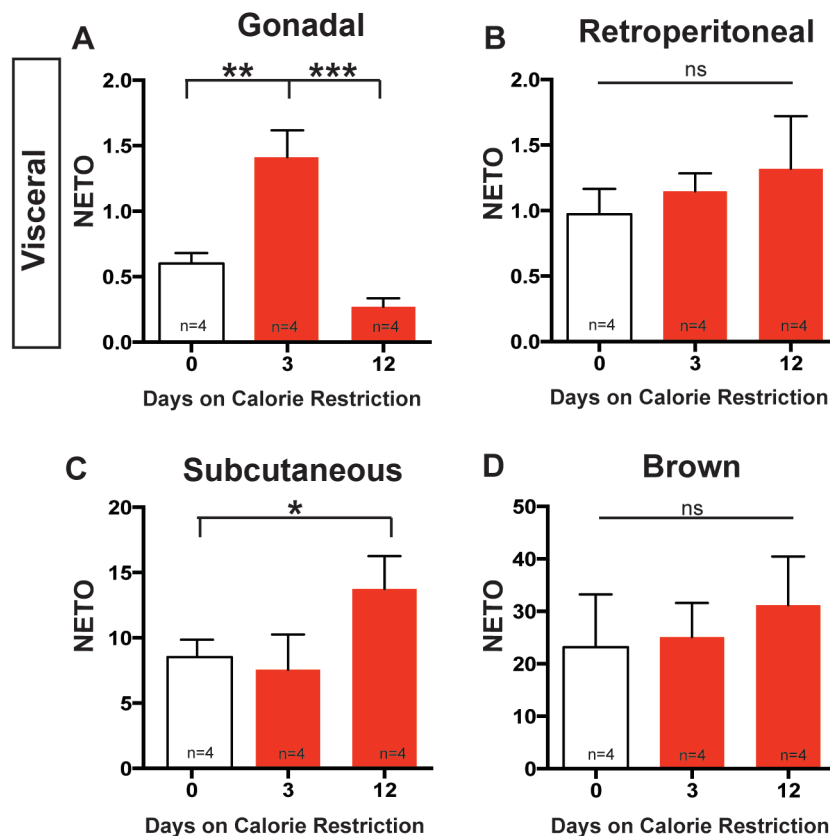


Figure 2.2 Non-uniform sympathetic activity to adipose depots after calorie restriction

- A. Norepinephrine turnover (NETO) in gonadal adipose tissue after 0, 3, or 12 days of calorie restriction. * $p=0.005$ day 0 compared to day 3, * $p=0.0005$ day 3 versus day 12
- B. NETO in retroperitoneal adipose tissue after 0, 3, or 12 days of calorie restriction. No significant differences
- C. NETO in subcutaneous adipose tissue after 0, 3, or 12 days of calorie restriction * $p=0.0374$ day 0 compared to day 12
- D. NETO in brown adipose tissue after 0, 3, or 12 days of calorie restriction. No significant differences

One way ANOVA with Tukey's multiple comparisons Data shown as \pm SEM

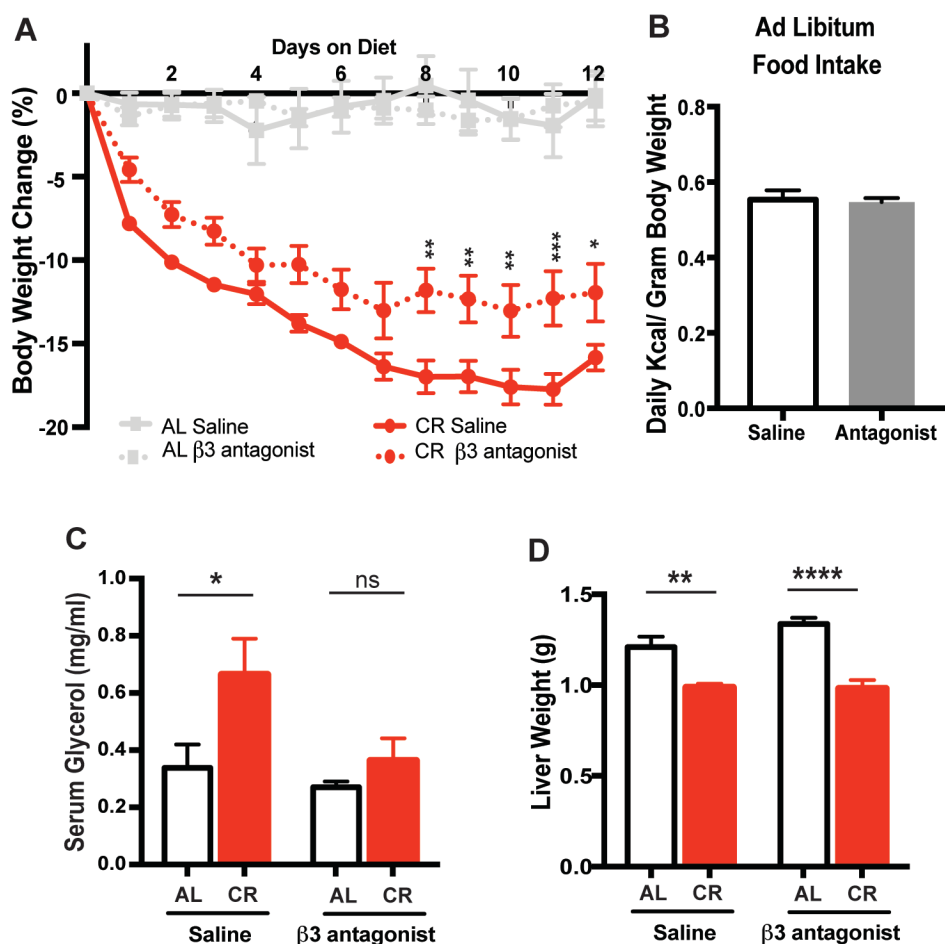


Figure 2.3 Inhibition of β 3-adrenergic receptor signaling prevents body weight loss and lipolysis in response to calorie restriction

A. C57BL/6 male mice at least 12 weeks of age and 25 grams were either fed *ad libitum* (AL) or only 75 percent of their average daily standard chow intake (CR). Mice were injected IP daily with saline or SR59230a (1mg/kg) prior to feeding. Mice were weighed daily and percent body weight change from starting body mass was calculated. * $p < 0.05$ Calorie Restriction Saline compared to Calorie Restriction SR59230A days 8-12

- B. Average daily food intake over 12 days by mice fed *ad libitum* either injected IP with saline or SR59230a (1mg/kg). $p=0.783$ (two sample t-test)
- C. Serum glycerol levels of mice after 12 days of *ad libitum* feeding or calorie restriction either injected IP with saline or SR59230a (1mg/kg) * $p=0.011$ *ad libitum* saline compared to calorie restriction saline, $p=0.956$ *ad libitum* SR59230a compared to calorie restriction SR59230a
- D. Dissected liver mass, weighed following 12 days of saline or SR59230a (1mg/kg) intraperitoneal injections while fed *ad libitum* or on calorie restriction. ** $p=0.0083$ *ad libitum* SR59230a compared to CR SR59230a, **** $p=0.0001$ CR saline compared to CR SR59230a

Two way ANOVA with Tukey's multiple comparisons. Data shown as \pm SEM

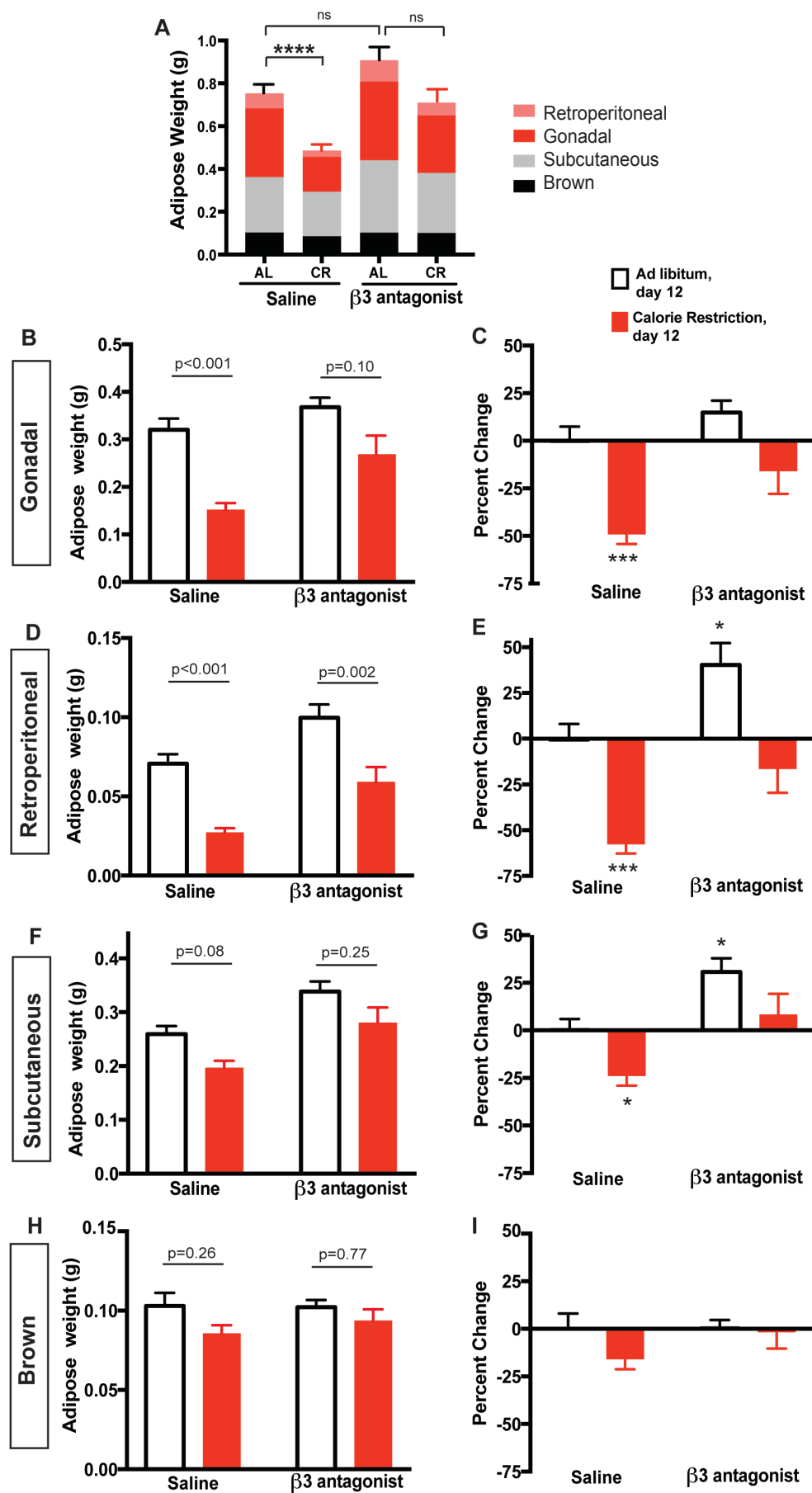


Figure 2.4 Inhibition of β_3 adrenergic signaling in adipose tissue prevents loss of visceral and subcutaneous adipose mass

- A. Dissected adipose depots were weighed following 12 days of saline or SR59230a (1mg/kg) intraperitoneal injections while fed *ad libitum* or on calorie restriction. The contribution of individual depots to the total adipose mass is shown. AL= *ad libitum*, CR= calorie restriction Pink=Retroperitoneal, Red= Gonadal, Gray= Subcutaneous, and Black= Brown. **** $p < 0.0001$ AL saline compared to CR, $p = 0.32$ AL saline compared to AL β_3 antagonist, $p = 0.14$ AL β_3 antagonist compared to CR 3 antagonist, ** $p = 0.0017$ calorie restriction saline compared to CR β_3 antagonist
- B. Gonadal Adipose tissue **** $p < 0.0001$ AL saline compared to CR Saline, $p = 0.1000$ AL β_3 antagonist compared to CR β_3 antagonist, $p = 0.6526$ AL saline compared to AL β_3 antagonist, * $p = 0.0112$ CR saline compared to CR β_3 antagonist,
- C. Percent change in gonadal adipose mass when compared to the average of AL fed saline treated mass. * $p < 0.001$ AL saline compared to CR Saline, $p = 0.5288$ AL saline compared to AL β_3 antagonist, $p = 0.3544$ AL saline compared to CR β_3 antagonist
- D. Retroperitoneal Adipose tissue **** $p < 0.0001$ AL saline compared to CR Saline, ** $p = 0.0026$ AL β_3 antagonist compared to CR β_3 antagonist, * $p = 0.0381$ AL saline compared to AL β_3 antagonist, ** $p = 0.0060$ CR saline compared to CR β_3 antagonist,

- E. Percent change in retroperitoneal adipose mass when compared to the average of AL fed saline treated mass. * $p < 0.0001$ AL saline compared to CR Saline, $p = 0.0239$ AL saline compared to AL $\beta 3$ antagonist, $p = 0.4696$ AL saline compared to CR $\beta 3$ antagonist
- F. Subcutaneous adipose tissue $p = 0.0838$ AL saline compared to CR Saline, $p = 0.2587$ AL $\beta 3$ antagonist compared to CR $\beta 3$ antagonist, $p = 0.0558$ AL saline compared to AL $\beta 3$ antagonist, * $p = 0.0144$ CR saline compared to CR $\beta 3$ antagonist,
- G. Percent change in subcutaneous adipose mass when compared to the average of AL fed saline treated mass. * $p = 0.048$ AL saline compared to CR Saline, $p = 0.0318$ AL saline compared to AL $\beta 3$ antagonist, $p = 0.7517$ AL saline compared to CR $\beta 3$ antagonist
- H. Brown adipose tissue, No significant differences
- I. Percent change in brown adipose mass when compared to the average of AL fed saline treated mass.

A,B,D,F,H- Two way ANOVA with Tukey's multiple comparisons C,E,G,I- Two way ANOVA with Dunnett's multiple comparisons against the control (AL) Data shown as \pm SEM

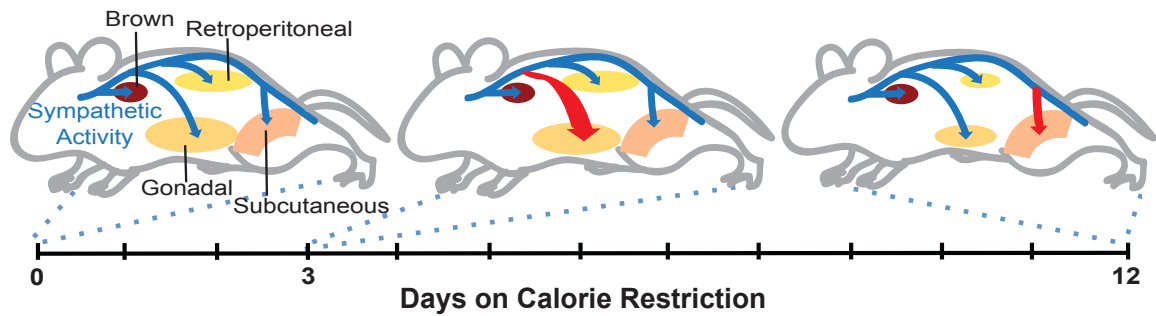


Figure 2.5 Model of hierarchical dynamics of sympathetic outflow during calorie restriction

The sympathetic nervous system (blue) innervates the visceral adipose depots gonadal and retroperitoneal, the subcutaneous depot, and the intrascapular brown adipose depot. After three days of calorie restriction sympathetic outflow is increased to the gonadal adipose tissue (red arrow). The sympathetic activity causes the gonadal adipose depot to shrink significantly by day 3 and reduce by half of the original size at day 12. By day 12 of calorie restriction, sympathetic outflow to gonadal adipose returns to normal, while the activity to subcutaneous adipose increases. The sympathetic drive to retroperitoneal adipose does change as a function of diet, however the depot reduces in mass by day 12 perhaps by SNS independent mechanisms. The brown adipose depot experiences no changes in sympathetic drive or adipose mass during the 12 days of calorie restriction.

DISCUSSION

Here we demonstrate that sympathetic drive regulates preferential loss of visceral adipose mass after acute calorie restriction. Clinical reports in humans show visceral adipose tissue is preferentially lost during acute weight loss diets (Chaston and Dixon, 2008b; Li et al., 2003). We suggest that the mechanism underlying this phenomenon is via selective sympathetic drive to visceral depots during calorie restriction. This also suggests that the SNS may be a relevant therapeutic target for human obesity since excess visceral adipose is linked to several co-morbidities including Type II diabetes, cardiovascular disease, and some cancers (Gasteyger and Tremblay, 2002).

In the past, it has been suggested that the SNS fires *en masse* (Morrison, 2001). However, in response to diet we found that not only can the dynamics of sympathetic drive differ between organs but also within the same organ. A similar conclusion was made using Siberian hamsters, when, in response to fasting, SNS activity toward visceral gonadal depot was elevated while activity remained unchanged in both subcutaneous white adipose and brown adipose tissue (Brito et al., 2008a).

The differences in sympathetic outflow dynamics in response to calorie restriction suggest that adipose depots may be used in a hierarchical manner as lipolytic sources and may represent a general logic for energy homeostasis. In our model of dietary weight loss we observed an initial increase of sympathetic drive to the visceral gonadal adipose depot. This was the only depot to significantly decrease in mass after 3 days of calorie restriction (Figure 2.1C). This suggests that gonadal depots are an early source of lipolysis in conditions of energy deprivation.

Sympathetic drive to adipose tissue may define the preference or hierarchy of lipolytic sources to be used for energy. Indeed, we observe elevated SNS activity first toward visceral depots during calorie restriction and then switching to subcutaneous depots later in the diet. Whether this switch is dependent of depletion of visceral stores remains an open question. After 12 days of calorie restriction the sympathetic drive to gonadal adipose tissue decreases below baseline, while the drive to subcutaneous adipose becomes significantly elevated (Figure 2.2A, C).

It is important to note, that tissues are not uniformly sensitive to NE due to regulation of adrenergic receptors or downstream signaling (Penn et al., 2006). In fact, subcutaneous adipose tissue has increased expression of $G_{\alpha i}$ coupled α -AR relative to visceral depots, which would inhibit the signals for lipolysis and resist loss of adipose mass (Bartness et al., 2010a; Langin, 2006). This may explain why we observe only a slight decrease in subcutaneous adipose mass by twelve days of calorie restriction, despite observing elevated NE turnover to this depot (Figure 2.1B, 2.1E, 2.4C). It will be interesting in the future to examine the dynamics of adrenergic receptor expression in this and other adipose depots as a function of time on calorie restriction.

Diet induced changes in sympathetic activity appear to be required for adipose loss. When mice were treated with a β_3 antagonist, the visceral adipose depots no longer significantly decreased in mass after calorie restriction (Fig4A, B-E). This finding has clinical relevance, because β -AR blockers are a common treatment for obesity-induced hypertension. Consistent with our findings, patients on β -AR blockers gained 1.2 kg in the first 2 years (Sharma et al., 2001; Tentolouris et al., 2006).

Not all adipose loss required dynamic SNS activity. The retroperitoneal depot lost mass in a similar fashion to gonadal adipose, however there was no significant increase in NE turnover as a function of time on diet (Figure 1G-H, 2B). Interestingly, the β 3-AR inhibitor, SR52930a, protects this adipose depot from diet-induced loss of mass and increased the mass while fed *ad libitum*. This indicates that while SNS activity wasn't changed in the time points assessed, it may still be involved in adipose maintenance and energy storage within the retroperitoneal depot.

The mechanisms underlying increased or decreased sympathetic drive to particular adipose depots are not well understood. Since parasympathetic nerves do not innervate any adipose depot, the sympathetic drive to adipose is without the regulatory counterbalance typical of the autonomic nervous system (Bartness et al., 2005; Giordano et al., 2006). There are several possible mechanisms by which autonomic drive to adipose tissue might be tuned: 1. A sensory feedback mechanism, whereby axons respond to lipolysis breakdown products, adipose mass, lipid stores, or leptin levels to control adipose specific sympathetic circuits (Bartness et al., 2010b; Fishman and Dark, 1987; Jéquier, 2002; Mark et al., 2003; Murphy et al., 2013) A circuit whereby sensory afferents directly or indirectly feedback onto sympathetic outflow is an attractive model for how adipose tissue may tune homeostatic energy liberation (Esler et al., 2006a). Indeed, points of sympathetic and sensory interaction have recently been identified for brown adipose tissue, such as the raphe pallidus nucleus, nucleus of the solitary tract, periaqueductal gray, hypothalamic paraventricular nucleus, and medial preoptic area (Ryu et al., 2015). 2. Differential sympathetic drive may also be explained by an endocrine feedback loop where adipose derived signals travel through the bloodstream

directly to the CNS or perhaps postganglionic neurons to regulate activity. We do not favor this model because it is difficult to envision a mechanism whereby activity to particular depots is selectively regulated.

We have determined the dynamics of the SNS activity toward visceral, subcutaneous and brown adipose tissue. Our findings suggest that sympathetic drive defines preferential changes in adipose depots, which represents a critical therapeutic target. In the future, it will be important to examine the dynamics of the SNS in other dietary challenges (*i.e.* high fat or ketogenic) as well as potential changes in sex and age. The potentially hierarchical dynamics of the SNS activity in response to persistent dietary challenge represent a novel mechanism for body weight maintenance and energy homeostasis.

Chapter 3. Mice deficient in p75 Neurotrophin Receptor are resistant to diet induced weight loss

INTRODUCTION

The sympathetic nervous system (SNS) governs the discrete adipose depots used for the body's lipolytic needs during dietary challenge. The activation of specific adipose depots by the SNS is dynamic throughout diet. Although, we have observed an apparent hierarchical regulation of lipolysis from different adipose depots in response to diet, we do not know the importance of this observation. What is the consequence of disrupting the preferential sympathetic drive or the timing of activation to adipose depots? How do discrete sympathetic circuits "match" to a particular depot such that different adipose depots can be regulated over the course of a diet? To answer these questions, we will take advantage of p75 Neurotrophin Receptor (p75NTR) deficient mice, which have been shown to be defective in developmental synapse refinement between neurons of the intermediolateral nucleus and postganglionic neurons (Sharma et al 2010). We predicted that this overabundance of synapses would lead to: 1. Diluted sympathetic outflow to any given target and 2. An inability for the sympathetic circuit to define the correctly matched target.

While p75NTR has sympathetic neuron autonomous roles in sympathetic development, it also has adipocyte autonomous roles in regulating sensitivity to NE signaling. As such, it is necessary to parse out the cell autonomous roles of p75NTR during a calorie restriction challenge. p75NTR functions in adipocytes to decrease energy expenditure and catecholamine induced lipolysis. Based on the functions of p75NTR

within adipocytes and sympathetic neurons, we expect opposing mechanisms of p75NTR during changes in energy homeostasis.

How does p75NTR regulate overall energy homeostasis in its diverse functions within organ systems? In this chapter, we determine the role of p75NTR in energy homeostasis specifically during the energy limited state of calorie restriction. We begin to elucidate the cell autonomous role of p75NTR in the SNS and cement the importance of differential sympathetic activity to adipose tissue throughout calorie restriction.

RESULTS

Mice deficient in p75NTR are resistant to diet induced body weight loss and adipose mass loss

To test how p75NTR influences energy homeostasis, we employed a calorie restriction model for dietary weight loss. Mice deficient in *p75NTR* and their littermate controls (*p75NTR^{+/+}*) were given 75% of their individual average standard chow intake. Mice on calorie restriction were weighed and fed the allotted amount of food at the start of the dark portion of the 12h:12h light:dark cycle for 12 days. *p75NTR^{-/-}* mice were resistant to diet induced weight loss. A significant difference was observed starting on day 6 of calorie restriction, where *p75NTR^{-/-}* mice only lost 7.04±1.01 percent of their starting body weight compared to their littermate controls, which lost 12.13±2.85 percent (Figure 3.1A). The percent body weight loss of *p75NTR^{-/-}* continued to be less than littermate controls through day 12 of the calorie restricted diet (Figure 3.1A). Importantly, the starting body weight of *p75NTR^{-/-}* mice was not significantly different from littermate controls (Figure 3.1B). In addition, the daily food intake was not different

between groups as measured by kcal/body weight (Figure 3.1C) or absolute grams of food (data not shown). Mice deficient in p75NTR were resistant to diet induced body weight loss, independent of starting body weight or food intake.

Next, we focused on the loss of adipose mass during calorie restriction. We first examined the summed mass of four adipose depots: gonadal, retroperitoneal, subcutaneous, and brown. Following 12 days of calorie restriction in *p75NTR^{+/+}* animals, total dissected adipose mass was significantly decreased compared to *ad libitum* fed animals (Figure 3.1D). In *p75NTR^{-/-}* mice however, the adipose mass was not significantly different between *ad libitum* fed and calorie restricted mice (Figure 3.1D). *p75NTR^{-/-}* mice begin with slightly less total dissected adipose mass, however this change is not significant between AL and CR ($p=0.09$). When represented as percent change from *ad libitum* adipose mass, *p75NTR^{-/-}* mice on calorie restriction had a significantly lower percent change in total adipose mass compared to *p75NTR^{+/+}* on after calorie restriction (Figure 3.1E). We previously showed the gonadal adipose tissue was preferentially lost following acute calorie restriction (Sipe et al., 2017). Consistent with these results, we found that gonadal depots in *p75NTR^{+/+}* animals decreased from 0.40 ± 0.17 grams to 0.12 ± 0.04 grams, which amounts to a 70% reduction in mass (Figure 3.1F). The gonadal depot of *p75NTR^{-/-}* mice did not significantly decrease following calorie restriction ($p=0.055$) (Figure 3.1F). However, the starting gonadal adipose mass in *p75NTR^{-/-}* mice was significantly lower than compared to their littermates (Figure 3.1F). This may be attributed to an adipocyte autonomous role of p75NTR to increase lipolysis and fatty acid oxidation, which will be discussed further below (Bernat et al., 2016). While *p75NTR^{-/-}* mice do not display significant reduction in gonadal adipose mass

following calorie restriction, the final weight of the depot is similar to that of the $p75NTR^{+/+}$ control (Figure 3.1F). As reported in our previous work, the subcutaneous depot and brown adipose depot did not lose significant mass by day 12 of calorie restriction (Figure 3.1G and data not shown) (Sipe et al., 2017). Mice also lose lean mass in response to 75% caloric restriction. Both $p75NTR^{+/+}$ and $p75NTR^{-/-}$ mice lost significant liver mass by day 12 on calorie restriction (Figure 3.1H).

Mice deficient in p75NTR have altered sympathetic drive to adipose tissue during calorie restriction

Our lab previously reported that elevated sympathetic drive to visceral adipose depots is necessary for body weight and specifically adipose weight loss in response to calorie restriction (Sipe et al., 2017). Since $p75NTR^{-/-}$ mice do not lose adipose mass in response to calorie restriction, we hypothesized that sympathetic drive was decreased in these mice. Simply measuring the concentration of NE in a tissue is likely more reflective of innervation density rather than release onto the tissue (Youngstrom and Bartness, 1995). Therefore, we turned to a classic method to measure of sympathetic activity, the NE turnover (NETO) assay (Brownstein and Axelrod, 1974; De Champlain et al., 1969; Schwartz et al., 1983; Vaughan et al., 2014). The detailed methods and description can be found in Chapter 1, page 15 and Chapter 5, page 91.

There were no changes in *ad libitum* fed NE turnover between $p75NTR^{+/+}$ and $p75NTR^{-/-}$ in any adipose depot analyzed (Figure 3.2A, B, C). Our previous work demonstrate, on day 12 of calorie restriction in C57BL6 mice, NE turnover toward the gonadal adipose matched basal levels whereas drive to subcutaneous adipose was

elevated from basal levels (Sipe et al., 2017). In agreement with those findings, $p75NTR^{+/+}$ mice exhibited no significant change in NE turnover to gonadal adipose tissue and a significant increase in NE turnover to subcutaneous adipose tissue (Figure 3.2A, B). We predict that similar to C57BL6 mice, $p75NTR^{+/+}$ mice would have elevated NE turnover to gonadal adipose tissue during the early stages of calorie restriction, which was necessary for gonadal adipose loss. In subcutaneous adipose tissue, the NE turnover of $p75NTR^{+/+}$ was significantly increased after 12 days of calorie restriction, this increase did not occur in $p75NTR^{-/-}$ mice (Figure 3.2B). Overall, the sympathetic drive to white adipose tissue in $p75NTR^{-/-}$ was reduced during calorie restriction. We know the sympathetic drive to white adipose tissue is necessary for loss of adipose mass during calorie restriction. Therefore the sympathetic drive to adipose represents a mechanism by which $p75NTR^{-/-}$ mice have impaired adipose loss after calorie restriction.

Following calorie restriction, we previously showed no change in sympathetic drive to brown adipose tissue, which is replicated in $p75NTR^{+/+}$ mice. However, in $p75NTR^{-/-}$ mice there was a significant increase in NE turnover to brown adipose tissue on day 12 of calorie restriction (Figure 3.2C). Increased sympathetic drive to brown adipose tissue stimulates thermogenesis and UCP1 expression, which are associated with increased energy expenditure. Ultimately, we would expect increases in NE turnover to promote weight loss, whereas $p75NTR^{-/-}$ mice experience less weight loss. More experiments will be necessary to determine the impact of this increase in sympathetic drive to brown adipose tissue on $p75NTR^{-/-}$ energy homeostasis.

As previously stated, the concentration of NE in a tissue is more reflective of innervation density rather than release onto the tissue (Youngstrom and Bartness, 1995).

p75NTR^{+/+} and *p75NTR*^{-/-} mice have similar levels of NE during *ad libitum* conditions in all adipose depots, indicating no changes in sympathetic innervation (Figure 3.2D-F).

During development of the SNS, mice deficient in p75NTR have higher presynaptic and postsynaptic density markers, synaptophysin and MAGUK respectively (Sharma et al., 2010). A possible mechanism for decreased sympathetic drive and lack of differential sympathetic drive could be the increase in synapses during development, which not only dilutes sympathetic outflow to target organs but also prevents sympathetic circuits from matching to a particular target. If this were true, we would predict that the elevation in synapse number observed in *p75NTR*^{-/-} mice during development would persist in to adulthood. We found that mice deficient in p75NTR fed *ad libitum* had significantly higher MAGUK expression compared to *p75NTR*^{+/+} controls (Figure 3.3A, B). This increase in synapses could lead to incorrect target matching or dilution of the preganglionic signal, both leading to impaired strength of and discrete control of sympathetic drive (Figure 3.3C)

***p75NTR*^{-/-} mice display no changes in food intake over time on diet**

While the decrease in sympathetic drive to adipose tissue could lead to impaired adipose mass loss, other mechanisms could also explain this resistance to weight loss. Previous studies have reported variances in weight loss from caloric restriction due to differences in energy expenditure and activity levels. To address these factors, we placed mice in metabolic cages while fed *ad libitum*, during days 0-2 of calorie restriction, or during days 9-11 of calorie restriction. The data presented in figures 3.3, 3.4, and 3.5 are depicting the middle day in the metabolic cage.

Both $p75NTR^{+/+}$ and $p75NTR^{-/-}$ mice fed *ad libitum* consumed 81.1 and 80.8 percent of their total food intake during the dark cycle, respectively (Figure 3.4A). By day one of calorie restriction (CR1), both $p75NTR^{+/+}$ and $p75NTR^{-/-}$ consumed 100% of their food during the dark cycle (Figure 3.4B). At CR10, mice consume their food rapidly, finishing all of the allotted food within 6 hours (Figure 3.4C). There was no difference in time to consume the food or gorging between genotypes (Figure 3.4C). As such, this may also reflect an intermittent fasting protocol as calorie restricted mice are without food for 18 hours.

p75NTR^{-/-} mice do not compensate for the energy deficient state of calorie restriction

Activity

$p75NTR^{+/+}$ mice exhibit decreased activity levels, as measured by ambulatory beam breaks, after calorie restriction, which is thought to be a homeostatic response to conserve energy. This is evidenced by the significant decrease in activity levels of $p75NTR^{+/+}$ mice between *ad libitum* dark cycle versus the dark cycle of CR10 (Figure 3.4D, F, G). In sharp contrast, $p75NTR^{-/-}$ mice increase activity levels after calorie restriction (Figure 3.4D, F, G). The activity levels of $p75NTR^{-/-}$ mice at CR10 are significantly higher than $p75NTR^{+/+}$ mice at CR10 and even $p75NTR^{+/+}$ and $p75NTR^{-/-}$ mice fed *ad libitum* (Figure 3.4D, F, G). This is a striking finding, as increased activity levels would predict increased weight loss in response to diet, which is the opposite of what we observe (Figure 3.1A). We noticed that $p75NTR^{-/-}$ mice increased activity at times surrounding changes in food availability. Therefore, we analyzed the total beam breaks in the last 6 hours of the dark cycle to represent post-meal activity. Mice deficient

in $p75NTR$ had increased activity following consumption of the meal (Figure 3.4H). This may indicate mice are searching for more food. We next analyzed the total beam breaks in the 2 hours prior to the dark cycle, when they receive their daily food, to measure anticipation for the meal. $p75NTR^{-/-}$ mice have significantly higher meal anticipation activity (Figure 3.4I). These changes in activity in relation to the timing of food intake could point to a mechanism, whereby $p75NTR$ is working in the CNS, where it influences the integration of circadian rhythms, foraging, and anticipatory activity.

Heat

Heat production (kcal/hr) was lower for both $p75NTR^{+/+}$ and $p75NTR^{-/-}$ during the light cycle. As calorie restriction progressed, both $p75NTR^{+/+}$ and $p75NTR^{-/-}$ reduced in body heat, however $p75NTR^{-/-}$ had significantly higher heat production during the light cycle of CR10 (Figure 3.5A). The increase in heat production seen in the $p75NTR^{-/-}$ mice, could be due to increased sympathetic activity to brown adipose tissue late in diet (Figure 3.2C).

Resting Metabolic Rate

Resting metabolic rate (RMR) is the metabolic rate during the point of lowest activity levels for each mouse over the 72-hour period in the metabolic cage. In $p75NTR^{+/+}$ mice, the RMR declined over diet and was significantly lower by day 12 on calorie restriction (Figure 3.5B). This decrease in RMR is likely to conserve energy. In contrast, mice deficient in $p75NTR$ had no change in RMR due to diet (Figure 3.5B). The

elevated RMR after calorie restriction in $p75NTR^{-/-}$ mice could be due to higher overall activity levels, since RMR is measured at the point of lowest activity.

The increased activity, heat production, and RMR reflect the inability of $p75NTR^{-/-}$ mice to compensate for the low energy state associated with calorie restriction. These changes also reflect a phenotype of a mouse that would lose more weight on calorie restriction, which is the opposite case for $p75NTR^{-/-}$ mice. We hope to analyze other metabolic pathways as well as the cell autonomous role of p75NTR.

Calorie Restriction produces intermittent fasting-like changes in RER

The respiratory exchange ratio (RER) typically fluctuates between 1.0 in the dark cycle and 0.8 light cycle, representing the use of carbohydrates (RER 1.0) as an energy source during the dark phase and lipids (RER 0.7) during the light phase. Indeed, in mice fed ad libitum, phasic RER was observed (Figure 3.6A). During this model of calorie restriction, mice consumed their food rapidly at the start of dark cycle and therefore were fasting for upwards of 18 hours before their next meal. This intermittent fasting is reflected in changes of the RER. On day 1 of calorie restriction, both $p75NTR^{+/+}$ and $p75NTR^{-/-}$ mice showed a reduction of RER before the start of the light cycle (Figure 3.6B). Once the RER declined to 0.8, it remained level throughout the entire light cycle, which indicates use of non-carbohydrate energy reserves such as lipids and some proteins. Upon feeding, both $p75NTR^{+/+}$ and $p75NTR^{-/-}$ had sharp increases of RER to 1.0, reflecting the switch to carbohydrates from the food as the energy source (Figure 3.6B, C). By CR10, $p75NTR^{+/+}$ mice no longer reduced RER to 0.8 before the start of the light cycle (Figure 3.6C). This suggests $p75NTR^{+/+}$ mice were capable of restricting the use of

carbohydrates from food over time. On CR10, $p75NTR^{-/-}$ mice had significantly reduced RER during the light cycle (Figure 3.6C, D). Therefore, $p75NTR^{-/-}$ mice were relying on lipids as fuel. Since RER is a ratio of oxygen consumption and CO₂ production, we analyzed those during calorie restriction day 10, when the RER was significantly different between genotypes. There were no significant differences between genotypes in oxygen consumption or carbon dioxide production when measured over a twelve hour period. (Figure 3.6E, F, and data not shown).

p75NTR expression in the sympathetic nervous system is necessary for reduction in adipose mass following calorie restriction

p75NTR is expressed in many metabolically active tissues (adipose, skeletal muscle, liver) as well as in neuronal tissues that regulate metabolism (hypothalamus, SNS). When placed on calorie restriction, $p75NTR^{-/-}$ mice are resistant to adipose mass loss, despite increased activity, heat production, and metabolic rate. Since p75NTR is known to have diverse and opposing roles in different tissues, it will be important to dissect the cell autonomous roles of p75NTR. We started with p75NTR expression in sympathetic neurons.

Conditional knockouts were made with p75NTR flox mice crossed to the tyrosine hydroxylase cre ($p75^{(fl/fl)}; THCre^{(+/cre)}$). Mice deficient in p75NTR specifically in the SNS were placed on 75% calorie restriction for 12 days. $p75^{(fl/fl)}; THCre^{(+/cre)}$ mice lost less total body weight compared to the littermate controls, $p75^{(fl/fl)}; THCre^{(+/+)}$, despite the same starting body weight and food intake (Figure 3.7A-C). At the end of the 12 day calorie restriction, $p75^{(fl/fl)}; THCre^{(+/cre)}$ mice were left with increased total dissected

adipose mass, gonadal adipose mass, and subcutaneous adipose mass (Figure 3.7D-F). The $p75^{(fl/fl)}$; $THCre^{(+/cre)}$ mice replicate the weight loss phenotype seen in the whole body $p75NTR^{-/-}$ mice. The role of p75NTR within sympathetic nerves is necessary for the adipose mass loss following calorie restriction. In $p75NTR^{-/-}$ mice, the sympathetic drive was reduced and synapses at the ganglia were increased. We expect this data to be replicated in the $p75^{(fl/fl)}$; $THCre^{(+/cre)}$ mice.

p75NTR expression in sympathetic nervous system does not alter activity levels following calorie restriction

p75NTR expression in the SNS was necessary for reduction in adipose mass after calorie restriction. Is p75NTR expression in the SNS responsible for the increases in activity after calorie restriction seen in whole body knockouts? The activity of $p75^{(fl/fl)}$; $THCre^{(+/cre)}$ and littermate was monitored by ambulatory beam breaks. Importantly, mice were in their natural cages with bedding, as opposed to the metabolic cages with wire bottoms. $p75^{(fl/fl)}$; $THCre^{(+/cre)}$ mice showed no changes in activity levels compared to littermate controls, $p75^{(fl/fl)}$; $THCre^{(+/+)}$, at CR1 or CR10 (Figure 3.8A, B). Furthermore, the meal anticipatory behavior was not significantly altered on at CR10 (Figure 3.8C). We conclude changes in activity surrounding feeding times are more likely a centrally mediated effect of p75.

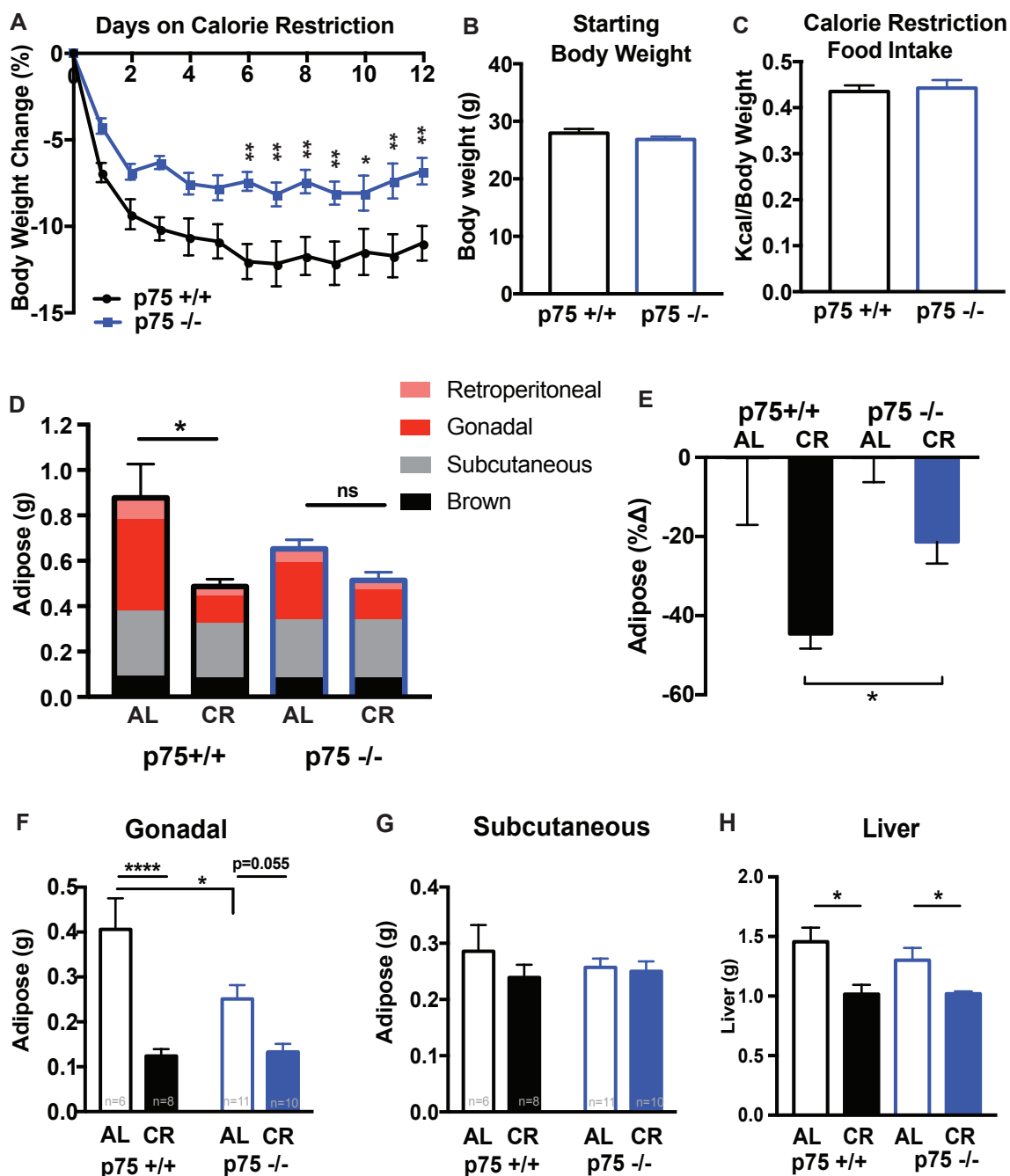


Figure 3.1 Mice deficient in p75 Neurotrophin Receptor are resistant to diet induced weight loss.

A. *p75NTR*^{-/-} mice and littermate controls were fed 75 percent of the average daily standard chow intake for 12 days. Mice were weighed daily and percent body weight change from starting body mass was calculated. Significant difference between groups on

days 6-12 of calorie restriction. Two way ANOVA, Tukey's multiple comparisons (n=8 WT, n=10 KO)

B. Starting body weight in grams of mice placed on calorie restriction. Students t-test. (n=8 $p75NTR^{+/+}$, n=10 $p75NTR^{-/-}$)

C. Daily food given on calorie restriction in kcal per starting body weight in grams. Students t-test. (n=8 $p75NTR^{+/+}$, n=10 $p75NTR^{-/-}$)

D. Total adipose weight of dissected adipose depots for *ad libitum* fed or 12 days of calorie restricted mice. The contribution of individual depots to the total dissected adipose mass is shown. Pink=Retroperitoneal, Red= Gonadal, Gray=Subcutaneous, and Black= Intrascapular brown.

E. Percent change in total dissected adipose compared to *ad libitum*.

F. Dissected gonadal adipose mass for *ad libitum* fed or 12 days of calorie restriction.

G. Dissected subcutaneous adipose mass for *ad libitum* fed or 12 days of calorie restriction.

H. Dissected liver mass for *ad libitum* fed or 12 days of calorie restriction.

Statistical analysis of two way ANOVA and Tukey's multiple comparisons unless stated otherwise (n=6 $p75NTR^{+/+}$ AL, n=8 $p75NTR^{+/+}$ CR, n=11 $p75NTR^{-/-}$ AL, n=10 $p75NTR^{-/-}$

CR). *p<0.05, **p<0.01, ***p<0.001, ****p<0.0001

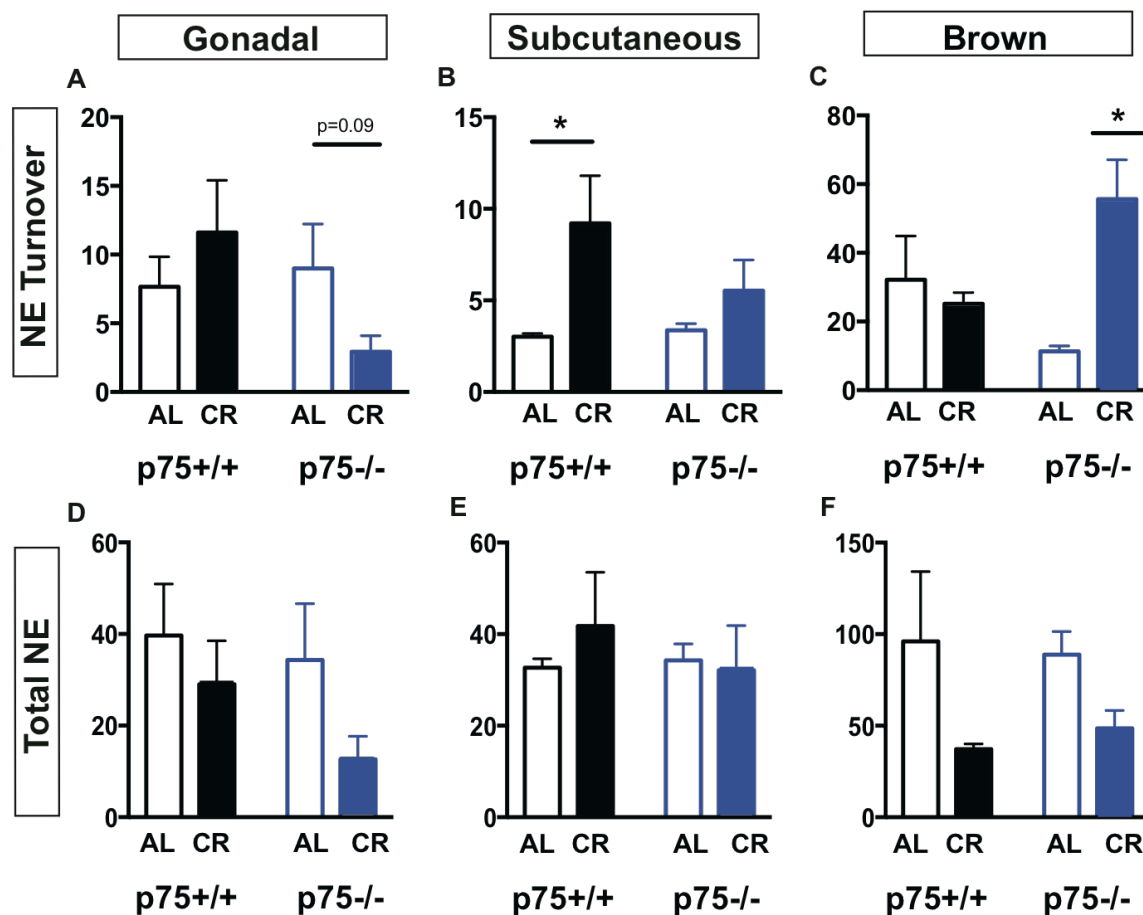


Figure 3.2 Sympathetic drive to adipose tissue is reduced in p75NTR deficient mice

A-C Norepinephrine turnover in gonadal (A), subcutaneous (B) or brown (C) adipose tissue in *ad libitum* (AL) or after 12 days of calorie restriction (CR)

D-F Total NE (ng) per adipose depot in gonadal (D), subcutaneous (E) or brown (F) adipose tissue in *ad libitum* (AL) or after 12 days of calorie restriction (CR)

Statistical analysis of two way ANOVA and Tukey's multiple comparisons unless stated otherwise, n=4, data plotted as mean \pm SEM, *p<0.05

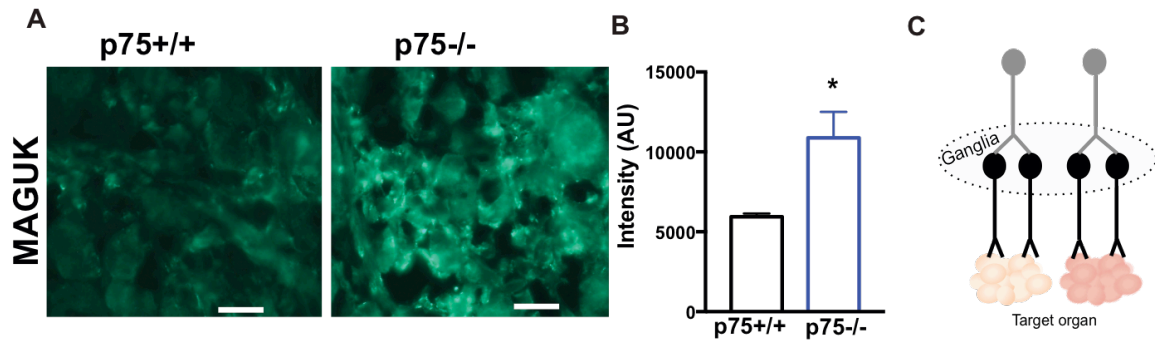


Figure 3.3 Mice deficient in p75NTR have increased postsynaptic markers

A. Immunostaining of MAGUK, marker of post-synaptic specializations, in the superior cervical sympathetic ganglia from $p75NTR^{+/+}$ or $p75NTR^{-/-}$ adult mice fed *ad libitum*.

Scale bar 20um

B. Quantification of MAGUK intensity in image j, students t-test n=3

C. Schematic of the sympathetic nervous system innervating the target adipose organ.

Preganglionic neurons (gray) synapse at the ganglia onto postganglionic neurons (black), which innervate the target adipose organ. MAGUK staining at the ganglia measures synapses on the postganglionic neuron.

n=3, data plotted as mean \pm SEM, * $p < 0.05$

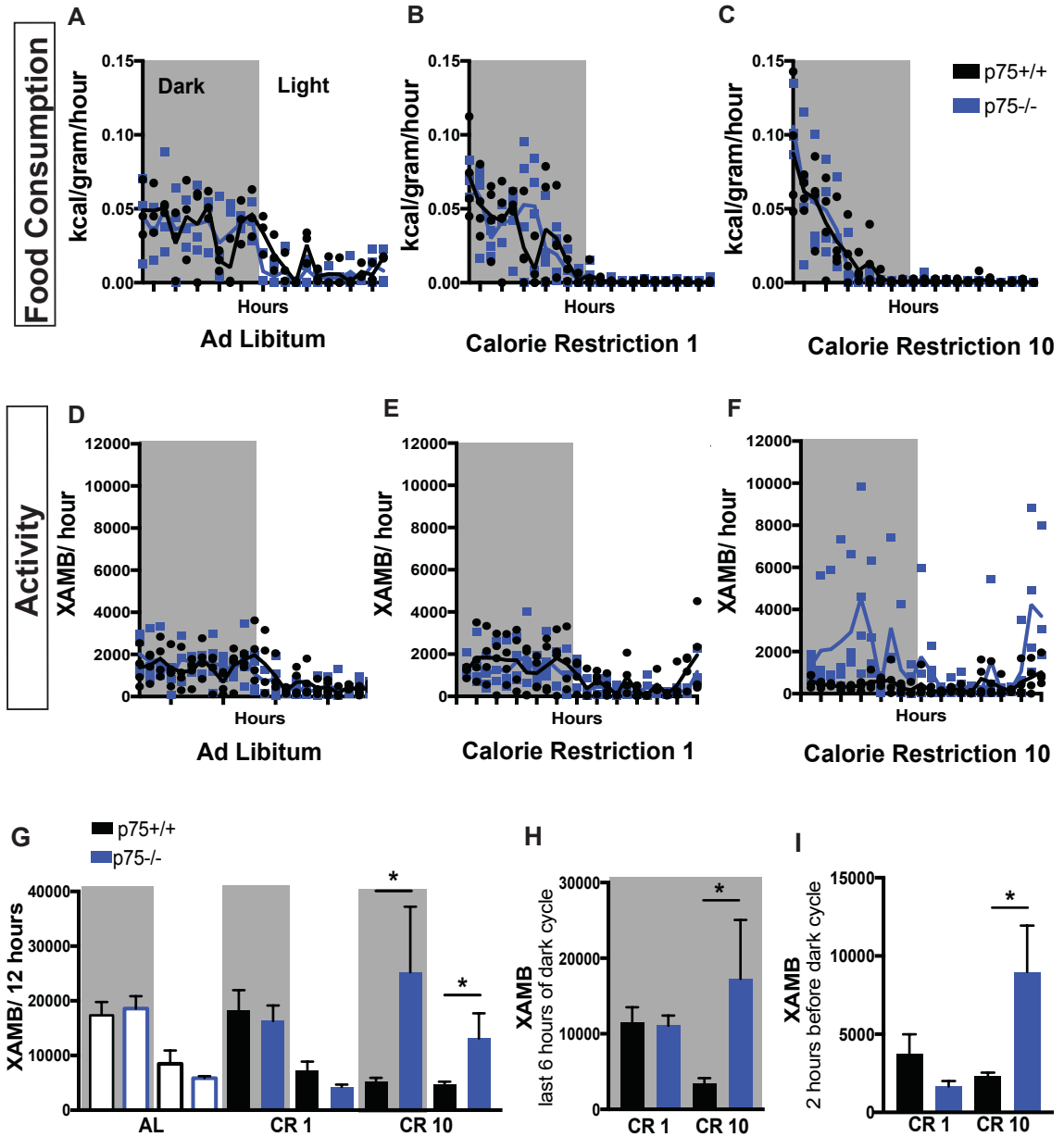


Figure 3.4 Food consumption and activity levels in $p75NTR^{+/+}$ and $p75NTR^{-/-}$ mice following calorie restriction

A-C. Food consumed per hour, measured in grams, represented as kcal per grams body weight during *ad libitum* (A), calorie restriction day one (B) and calorie restriction day 10 (C). Gray background represents dark cycle, and clear background represents light cycle.

D-F. Ambulatory activity count (XAMB) per hour, measured by beak breaks, during *ad libitum* (D), calorie restriction day one (E) and calorie restriction day 10 (F)

G. Total Ambulatory activity count per 12 hours during cycle *ad libitum* (AL), calorie restriction day one (CR1) and calorie restriction day 10 (CR10), gray stripes indicate dark cycle

H. Total ambulatory activity count in the last 6 hours of the dark cycle *ad libitum* (AL), calorie restriction day one (CR1) and calorie restriction day 10 (CR10).

I. Total ambulatory activity count in the 2 hours before the dark cycle during calorie restriction day one (CR1) and calorie restriction day 10 (CR10).

A-F individual data points traces fitted to mean, G-I data plotted as mean \pm SEM, Statistical analysis of One way ANOVA with Tukey's multiple comparisons. N=4.

*p<0.05

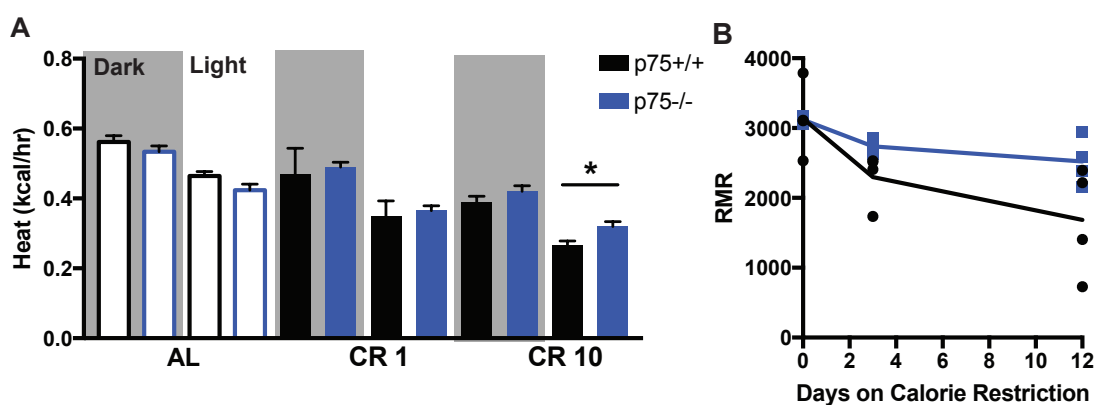


Figure 3.5 Mice deficient in p75NTR do not decrease heat production or resting metabolic rate during calorie restriction

A. Average heat (kcal/hr), measured by $\dot{V}O_2$ and $\dot{V}CO_2$ levels, over 12 hour dark (gray stripes) or light cycle (solid bar) during cycle *ad libitum* (AL), calorie restriction day one (CR1) and calorie restriction day 10 (CR10). Data plotted as mean \pm SEM

B. Resting metabolic rate, measured by $\dot{V}O_2$, at the lowest points of activity during the 72 hour metabolic cage run. Data plotted as individual data points

N=4 Statistical analysis of One way ANOVA with Tukey's multiple comparisons.

* $p < 0.05$

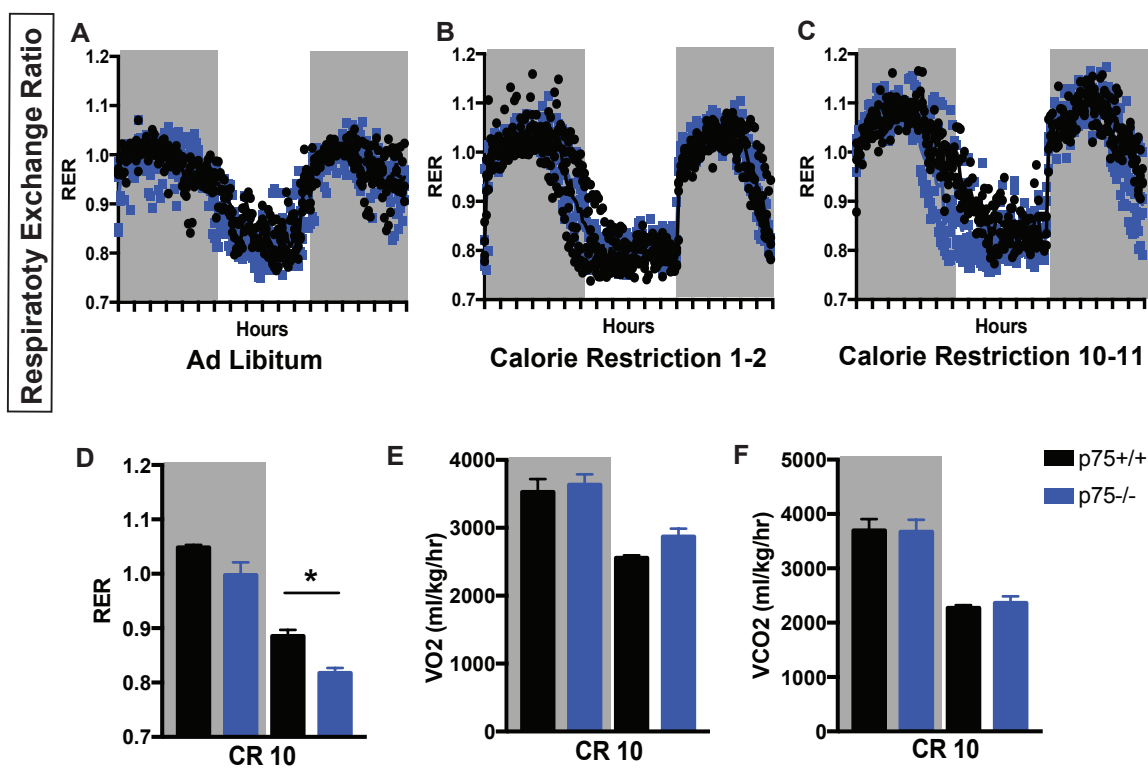


Figure 3.6 Calorie Restriction produces intermittent fasting-like changes in RER

A-C Respiratory exchange ratios (RER), measured by $\dot{V}CO_2/\dot{V}O_2$, every 15 minutes over 36 hours, during *ad libitum* (A), calorie restriction day one and two (B) and calorie

restriction day 10 and 11 (C). Gray background represents dark cycle, and clear background represents light cycle.

D. Average RER over 12 hours during calorie restriction day 10 and 11, gray stripes represent dark cycle

E. Average Oxygen consumption (VO_2) over 12 hours during calorie restriction day 10, gray stripes represent dark cycle

F. Average Carbon dioxide production ($VC O_2$) over 12 hours during calorie restriction day 10, gray stripes represent dark cycle

N=4, A-C Data represented as individual mice, D-F data represented as mean \pm SEM, Statistical analysis of One way ANOVA with Tukey's multiple comparisons.

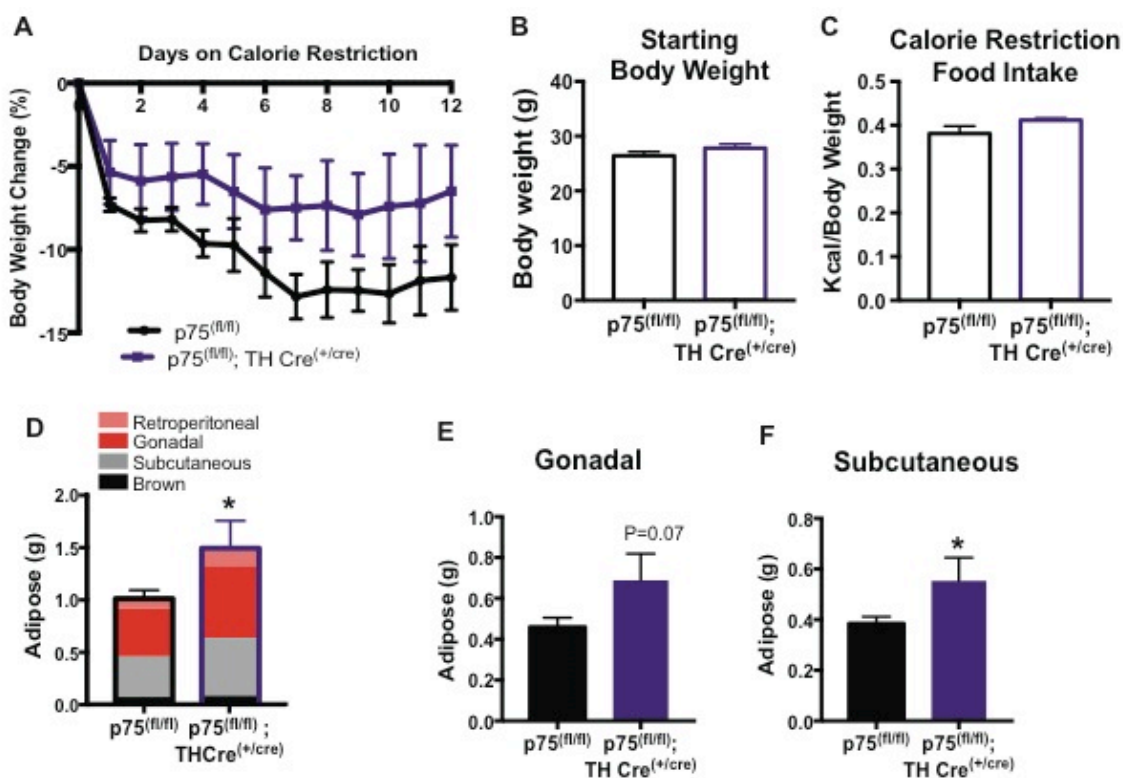


Figure 3.7 p75NTR expression in the sympathetic nervous system is necessary for reduction in adipose mass following calorie restriction

A. $p75^{(fl/fl)};THCre^{(+/-cre)}$ mice and littermate controls were fed 75 percent of the average daily standard chow intake for 12 days. Mice were weighed daily and percent body weight change from starting body mass was calculated. Two way ANOVA, Tukey's multiple comparisons ($n=5$ $p75^{(fl/fl)};THCre^{(+/+)}$ $n=3$ $p75^{(fl/fl)};THCre^{(+/-cre)}$)

B. Starting body weight in grams of mice placed on calorie restriction.

C. Daily food given on calorie restriction in kcal per starting body weight in grams.

D. Total adipose weight of dissected adipose depots for *ad libitum* fed or 12 days of calorie restricted mice. The contribution of individual depots to the total dissected adipose mass is shown. Pink=Retroperitoneal, Red=Gonadal, Gray=Subcutaneous, and Black= Intrascapular brown.

E. Dissected gonadal adipose mass for *ad libitum* fed or 12 days of calorie restriction.

F. Dissected subcutaneous adipose mass for *ad libitum* fed or 12 days of calorie restriction.

G. Statistical analysis of student's t-test unless stated otherwise * $p < 0.05$, ($n = 5$ $p75^{(fl/fl)}$; $THCre^{(+/+)}$ $n = 3$ $p75^{(fl/fl)}$; $THCre^{(+/-cre)}$)

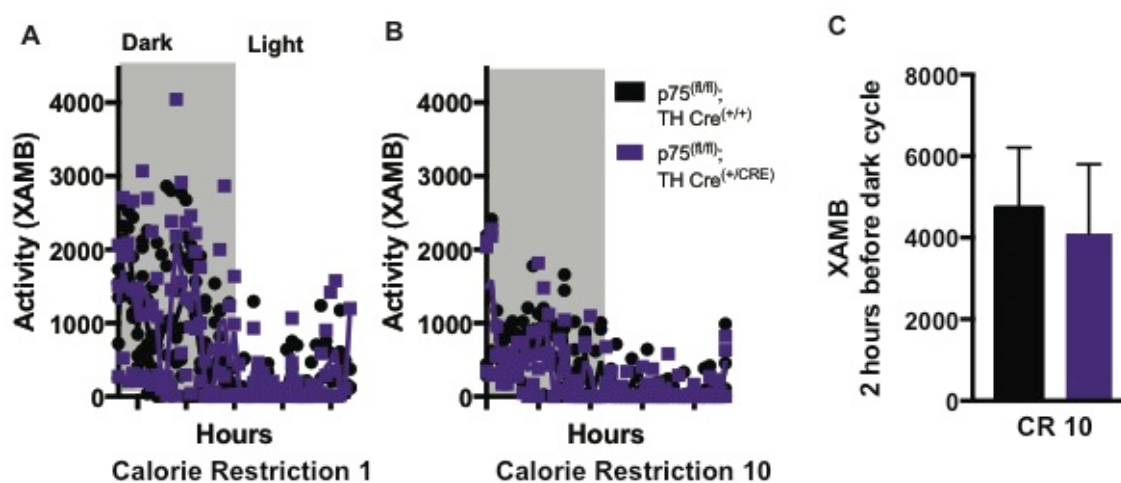


Figure 3.8 $p75$ expression in sympathetic nervous system does not alter activity levels following calorie restriction

A-B Ambulatory activity count (XAMB) per hour, measured by beak breaks, during calorie restriction day one (A) and calorie restriction day 10 (B)

C. Total ambulatory activity count in the 2 hours before the dark cycle during calorie restriction day 10. Student's t-test.

H. A-B data represented as individual data points, C data plotted as mean \pm SEM, $N = 4$. * $p < 0.05$. ($n = 5$ $p75^{(fl/fl)}$; $THCre^{(+/+)}$ $n = 3$ $p75^{(fl/fl)}$; $THCre^{(+/-cre)}$)

DISCUSSION

We established that differential sympathetic drive to adipose tissue is essential for reduction of adipose mass during calorie restriction. How does altered development of sympathetic drive change adipose utilization on calorie restriction? Through using the p75NTR knockout mouse, we hypothesized the disrupted development of the SNS would lead to disrupted function and ultimately impaired regulation of energy homeostasis as an adult. In addition to changes in the SNS to impact energy homeostasis, mice deficient in p75NTR could have impacts on many metabolically active tissues (adipose, skeletal muscle, liver) as well as in neuronal tissues that regulate metabolism (hypothalamus) due to the broad expression and function of p75NTR. With this in mind, we aimed to determine the role of p75NTR in energy homeostasis specifically during the energy deficient state of calorie restriction. We focused on the differential sympathetic activity to adipose tissue throughout calorie restriction due to the role of p75NTR in sympathetic development and synapse formation. Overall, we found that p75NTR is essential for adipose loss in response to calorie restriction. We begin to elucidate the cell autonomous role of p75NTR in the SNS and cement the importance of differential sympathetic activity to adipose tissue throughout calorie restriction.

Mice deficient in p75NTR are resistant to body weight loss following calorie restriction, independent of changes in starting body weight or food intake (Figure 3.1). *p75NTR*^{-/-} mice lose significantly less visceral adipose mass following calorie restriction compared to the littermate controls (Figure 3.1). We have previously shown sympathetic drive to adipose tissue is necessary for adipose loss in response to calorie restriction

(Figure 2.4). In $p75NTR^{-/-}$ mice, sympathetic drive is reduced after 12 days of calorie restriction (Figure 3.2). We hypothesize the reduction in sympathetic drive is the mechanism for losing less weight on calorie restriction. In line, the conditional knockout of p75NTR in SNS replicated the total knockout phenotype of losing less adipose mass after calorie restriction (Figure 3.6). One possible mechanism for the reduction in sympathetic drive in p75NTR deficient mice is the increase of synapses at the sympathetic ganglia (Figure 3.2). We hypothesize the increase in synapses could lead to diffused preganglionic signal and incorrect target matching; both would impair differential sympathetic drive.

When mice and humans undergo caloric restriction, they undergo compensatory changes in energy expenditure. This is the body's natural mechanism to maintain energy homeostasis (Faulks et al., 2006; Rosenbaum and Leibel, 2014). Some of the ways to conserve energy are to decrease activity levels, heat production, and RMR, which was observed in $p75NTR^{+/+}$ mice. In contrast, $p75NTR^{-/-}$ mice displayed increased activity, heat production, and RMR, which in sum increase energy expenditure (Figure 3.3 and Figure 3.4). Based on the conservation of energy, mice with increased energy expenditure should display a phenotype of increased weight loss, the opposite phenotype seen in $p75NTR^{-/-}$ mice (Vaanholt et al., 2015).

Moving forward, I am interested in exploring the following avenues to further analyze the conflicting $p75NTR^{-/-}$ phenotypes (1) the reduction of sympathetic drive to white adipose (2) the opposing and diverse cell autonomous roles of p75NTR and (3) the absorption and metabolism of calories.

Reduction of sympathetic drive to white adipose tissue

As mentioned, we established the sympathetic drive as facilitator of adipose loss during calorie restriction. In $p75NTR^{-/-}$ mice, sympathetic drive to white adipose does not increase after 12 days of calorie restriction. This is a relatively modest change in sympathetic drive, therefore more evidence is needed to confirm that changes in sympathetic drive are necessary for the resistance to weight loss seen in $p75NTR^{-/-}$ mice. First, it is important to examine the sympathetic drive during early weight loss when we established it is increased to gonadal adipose depots (Figure 2.2A). Since the gonadal adipose tissue is the only adipose depot to reduce in volume in $p75NTR^{+/+}$ or $p75NTR^{-/-}$ mice, it will be important to analyze sympathetic drive during the relevant time on diet. Next, it is imperative to determine if reductions in sympathetic drive led to functional consequences in NE signaling that control energy expenditure. NE signals to white adipose to promote lipolysis, therefore reductions in serum glycerol levels and phosphorylation of HSL are expected. Finally, if reduced sympathetic drive is the mechanism behind the phenotype of $p75NTR^{-/-}$ mice resistance to weight loss, then increasing sympathetic drive would rescue the phenotype. Sympathetic drive can be rescued pharmacologically, with β_3 -AR agonists, and genetically, with expression of p75NTR specifically in sympathetic nerves. The genetic rescue will be a novel model, where p75NTR is overexpressed in a cre-dependent manner on a background of $p75NTR^{-/-}$ mice. If p75NTR is solely expressed in sympathetic nerves, and the sympathetic drive is the dominant regulator of adipose mass loss, then we would expect a phenotype of normal adipose mass loss in response to calorie restriction.

Diverse cell autonomous roles of p75NTR

p75NTR is known to have diverse and sometimes opposing roles in varying organ systems (Gentry et al., 2004; Lee et al., 1992, 1994). A way to explain the various phenotypes is through the opposing roles of p75NTR in different organ systems. While we have focused on the role of p75NTR in SNS to regulate energy homeostasis, we must also discuss the contributions of p75NTR in adipocytes and the CNS. First, p75NTR functions specifically within adipocytes to increase in energy expenditure and oxygen consumption. Bernat and colleagues determined p75NTR directly binds to the regulatory and catalytic subunits of PKA, to inhibit PKA signaling. In the absence of inhibition by p75NTR, active PKA leads to an increase in lipolysis, fat oxidation, and UCP-1 expression (Bernat et al., 2016). The function of p75NTR within adipocytes increases energy expenditure, which could explain the changes in metabolic rate and heat production in *p75NTR^{-/-}* mice during calorie restriction. In addition, this role of p75NTR within adipocytes might explain why *p75NTR^{-/-}* mice have decreased gonadal adipose mass in *ad libitum* fed conditions. It will be important to analyze the conditional knockout of p75NTR in adipocytes. We hypothesize these mice will have increased energy expenditure during calorie restriction, which could lead to increased weight loss.

p75NTR is expressed throughout the CNS. Our collaborator, Sung Ok Yoon, recently established p75NTR expression in the hypothalamus, a key area for regulation of energy homeostasis (unpublished data). We hypothesize the changes in activity surrounding changes in food availability are due to p75NTR function in the CNS. p75NTR deficient mice were previously shown to have increased activity levels when

circadian rhythmicity was disrupted (Baeza-Raja et al., 2013). Interestingly, $p75NTR^{-/-}$ mice had increased activity levels 2 hours prior to feeding, similar to food anticipatory activity. Dopamine is a key signal that integrates circadian rhythm and food intake to create food anticipatory behavior. Inhibition of dopamine receptors pharmacologically or genetically reduces food anticipatory behavior (Liu et al., 2012). In the $p75^{(fl/fl)};THCre^{(+/-cre)}$ mice, p75NTR would also be deleted from dopamine synthesizing neurons. However, we did not see increases in food anticipatory activity in $p75^{(fl/fl)};THCre^{(+/-cre)}$ (Figure 3.8). Therefore, I hypothesize that p75NTR functions in dopamine receptor expressing neurons, rather than dopamine synthesizing neurons. Perhaps p75NTR interacts with the dopamine receptor specifically to exert changes in food anticipation behaviors.

Absorption and metabolism of calories

While the interesting phenotypes could be explained by the opposing roles of p75NTR within different tissues, the fact remains that $p75NTR^{-/-}$ are resistant to diet induced weight loss while displaying increased activity and metabolic rate. The $p75NTR^{-/-}$ mice perplexingly increased energy expenditure, through increased ambulatory activity, heat production, and resting metabolic rate. One possible explanation for the phenotype, is $p75NTR^{-/-}$ mice are capable of absorbing greater amounts of calories from the food. To measure this, we will use fecal bomb calorimetry and analyze the calories excreted (Yang and Van Itallie, 1976). The expression of p75NTR in intestinal cells or the function of p75NTR as a regulator of the microbiome is currently unknown.

In conclusion, p75NTR functions in multiple ways and in multiple organ systems to regulate energy homeostasis. I outlined several ways the p75NTR functions in energy homeostasis to impact weight loss on calorie restriction. *p75NTR^{-/-}* mice are resistant to diet induced weight loss while displaying increased activity and metabolic rate. Our best explanation of this phenotype is the role of p75NTR in governing sympathetic activity toward white adipose tissue. The diverse roles of p75NTR in energy expenditure open up a new understanding of metabolic health and the regulation of energy expenditure.

Chapter 4. Discussion and Future Directions

We determined the dynamics of the SNS activity toward visceral, subcutaneous, and brown adipose tissue across diet. Our findings suggest that the SNS preferentially activates adipose depots, which is a novel mechanism explaining adipose loss in response to diet. Next, we determined that disruption in the sympathetic drive to adipose tissue in mice deficient in p75NTR led to reduced weight loss in response to calorie restriction. We established that differential sympathetic drive is essential for adipose loss from calorie restriction. Our future work will address how differential sympathetic drive to adipose tissue is regulated, which will lead to advances in metabolic health and a better understanding of energy homeostasis.

The sympathetic drive to adipose depots is one distinguishing difference between adipose depots. Visceral adipose is more highly associated with metabolic risk factors such as cardiovascular disease, diabetes, metabolic syndrome, and non-alcoholic fatty liver disease (Fox et al., 2007). Luckily, weight loss in humans and mice promotes preferential loss in visceral adipose compared to subcutaneous adipose tissue (Doucet et al., 2002; Sipe et al., 2017). We established that sympathetic drive specifically to visceral adipose tissue in early stages of weight loss is the mechanism behind reduction of visceral adipose first (Sipe et al., 2017). If we could define how the discrete sympathetic drive to adipose depots is regulated we could put forth impactful therapeutic targets to treat obesity that mimics early weight loss or prolongs sympathetic activation to the pathological visceral adipose.

We were the first to show the sympathetic outflow in early calorie restriction was increased to the visceral gonadal adipose tissue. The sympathetic activity causes the gonadal adipose depot to be reduced to half of its original size by day 12, at which time, sympathetic outflow to gonadal adipose returns to normal, and the activity to subcutaneous adipose increases. This represents a switch in the body's lipolytic source once the gonadal adipose depot is depleted. The switch in sympathetic nerve activity to the subcutaneous depot is an important point of regulation for future studies.

The sensory nervous system could act as an important feedback mechanism, whereby axons respond to adipose mass, lipolysis breakdown products, lipid stores, or leptin levels to control adipose specific sympathetic circuits (Bartness et al., 2010b; Fishman and Dark, 1987; Jéquier, 2002; Mark et al., 2003; Murphy et al., 2013). A circuit whereby sensory afferents directly feedback onto sympathetic outflow is an attractive model for how adipose tissue may tune homeostatic energy liberation (Esler et al., 2006a). Indeed, points of sympathetic and sensory interaction have recently been identified for brown adipose tissue, such as the raphe pallidus nucleus, nucleus of the solitary tract, periaqueductal gray, hypothalamic paraventricular nucleus, and medial preoptic area (Ryu et al., 2015). Furthermore, after sensory nerve loss to one adipose depot, a compensatory increase in the mass of the remaining adipose depots occurs (Bartness et al., 2010b). This suggests that at least one of the functions of sensory innervation of white adipose tissue is to inform the brain of white adipose mass.

One indicator of adipose mass is the adipokine leptin, which is expressed proportionally to adipose mass and therefore could be the signal to the sensory nerves indicating adipose lipid stores. Indeed, the sensory nerves innervating adipose tissue

express leptin receptors and respond to leptin signals (Murphy et al., 2013). Based on this evidence, we suggest that leptin responsive sensory nerves feedback onto the SNS to inform the circuit of adipose stores. In our model of calorie restriction, after early loss in gonadal adipose mass the sensory nerves would register low leptin levels. This signal would relay to the CNS, where the switch of sympathetic drive to subcutaneous depot is implemented. To test this hypothesis, we are currently generating mice where the leptin receptor is conditionally knocked out in the sensory nervous system. When the leptin receptor is knocked out specifically in sensory nerves, the circuit would no longer be receiving information on the adipose mass and the sympathetic drive to gonadal adipose would go unchecked and remain elevated. Alternatively, the lack of leptin signaling would convey no adipose mass which would disrupt the differential sympathetic drive altogether. The sensory nerves, and specifically leptin signaling in the sensory nerves, are a potential regulator of differential sympathetic drive.

There is very little known about the subtypes or gene expression profile of the sensory neurons that innervate different adipose depots. An important future direction stemming from this work is to define the neuronal subtypes that innervate distinct adipose depots. Currently, the Deppmann, Zunder, and Liu labs are establishing mass cytometry technology at the University to proteomically identify neuronal populations. Mass cytometry is a single cell analysis tool that can identify over 40 markers in a single run. This is a novel application of mass cytometry and specific antibody panels will be established to examine sensory neurons or hypothalamic neurons. First, to identify sensory neurons innervating the adipose depots, the individual adipose depots will be injected with metal labeled retrograde tracers, which are detectable via mass cytometry

and will tag the neuron subtypes that innervate a particular fat pad. The sensory neurons will be collected at the dorsal root ganglia and dissociated into a single cell suspension. Currently, some information about the subtypes of sensory neurons innervating the adipose tissue is known, but much remains to be learned including adipose specific markers and signaling events. Canonical sensory markers such as TRPV1 and CGRP have been found in adipose depots (Bartness et al., 2010b). Receptors more relevant to adipose tissue, such as the leptin receptor, are of great interest for analysis in these mass cytometry experiments. Between sensory neurons innervating different adipose depots, I do not expect there to be great differences in the sensory subtypes or receptor expression, but there might be differences in level of receptor expression and the signaling events. A benefit to mass cytometry is the ability to analyze kinase signaling through phospho-specific antibodies. Signaling such as, the leptin receptor induction of phosphorylation of STAT3, can be different between adipose depots and also across diet. If we find distinct sensory neuron molecular profiles that vary based on innervated adipose depot, we could exploit them as calorie restriction mimetics for the treatment of obesity.

To determine the descending circuitry controlling sympathetic neurons that innervate the adipose depots, individual adipose depots will be injected with a retrograde tracer labeling the efferent neurons. Either the whole brain or specific region dissections will be dissociated into single cell suspension. The hypothalamus is a region of particular interest in these experiments due to its regulation of energy homeostasis and known roles in SNS activity to adipose tissue. Previous tracing studies found POMC positive neurons labeled with retrograde tracer injected into adipose depots and activation of POMC neurons induces SNS activity to brown and white adipose tissue (Dodd et al., 2015;

Stefanidis et al., 2014). The identification of POMC positive neurons in these tracing studies was done with traditional immunostaining, which is limited by the number of markers that can be analyzed. By employing mass cytometry, over 40 markers can be analyzed to accurately identify the hypothalamic neuronal types involved in the regulation of adipose tissue. This is especially important in the hypothalamus, which contains the highest diversity of neurons in the brain with over 60 distinct neuronal subtypes (Romanov et al., 2017). These experiments will open up interesting new pathways in the hypothalamic-adipose axis to control discrete sympathetic drive to adipose depots.

Differential sympathetic drive could be regulated through endocrine mechanisms. This may also be explained by an endocrine feedback loop where adipose derived signals travel through the bloodstream directly to the CNS or perhaps postganglionic neurons to regulate activity. When gonadal adipose tissue is devoid of lipids to fuel the body during the energy deficit the depot will not carry out lipolysis even if acted on by the SNS. The CNS may be responding to the reductions in free fatty acids in the serum and increasing drive to other depots to fulfill the lipolytic needs. Although a formal possibility, we do not favor the endocrine model because it is difficult to envision a mechanism whereby activity to particular depots is selectively regulated.

Another way to determine the regulation of differential sympathetic drive is to analyze additional variables whereby the differential drive would be altered. We defined the pattern of sympathetic activation during calorie restriction for non-obese male mice. It is possible the same pattern of sympathetic activity would not be observed in mice that are obese, or female, which represent important future directions. We can hypothesize

how the sympathetic drive during weight loss would be altered based on evidence of specific adipose depot loss in obese or female humans and mice. Obese male patients still lose visceral adipose tissue preferentially. During obesity, the sympathetic drive to the cardiovascular system is elevated, however drive to adipose has not been directly tested. Female patients, however, generally lose equal amounts of visceral and subcutaneous adipose mass during weight loss treatments. This indicates that sympathetic drive is activated to both visceral and subcutaneous adipose during early weight loss.

Following calorie restriction the C57BL6, $p75NTR^{+/+}$, and $p75NTR^{-/-}$ mice, the resulting gonadal adipose tissue reached the same final mass. This opened the question, is there a lower limit to the mass of gonadal adipose tissue? Does the sympathetic drive to gonadal adipose tissue stop because there are simply no lipid stores left? It will be important to perform histological analysis on the gonadal adipose tissue after calorie restriction. We will stain with oil-red-o to assay the level of lipid stores. Then, to ensure that reduction of mass is only due to loss of lipids and not the loss of adipocytes, we will stain for apoptotic markers. The lower limit of gonadal adipose mass could also add an alternative outlook on the reduced weight loss in $p75NTR^{-/-}$ mice. Since $p75NTR^{-/-}$ mice begin with less gonadal adipose mass, mice more quickly reach the lower limit of adipose tissue mass. This will be an important alternative perspective for future work on $p75NTR^{-/-}$ mice.

The differential sympathetic drive is likely established during the development of the SNS. In this dissertation, we analyzed $p75NTR^{-/-}$ mice that present with increased synapses at the sympathetic ganglia. The increase in synapses caused diffused preganglionic signaling, as evidenced by the reduced NE turnover. We currently

hypothesize that incorrect target matching is disrupting discrete sympathetic drive. To test this hypothesis, we will inject retrograde tracers into the individual adipose depots and analyze the innervating circuitry. Bartness and colleagues found individual adipose depots have distinct central circuitry. If target matching has been compromised during development in $p75NTR^{-/-}$, then the retrograde tracers would show increased overlap at the preganglionic level and in the central neurons between adipose depots (Figure 3.9).

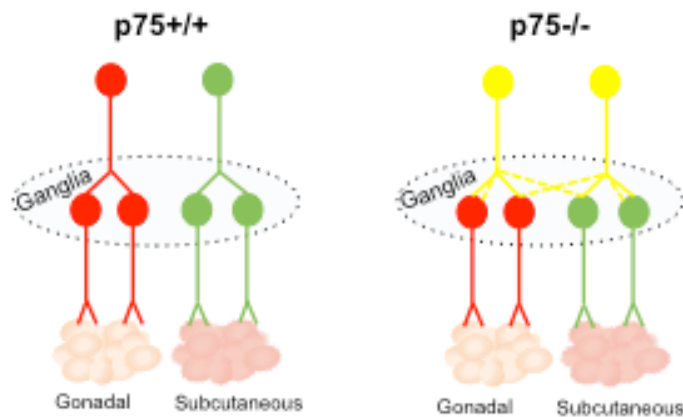


Figure 3.9

Schematic representation of the hypothesis that increased synapses at the sympathetic ganglia would lead to incorrect target matching. The gonadal and subcutaneous adipose depots will be injected with retrograde tracers (red or green), which will label preganglionic and central neurons. If $p75NTR^{-/-}$ mice display incorrect target matching, the retrograde tracers will have increased overlap (yellow) in projected regions.

An implication of this research is the diverse roles of p75NTR. Previously, *p75NTR*^{-/-} mice were shown to be resistant to diet-induced obesity (Bernat et al., 2016). p75NTR expression was increased in obesity and p75NTR directly interacted with PKA to inhibit energy expenditure. The roles of p75NTR within adipocytes to increase energy expenditure were established during obese conditions. If the role of p75NTR to decrease energy expenditure held true in calorie restriction conditions, we would expect *p75NTR*^{-/-} mice to lose more weight on calorie restriction. Instead, I hypothesize that the calorie restriction state engages the SNS, which makes p75NTR functions within the SNS the main contributor to energy homeostasis. Whereas during obesity, sympathetic activity to adipose tissue is generally decreased, unmasking the role of p75NTR function within adipocytes. Ultimately mice deficient in p75NTR are more confined in their energy homeostasis, implying that p75NTR acts as a novel energy homeostatic marker. Interestingly, the opposing roles of p75NTR indicate that the same things that prevent weight gain don't necessarily help with weight loss. This will be an important perspective for future research in the field of energy homeostasis.

Chapter 5. Materials and Methods

Mice and diets

All experiments were carried out in compliance with the Association for Assessment of Laboratory Animal Care policies and approved by the University of Virginia Animal Care and Use Committee (ACUC). The C57BL/6J (B6) mice were obtained from Jackson Laboratory (Bar Harbor, ME). Mice used in all studies were adult male mice between 12 and 16 weeks of age and weighed at least 25 grams. Mice were housed individually in a temperature-regulated room at 22°C and kept on a 12 hour light-dark cycle. Water was provided *ad libitum*.

The standard chow diet (8604 Teklad rodent diet) was provided to mice *ad libitum*. The daily food intake of mice on standard chow was measured for 4 days and an average food intake was calculated. Mice on calorie restriction were given 75 percent of their daily standard chow intake. Calorie Restricted mice were fed daily within one hour of the start of the dark cycle. Due to ACUC regulations, mice on calorie restriction were not permitted to lose more than 20 percent of their starting body weight. All tissue and serum harvests were performed within 2 hours of the dark cycle and before their daily allotment of food. Tissues were weighed immediately after dissection before being flash frozen in liquid nitrogen.

Norepinephrine turnover

Norepinephrine turnover (NETO) was measured using chemical inhibition of NE synthesis by alpha-methyl-p-tyrosine (AMPT) as described previously (Vaughan et al., 2014). The amount of NE in a tissue is a balance between production and degradation. NE is degraded rapidly after it is released into the synapse, therefore NE degradation is dependent and roughly equivalent to NE release (Axelrod, 1971). The total NE in adipose tissue before and after AMPT treatment was measured to obtain a rate of NE degradation independent of NE synthesis. The rate of NE degradation is multiplied by the total NE in the tissue as the final value of NETO (Brito et al., 2008a; Landsberg and Young, 1978; Vaughan et al., 2014). NETO is determined on a whole adipose depot basis to reflect the overall sympathetic drive and physiological impact for each tissue. The following two groups were used to determine the intra-animal decline of NE in tissues: (1) Mice not treated with AMPT and (2) mice treated with AMPT for four hours. AMPT was administered by intraperitoneal injection at time 0 hour (300 mg/kg, 20mg/ml) and at time 2 hours (150mg/kg, 20mg/ml). Adipose tissues were harvested and weighed four hours after injection. NE was extracted from the tissue using a protocol adapted from Bartness and colleagues (Vaughan et al. 2014). In brief, an entire adipose depot was minced in 0.2M perchloric acid and 3ug/ml Ascorbic acid. These samples were homogenized using the Bullet Blender (Next Advance, Averill Park, NY) and the supernatants were column filtered prior to analyzing via HPLC.

The HPLC system consisted of a Jasco model PU-2080*Plus* isocratic pump and AS-950 Intelligent Autosampler, (Jasco Inc., Easton, MD), an Antec

Leyden Decade electrochemical detector (Antec Leyden, The Netherlands), pH 4.5 mobile phase with 4 mM decyl sulphonic acid/17% Acetonitrile, as described(Hardie and Hirsh, 2006).

NETO was calculated by subtracting the NE content (ng NE/ tissue) from control group from the AMPT treated group, to determine the rate of NE decline. Calculations were made according to the following formula: $k = (\lg[NE]^0 - \lg[NE]^4)/(0.434 \times 4)$ and $K = k[NE]^0$, where k is the constant rate of NE efflux, $[NE]^0$ is the initial NE concentration, $[NE]^4$ is the final NE concentration, and $K=NETO$ (Vaughan et al., 2014).

Measurement of serum metabolites

Blood was collected post euthanasia and centrifuged for one hour 3,000 g at 4C. Serum was collected then assayed for glycerol using the free glycerol reagent (Sigma).

Antagonist administration

Mice were either fed *ad libitum* or placed on calorie restriction. Placebo mice were IP injected with saline. Treated mice were IP injected with 1mg/kg SR59230a (Sigma) diluted in saline prior to being fed within one hour before the start of the dark cycle(Bexis and Docherty, 2009; Mizuno et al., 2002).

Sections were produced from fresh frozen sympathetic ganglia tissue and cryosectioned at a thickness of 10um, Sections were fixed in 4%PFA, blocked in 5% normal goat serum, incubated in primary antibody (anti MAGUK, Antibodies Inc 75-029) overnight

at 4C, and incubated in Alexa-Fluor conjugated secondary antibody for one hour at room temperature. Tissue was mounted with Dapimount. Images were taken at 40X on the Zeiss Observer Z1. Intensity of MAGUK staining was analyzed with ImageJ.

Metabolic cages

Oxygen consumption ($\dot{V}O_2$), carbon dioxide production ($\dot{V}CO_2$), food intake, and ambulatory activity were determined in an Oxymax metabolic chamber system (Comprehensive Laboratory Animal Monitoring System from Columbus Instruments, Columbus, OH). Respiratory exchange ratios (RER) were calculated as the ratio of carbon dioxide production to oxygen consumption ($\dot{V}CO_2/\dot{V}O_2$). Heat production was calculated by Oxymax software using gas exchange data with the following formula: heat ($\text{kcal} \cdot \text{kg body wt}^{-1} \cdot \text{h}^{-1}$) = $(3.815 + 1.232 \times \text{RER}) \times \dot{V}O_2$ (Hargett et al., 2016).

Statistical Analysis

All statistical comparisons were performed using Prism 7 (GraphPad). Specific statistical tests are explicitly stated in the figure legends. All data are expressed as the mean \pm SEM.

Appendix 1. Differential sympathetic drive to adipose does not regulate energy storage

We established the role of the SNS activity to adipose tissue as a discrete regulator of adipose mass and lipolysis. We next wanted to ask, how the SNS regulates energy storage. We employed two dietary challenges, both high in dietary fats, to ascertain the role of sympathetic drive in increasing adipose mass. The ketogenic diet consists of high levels of fats with low levels of carbohydrates and is generally a weight loss diet. It is an extreme dietary challenge, as dietary carbohydrates are restrictive and the body must rely on lipids, ketones, and gluconeogenesis for metabolic fuel (Kennedy et al., 2007). The second diet, a high fat diet, is used for mouse models of obesity. This diet is high in lipids and carbohydrates and leads to excess caloric intake and obesity (Gajda, 2008). These two diets both lead to increases in adipose mass, however divergent changes in total body weight. By measuring NE turnover during these diets, we will determine if the changes in sympathetic drive are responsible for increases in adipose mass.

Table Ap1. Calorie distribution of standard chow, ketogenic, and high fat diets

	Chow	Ketogenic	High Fat Diet
Macronutrient (%)	Teklad	Bioserv F3666	Bioserv F4282
Protein	23.5	8.6	20.5
Carbohydrates	17	3.2	35.7
Fat	60	75.1	36.0
<i>Kcal/g</i>	3.3	7.456	5.49

Ketogenic Diet

Mice placed on ketogenic diet lost 2.23 ± 0.89 grams in the first day of diet. This is a remarkable drop in body weight amounting to 7.42 ± 2.38 percent of their starting body weight (Figure Ap1A). The ketogenic diet is calorically dense, at 7.24 kcal/gram, therefore while the mice are consuming greater number of calories in the first day on diet the diet consumed is 1.43 grams less (Figure Ap1B, C). The decrease in body weight after the first day can be attributed to the reduction in grams of food and likely glycogen associated water weight (Kennedy et al., 2007). The white adipose depots decrease in mass after three days on the ketogenic diet, but rebound to the original mass after twelve days on diet (Figure Ap1D, E, F). The brown adipose mass does not change in response to ketogenic diet (Figure Ap1G). Even though the ketogenic diet is a weight loss diet, the high fat content requires adipose tissue to continue as a storage unit. This is why we do not see persistent reductions in adipose mass. The sympathetic nervous system responds to the early reduction in body weight and increases drive to the gonadal adipose tissue at day three (Figure Ap1I). This initial increase in NE turnover to gonadal adipose mirrors the response to calorie restriction. It is possible the sympathetic drive to gonadal adipose is the first response to a reduction in energy balance regardless of dietary type. The high fat content of the ketogenic diet necessitates adipose tissue to behave as a storage unit and therefore we expect low sympathetic drive to facilitate lipid storage. Indeed, NE turnover to the subcutaneous, retroperitoneal, and brown adipose all decrease in response to ketogenic diet (Figure Ap1H, J,K)

Although short term ketogenic diets produce weight loss, after 12 days on the diet mice begin to regain weight (Figure Ap1L). Mice on long term ketogenic diets do not show a difference in body weight to age matched chow fed mice and have increased adipose mass, especially in the visceral adipose tissue (Jornayvaz et al., 2010). To test how the SNS regulated adipose mass and lipolysis during the ketogenic diet, we employed the β 3-AR agonist, CL316243 (Sigma). During the first 12 days of diet, mice treated daily with the β 3-AR agonist lost the same amount of weight as saline treated controls (Figure Ap1L). However, when the saline controls began to regain weight after prolonged ketogenic diet, mice treated with the β 3-AR agonist remained lean (Figure Ap1L). This could be due to the β 3-AR agonist preventing increases in adipose mass from a prolonged ketogenic diet. Standard chow fed mice treated with β 3-AR agonist had significant increases in lipolysis, measured by serum glycerol (Figure Ap1M). However, when mice are fed the ketogenic diet high in dietary lipids, the β 3-AR agonist no longer increases lipolysis (Figure Ap1M). After twelve days on the ketogenic diet, the serum glycerol levels were as high as those mice treated with the agonist, indicating the ketogenic diet produces saturating levels of serum lipids (Figure Ap1M).

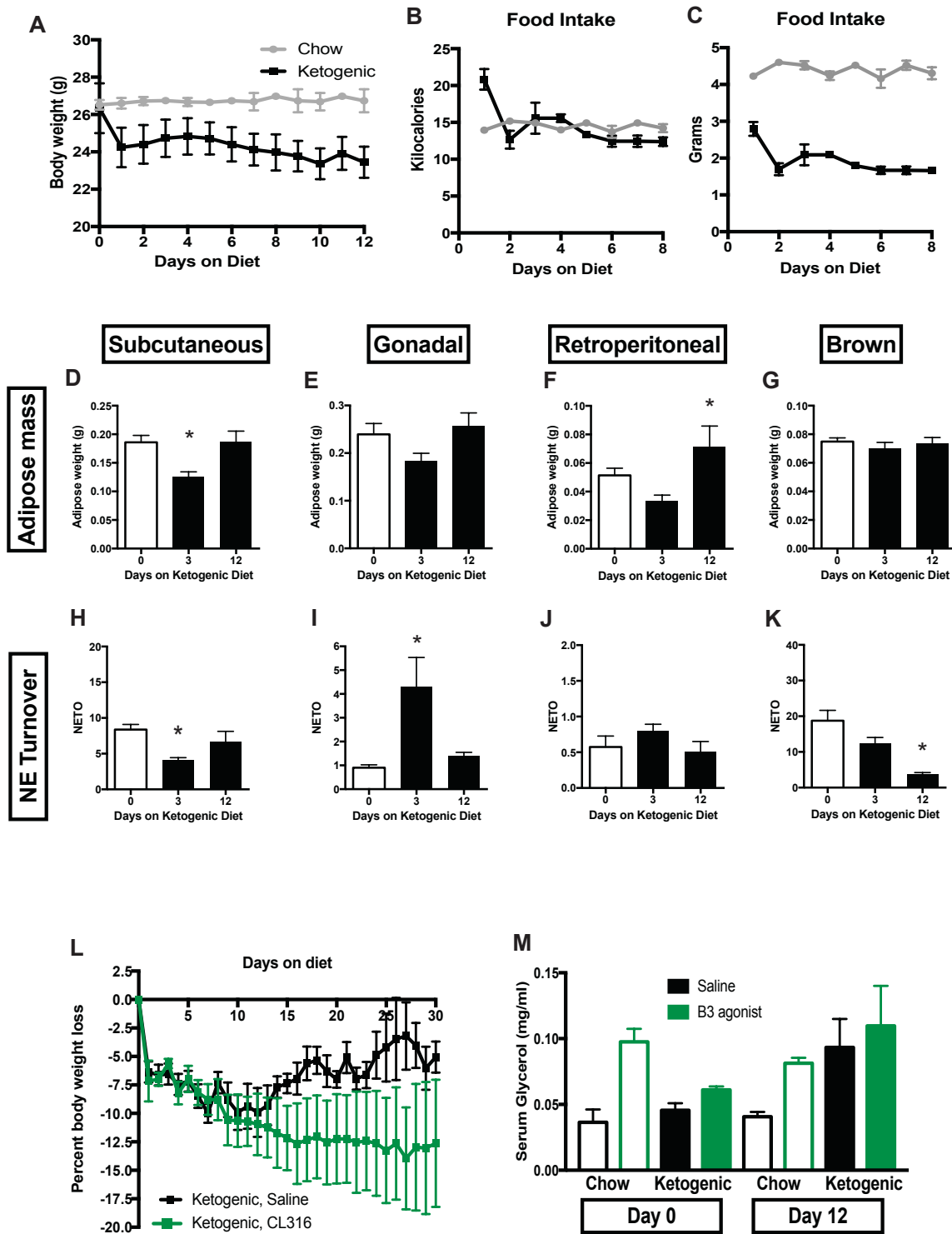


Figure Ap1 Ketogenic diet

A. C57BL/6 male mice at least 12 weeks of age and 25 grams were fed *ad libitum* with either standard chow or ketogenic diet. Mice were weighed daily.

B-C. Daily food intake of standard chow or ketogenic diet in kcal (B) or grams (C)

D-G. Dissected subcutaneous (D), gonadal (E), retroperitoneal (F), and brown (G) adipose mass after 0, 3, or 12 days of ketogenic diet

H-K. NE turnover in subcutaneous (H), gonadal (I), retroperitoneal (J), and brown (K) adipose depots after 0, 3, or 12 days of ketogenic diet

L. C57BL/6 male mice at least 12 weeks of age and 25 grams were fed ketogenic diet. Mice were injected IP daily with saline or CL316243 (1mg/kg) prior at the start of the dark cycle. Mice were weighed daily and percent body weight change from starting body mass was calculated.

M. Serum glycerol levels of mice fed standard chow or ketogenic diet injected IP with saline or CL316243 (1mg/kg)

One way ANOVA with Tukey's multiple comparisons Data shown as \pm SEM n=8

High Fat Diet

Mice on a high fat diet gained weight linearly, increasing by 1% body weight per day. We analyzed adipose mass and NE turnover after a 10% body weight gain (11 days on HFD) and after 20% body weight gain (19 days on HFD) (Figure Ap2A). During calorie restriction, the visceral adipose depots were lost preferentially due to targeted sympathetic drive (Sipe 2017). However when gaining weight from a high fat diet, all white adipose depots increased in mass at the same rate (Figure Ap2C, D, E). The brown

adipose mass did not significantly increase following a HFD (Figure Ap2F). Since sympathetic drive to adipose tissue signals lipolysis and results in decrease in adipose mass, we expect a decrease in sympathetic drive during weight gain. Indeed, the visceral adipose depots, gonadal and retroperitoneal, experienced decreased NE turnover. However NE turnover to the subcutaneous adipose was increased following 19 days on a HFD. This mis-match between sympathetic drive and adipose mass indicates the SNS is not controlling energy storage the same way as it controls energy liberation from adipose mass. Therefore, other mechanisms may regulate adipose mass during a high fat diet, while overall low sympathetic drive does not interfere. A likely mechanism is endocrine signaling, such as insulin, since all white adipose depots increase in adipose mass at the same rate. An endocrine mechanism would not be able to discern adipose depots in the same manner as the targeted sympathetic drive.

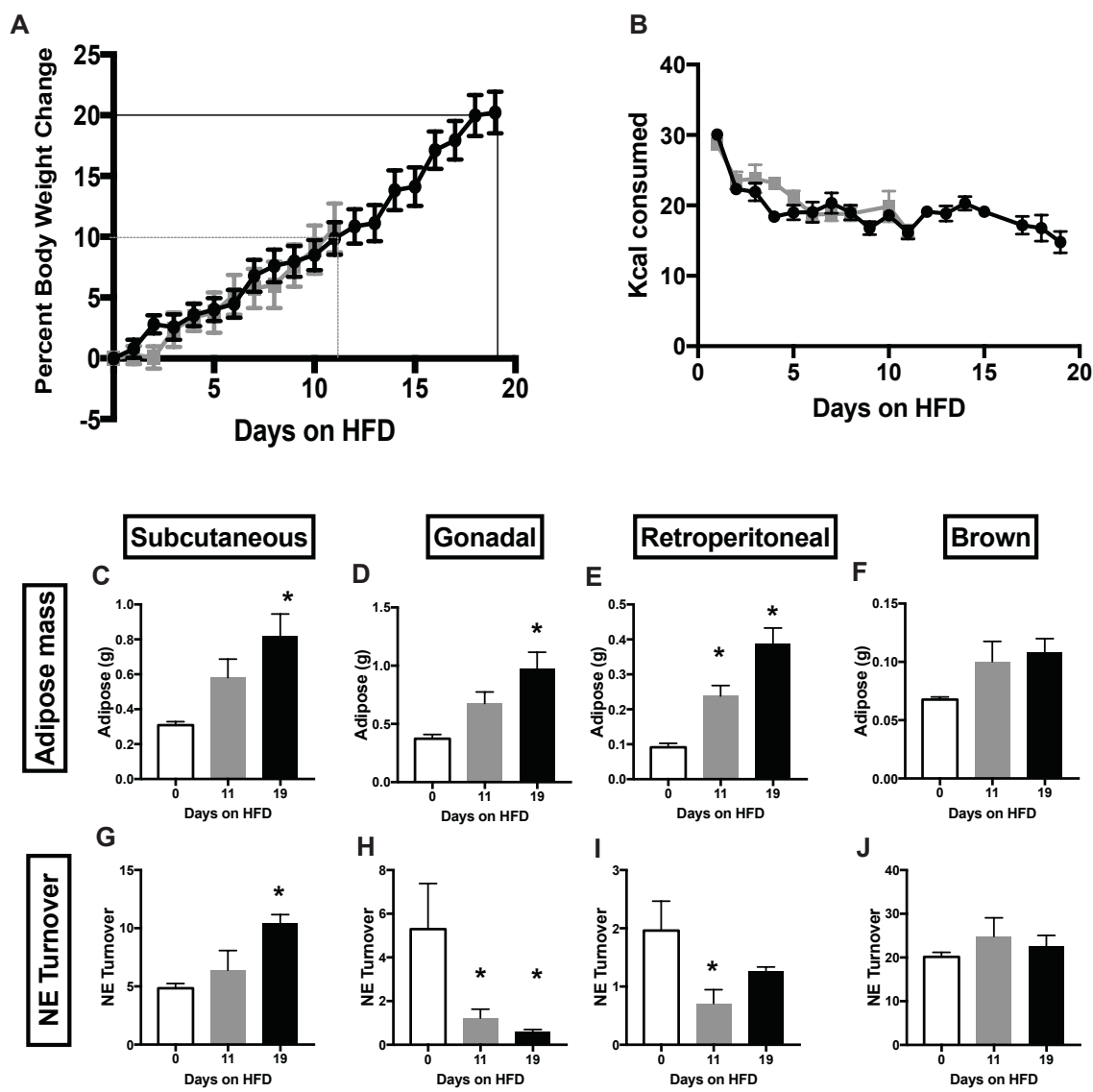


Figure Ap2. High Fat Diet

A. C57BL/6 male mice at least 12 weeks of age and 25 grams were fed *ad libitum* a high fat diet (HFD). Mice were weighed daily. Dotted boxes represents 10% body weight gain and 20% body weight gain.

B. Daily food intake of standard chow or ketogenic diet in kilocalories

C-F. Dissected subcutaneous (C), gonadal (D), retroperitoneal (E), and brown (F) adipose mass after 0, 11 or 19 days of high fat diet

G-J. NE turnover in subcutaneous (G), gonadal (H), retroperitoneal (I), and brown (J) adipose depots after 0, 3, or 12 days of high fat diet

One way ANOVA with Tukey's multiple comparisons Data shown as \pm SEM n=8

References

- Adler, E.S., Hollis, J.H., Clarke, I.J., Grattan, D.R., and Oldfield, B.J. (2012). Neurochemical Characterization and Sexual Dimorphism of Projections from the Brain to Abdominal and Subcutaneous White Adipose Tissue in the Rat. *J. Neurosci.* *32*, 15913–15921.
- Alvarez, G.E. (2002). Sympathetic Neural Activation in Visceral Obesity. *Circulation* *106*, 2533–2536.
- Alvarez, G.E., Ballard, T.P., Beske, S.D., and Davy, K.P. (2004). Subcutaneous obesity is not associated with sympathetic neural activation. *Am. J. Physiol. Heart Circ. Physiol.* *287*, H414-8.
- Arch, J.R., and Wilson, S. (1996). Prospects for beta 3-adrenoceptor agonists in the treatment of obesity and diabetes. *Int. J. Obes. Relat. Metab. Disord.* *20*, 191–199.
- Armitage, J.A., Burke, S.L., Prior, L.J., Barzel, B., Eikelis, N., Lim, K., and Head, G.A. (2012). Rapid onset of renal sympathetic nerve activation in rabbits fed a high-fat diet. *Hypertension* *60*, 163–171.
- Axelrod, J. (1971). Noradrenaline: Fate and Control of Its Biosynthesis. *Science* (80-). *173*, 598–606.
- van Baak, M.A. (2001). The peripheral sympathetic nervous system in human obesity. *Obes. Rev.* *2*, 3–14.
- Baeza-Raja, B., Li, P., Le Moan, N., Sachs, B.D., Schachtrup, C., Davalos, D., Vagena, E., Bridges, D., Kim, C., Saltiel, A.R., et al. (2012). p75 neurotrophin receptor regulates glucose homeostasis and insulin sensitivity. *Proc. Natl. Acad. Sci. U. S. A.* *109*, 5838–5843.

Baeza-Raja, B., Eckel-Mahan, K., Zhang, L., Vagena, E., Tsigelny, I.F., Sassone-Corsi, P., Ptáček, L.J., and Akassoglou, K. (2013). p75 neurotrophin receptor is a clock gene that regulates oscillatory components of circadian and metabolic networks. *J. Neurosci.* *33*, 10221–10234.

Bamji, S.X., Majdan, M., Pozniak, C.D., Belliveau, D.J., Aloyz, R., Kohn, J., Causing, C.G., and Miller, F.D. (1998). The p75 neurotrophin receptor mediates neuronal apoptosis and is essential for naturally occurring sympathetic neuron death. *J. Cell Biol.* *140*, 911–923.

Bamshad, M., Aoki, V.T., Adkison, M.G., Warren, W.S., and Bartness, T.J. (1998). Central nervous system origins of the sympathetic nervous system outflow to white adipose tissue. *Am J Physiol Regul. Integr. Comp Physiol* *275*, R291-299.

Barker, P.A. (2004). p75NTR Is Positively Promiscuous: Novel Partners and New Insights. *Neuron* *42*, 529–533.

Bartness, T.J., and Song, C.K. (2007). Thematic review series: adipocyte biology. Sympathetic and sensory innervation of white adipose tissue. *J. Lipid Res.* *48*, 1655–1672.

Bartness, T.J., Kay Song, C., Shi, H., Bowers, R.R., and Foster, M.T. (2005). Brain-adipose tissue cross talk. *Proc. Nutr. Soc.* *64*, 53–64.

Bartness, T.J., Vaughan, C.H., and Song, C.K. (2010a). Sympathetic and sensory innervation of brown adipose tissue. *Int. J. Obes. (Lond).* *34 Suppl 1*, S36-42.

Bartness, T.J., Shrestha, Y.B., Vaughan, C.H., Schwartz, G.J., and Song, C.K. (2010b). Sensory and sympathetic nervous system control of white adipose tissue lipolysis. *Mol. Cell. Endocrinol.* *318*, 34–43.

- Bartness, T.J., Liu, Y., Shrestha, Y.B., and Ryu, V. (2014). Neural innervation of white adipose tissue and the control of lipolysis. *Front. Neuroendocrinol.* *35*, 473–493.
- Bell-Anderson, K.S., and Bryson, J.M. (2004). Leptin as a potential treatment for obesity: progress to date. *Treat. Endocrinol.* *3*, 11–18.
- Benedict, C., Dodt, C., Hallschmid, M., Lepiorz, M., Fehm, H.L., Born, J., and Kern, W. (2005). Immediate but not long-term intranasal administration of insulin raises blood pressure in human beings. *Metabolism.* *54*, 1356–1361.
- Bernat, B.-R., Sachs, B.D., Li, P., Christian, F., Vagena, E., Davalos, D., Moan, N. Le, Ryu, J.K., Sikorski, S.L., Chan, J.P., et al. (2016). p75 neurotrophin receptor regulates energy balance in obesity. *Cell Rep.* *14*, 255–268.
- Bexis, S., and Docherty, J.R. (2009). Role of alpha 1- and beta 3-adrenoceptors in the modulation by SR59230A of the effects of MDMA on body temperature in the mouse. *Br. J. Pharmacol.* *158*, 259–266.
- BOUCHARD, C., DESPRÉS, J.-P., and MAURIÈGE, P. (1993). Genetic and Nongenetic Determinants of Regional Fat Distribution. *Endocr. Rev.* *14*, 72–93.
- Bowers, R.R., Festuccia, W.T.L., Song, C.K., Shi, H., Migliorini, R.H., and Bartness, T.J. (2004). Sympathetic innervation of white adipose tissue and its regulation of fat cell number. *Am. J. Physiol. Regul. Integr. Comp. Physiol.* *286*, R1167-75.
- Brito, N.A., Brito, M.N., and Bartness, T.J. (2008a). Differential sympathetic drive to adipose tissues after food deprivation, cold exposure or glucoprivation. *Am. J. Physiol. Regul. Integr. Comp. Physiol.* *294*, R1445-52.
- Brito, N. a, Brito, M.N., and Bartness, T.J. (2008b). Differential sympathetic drive to adipose tissues after food deprivation, cold exposure or glucoprivation. *Am. J. Physiol.*

Regul. Integr. Comp. Physiol. 294, R1445–R1452.

Brownstein, M., and Axelrod, J. (1974). Pineal gland: 24-hour rhythm in norepinephrine turnover. *Science* 184, 163–165.

Canello, R., Tordjman, J., Poitou, C., Guilhem, G., Bouillot, J.L., Hugol, D., Coussieu, C., Basdevant, A., Bar Hen, A., Bedossa, P., et al. (2006). Increased infiltration of macrophages in omental adipose tissue is associated with marked hepatic lesions in morbid human obesity. *Diabetes* 55, 1554–1561.

Catalano, K.J., Stefanovski, D., and Bergman, R.N. (2010). Critical role of the mesenteric depot versus other intra-abdominal adipose depots in the development of insulin resistance in young rats. *Diabetes* 59, 1416–1423.

De Champlain, J., Mueller, R.A., and Axelrod, J. (1969). Turnover and synthesis of norepinephrine in experimental hypertension in rats. *Circ. Res.* 25, 285–291.

Chaston, T.B., and Dixon, J.B. (2008a). Factors associated with percent change in visceral versus subcutaneous abdominal fat during weight loss: findings from a systematic review. *Int. J. Obes.* 32, 619–628.

Chaston, T.B., and Dixon, J.B. (2008b). Factors associated with percent change in visceral versus subcutaneous abdominal fat during weight loss: findings from a systematic review. *Int. J. Obes. (Lond).* 32, 619–628.

Cohen, P., Levy, J.D., Zhang, Y., Frontini, A., Kolodin, D.P., Svensson, K.J., Lo, J.C., Zeng, X., Ye, L., Khandekar, M.J., et al. (2014). Ablation of PRDM16 and Beige Adipose Causes Metabolic Dysfunction and a Subcutaneous to Visceral Fat Switch. *Cell* 156, 304–316.

Collins, S., Cao, W., and Robidoux, J. (2004). Learning new tricks from old dogs: beta-

adrenergic receptors teach new lessons on firing up adipose tissue metabolism. *Mol. Endocrinol.* *18*, 2123–2131.

Cooper, J.R., Bloom, F.E., and Roth, R.H. (2003). *The biochemical basis of neuropharmacology* (Oxford University Press).

Coppack, S.W., Horowitz, J.F., Paramore, D.S., Cryer, P.E., Royal, H.D., and Klein, S. (1998). Whole body, adipose tissue, and forearm norepinephrine kinetics in lean and obese women. *Am. J. Physiol.* *275*, E830-4.

Davy, K.P., and Orr, J.S. (2009). Sympathetic nervous system behavior in human obesity. *Neurosci. Biobehav. Rev.* *33*, 116–124.

Denny, C.A., Kasperzyk, J.L., Gorham, K.N., Bronson, R.T., and Seyfried, T.N. (2006). Influence of caloric restriction on motor behavior, longevity, and brain lipid composition in Sandhoff disease mice. *J. Neurosci. Res.* *83*, 1028–1038.

Deponti, D., Buono, R., Catanzaro, G., De Palma, C., Longhi, R., Meneveri, R., Bresolin, N., Bassi, M.T., Cossu, G., Clementi, E., et al. (2009). The low-affinity receptor for neurotrophins p75NTR plays a key role for satellite cell function in muscle repair acting via RhoA. *Mol. Biol. Cell* *20*, 3620–3627.

Deppmann, C.D., Mihalas, S., Sharma, N., Lonze, B.E., Niebur, E., and Ginty, D.D. (2008). A model for neuronal competition during development. *Science* *320*, 369–373.

Dodd, G.T., Decherf, S., Loh, K., Simonds, S.E., Wiede, F., Balland, E., Merry, T.L., Münzberg, H., Zhang, Z.-Y., Kahn, B.B., et al. (2015). Leptin and insulin act on POMC neurons to promote the browning of white fat. *Cell* *160*, 88–104.

Doucet, E., St-Pierre, S., Alméras, N., Imbeault, P., Mauriège, P., Pascot, A., Després, J.-P., and Tremblay, A. (2002). Reduction of visceral adipose tissue during weight loss. *Eur.*

J. Clin. Nutr. 56, 297–304.

Eisenhofer, G., Kopin, I.J., and Goldstein, D.S. (2004). Catecholamine Metabolism: A Contemporary View with Implications for Physiology and Medicine. *Pharmacol. Rev.* 56.

Esler, M., Straznicky, N., Eikelis, N., Masuo, K., Lambert, G., and Lambert, E. (2006a). Mechanisms of sympathetic activation in obesity-related hypertension. *Hypertension* 48, 787–796.

Esler, M., Straznicky, N., Eikelis, N., Masuo, K., Lambert, G., and Lambert, E. (2006b). Mechanisms of sympathetic activation in obesity-related hypertension. *Hypertension* 48, 787–796.

Faulks, S.C., Turner, N., Else, P.L., and Hulbert, A.J. (2006). Calorie restriction in mice: effects on body composition, daily activity, metabolic rate, mitochondrial reactive oxygen species production, and membrane fatty acid composition. *J. Gerontol. A. Biol. Sci. Med. Sci.* 61, 781–794.

Fishman, R.B., and Dark, J. (1987). Sensory innervation of white adipose tissue. *Am. J. Physiol.* 253, R942-4.

Foster, M.T., and Bartness, T.J. (2006). Sympathetic but not sensory denervation stimulates white adipocyte proliferation. *Am. J. Physiol. Regul. Integr. Comp. Physiol.* 291, R1630-7.

Fox, C.S., Massaro, J.M., Hoffmann, U., Pou, K.M., Maurovich-Horvat, P., Liu, C.-Y., Vasan, R.S., Murabito, J.M., Meigs, J.B., Cupples, L.A., et al. (2007). Abdominal Visceral and Subcutaneous Adipose Tissue Compartments: Association With Metabolic Risk Factors in the Framingham Heart Study. *Circulation* 116, 39–48.

Gajda, A. (2008). High fat diets for diet-induced obesity models. *Res. Diets* 2008–2010.

- Garrison, R.J., Kannel, W.B., Stokes, J., and Castelli, W.P. (1987). Incidence and precursors of hypertension in young adults: the Framingham Offspring Study. *Prev. Med. (Baltim)*. *16*, 235–251.
- Gasteyger, C., and Tremblay, A. (2002). Metabolic impact of body fat distribution. *J. Endocrinol. Invest.* *25*, 876–883.
- Gentry, J.J., Barker, P.A., and Carter, B.D. (2004). The p75 neurotrophin receptor: Multiple interactors and numerous functions. In *Progress in Brain Research*, (Elsevier), pp. 25–39.
- Gezginci-Oktayoglu, S., and Bolkent, S. (2011). 4-Methylcatechol prevents NGF/p75NTR-mediated apoptosis via NGF/TrkA system in pancreatic β cells. *Neuropeptides* *45*, 143–150.
- Giordano, A., Song, C.K., Bowers, R.R., Ehlen, J.C., Frontini, A., Cinti, S., and Bartness, T.J. (2006). White adipose tissue lacks significant vagal innervation and immunohistochemical evidence of parasympathetic innervation. *Am. J. Physiol. Regul. Integr. Comp. Physiol.* *291*, R1243-55.
- Hardie, S.L., and Hirsh, J. (2006). An improved method for the separation and detection of biogenic amines in adult *Drosophila* brain extracts by high performance liquid chromatography. *J. Neurosci. Methods* *153*, 243–249.
- Hargett, S.R., Walker, N.N., and Keller, S.R. (2016). Rab GAPs AS160 and Tbc1d1 play nonredundant roles in the regulation of glucose and energy homeostasis in mice. *Am. J. Physiol. Endocrinol. Metab.* *310*, E276-88.
- Harms, M., and Seale, P. (2013). Brown and beige fat: development, function and therapeutic potential. *Nat. Med.* *19*, 1252–1263.

- Ibáñez, C.F., and Simi, A. (2012). p75 neurotrophin receptor signaling in nervous system injury and degeneration: paradox and opportunity. *Trends Neurosci.* *35*, 431–440.
- Ibrahim, M.M. (2010). Subcutaneous and visceral adipose tissue: structural and functional differences. *Obes. Rev.* *11*, 11–18.
- Jéquier, E. (2002). Leptin signaling, adiposity, and energy balance. *Ann. N. Y. Acad. Sci.* *967*, 379–388.
- Jones, D.D., Ramsay, T.G., Hausman, G.J., and Martin, R.J. (1992). Norepinephrine inhibits rat pre-adipocyte proliferation. *Int. J. Obes. Relat. Metab. Disord.* *16*, 349–354.
- Jornayvaz, F.R., Jurczak, M.J., Lee, H.-Y., Birkenfeld, A.L., Frederick, D.W., Zhang, D., Zhang, X.-M., Samuel, V.T., and Shulman, G.I. (2010). A high-fat, ketogenic diet causes hepatic insulin resistance in mice, despite increasing energy expenditure and preventing weight gain. *Am. J. Physiol. Endocrinol. Metab.* *299*, E808-15.
- Kaplan, D.R., and Miller, F.D. (2000). Neurotrophin signal transduction in the nervous system. *Curr. Opin. Neurobiol.* *10*, 381–391.
- Kaufman, L.N., Young, J.B., and Landsberg, L. (1986). Effect of protein on sympathetic nervous system activity in the rat. Evidence for nutrient-specific responses. *J. Clin. Invest.* *77*, 551–558.
- Kennedy, A.R., Pissios, P., Otu, H., Roberson, R., Xue, B., Asakura, K., Furukawa, N., Marino, F.E., Liu, F.-F., Kahn, B.B., et al. (2007). A high-fat, ketogenic diet induces a unique metabolic state in mice. *Am. J. Physiol. Endocrinol. Metab.* *292*, E1724-39.
- Lambert, G.W., Straznicki, N.E., Lambert, E.A., Dixon, J.B., and Schlaich, M.P. (2010). Sympathetic nervous activation in obesity and the metabolic syndrome--causes, consequences and therapeutic implications. *Pharmacol. Ther.* *126*, 159–172.

- Landsberg, L. (1986). Diet, obesity and hypertension: an hypothesis involving insulin, the sympathetic nervous system, and adaptive thermogenesis. *Q. J. Med.* 61, 1081–1090.
- Landsberg, L., and Young, J.B. (1978). Fasting, feeding and regulation of the sympathetic nervous system. *N. Engl. J. Med.* 298, 1295–1301.
- Lane, M., Ingram, D.K., and Roth, G.S. (1999). Calorie restriction in nonhuman primates: effects on diabetes and cardiovascular disease risk. *Toxicol. Sci.* 52, 41–48.
- Langin, D. (2006). Adipose tissue lipolysis as a metabolic pathway to define pharmacological strategies against obesity and the metabolic syndrome. *Pharmacol. Res.* 53, 482–491.
- Lee, K.F., Li, E., Huber, L.J., Landis, S.C., Sharpe, A.H., Chao, M. V, and Jaenisch, R. (1992). Targeted mutation of the gene encoding the low affinity NGF receptor p75 leads to deficits in the peripheral sensory nervous system. *Cell* 69, 737–749.
- Lee, K.F., Bachman, K., Landis, S., and Jaenisch, R. (1994). Dependence on p75 for innervation of some sympathetic targets. *Science* 263, 1447–1449.
- Lefebvre, A.-M., Laville, M., Vega, N., Riou, J.P., Gaal, L. v., Auwerx, J., and Vidal, H. (1998). Depot-Specific Differences in Adipose Tissue Gene Expression in Lean and Obese Subjects. *Diabetes* 47, 98–103.
- Levri, K.M., Slaymaker, E., Last, A., Yeh, J., Ference, J., D’Amico, F., and Wilson, S.A. (2005). Metformin as treatment for overweight and obese adults: a systematic review. *Ann. Fam. Med.* 3, 457–461.
- Li, Y., Bujo, H., Takahashi, K., Shibasaki, M., Zhu, Y., Yoshida, Y., Otsuka, Y., Hashimoto, N., and Saito, Y. (2003). Visceral fat: higher responsiveness of fat mass and gene expression to calorie restriction than subcutaneous fat. *Exp. Biol. Med.* (Maywood).

228, 1118–1123.

Liu, Y.-Y., Liu, T.-Y., Qu, W.-M., Hong, Z.-Y., Urade, Y., and Huang, Z.-L. (2012).

Dopamine Is Involved in Food-Anticipatory Activity in Mice. *J. Biol. Rhythms* 27, 398–409.

Lomen-Hoerth, C., and Shooter, E.M. (1995). Widespread neurotrophin receptor expression in the immune system and other nonneuronal rat tissues. *J. Neurochem.* 64, 1780–1789.

Mahoney, L.B., Denny, C.A., and Seyfried, T.N. (2006). Caloric restriction in C57BL/6J mice mimics therapeutic fasting in humans. *Lipids Health Dis.* 5, 13.

Mark, A.L., Rahmouni, K., Correia, M., and Haynes, W.G. (2003). A leptin-sympathetic-leptin feedback loop: potential implications for regulation of arterial pressure and body fat. *Acta Physiol. Scand.* 177, 345–349.

Matsumara, S., MIZUSHIGE, T., YONEDA, T., IWANAGA, T., TSUZUKI, S., INOUE, K., and FUSHIKI, T. (2007). GPR expression in the rat taste bud relating to fatty acid sensing. *Biomed. Res.* 28, 49–55.

Messina, G., De Luca, V., Viggiano, A., Ascione, A., Iannaccone, T., Chieffi, S., and Monda, M. (2013). Autonomic nervous system in the control of energy balance and body weight: personal contributions. *Neurol. Res. Int.* 2013, 639280.

Misra, A., and Vikram, N.K. (2003). Clinical and pathophysiological consequences of abdominal adiposity and abdominal adipose tissue depots. *Nutrition* 19, 457–466.

Mizuno, K., Kanda, Y., Kuroki, Y., Nishio, M., and Watanabe, Y. (2002). Stimulation of beta(3)-adrenoceptors causes phosphorylation of p38 mitogen-activated protein kinase via a stimulatory G protein-dependent pathway in 3T3-L1 adipocytes. *Br. J. Pharmacol.*

135, 951–960.

Morris, N.J., Ross, S.A., Lane, W.S., Moestrup, S.K., Petersen, C.M., Keller, S.R., and Lienhard, G.E. (1998). Sortilin is the major 110-kDa protein in GLUT4 vesicles from adipocytes. *J. Biol. Chem.* 273, 3582–3587.

Morrison, S.F. (2001). Differential control of sympathetic outflow. *Am. J. Physiol. Regul. Integr. Comp. Physiol.* 281, R683-98.

Morrison, S.F., Madden, C.J., and Tupone, D. (2014). Central Neural Regulation of Brown Adipose Tissue Thermogenesis and Energy Expenditure. *Cell Metab.* 19, 741–756.

Muntzel, M.S., Al-Naimi, O.A.S., Barclay, A., and Ajasin, D. (2012). Cafeteria diet increases fat mass and chronically elevates lumbar sympathetic nerve activity in rats. *Hypertension* 60, 1498–1502.

Murphy, K.T., Schwartz, G.J., Nguyen, N.L.T., Mendez, J.M., Ryu, V., and Bartness, T.J. (2013). Leptin-sensitive sensory nerves innervate white fat. *Am. J. Physiol. Endocrinol. Metab.* 304, E1338-47.

Nguyen, N.L.T., Randall, J., Banfield, B.W., and Bartness, T.J. (2014). Central sympathetic innervations to visceral and subcutaneous white adipose tissue. *Am. J. Physiol. Regul. Integr. Comp. Physiol.* 306, R375-86.

Nisoli, E., Tonello, C., Benarese, M., Liberini, P., and Carruba, M.O. (1996a). Expression of nerve growth factor in brown adipose tissue: implications for thermogenesis and obesity. *Endocrinology* 137, 495–503.

Nisoli, E., Tonello, C., Landi, M., and Carruba, M.O. (1996b). Functional studies of the first selective beta 3-adrenergic receptor antagonist SR 59230A in rat brown adipocytes.

Mol. Pharmacol. 49, 7–14.

Ootsuka, Y., Kulasekara, K., de Menezes, R.C., and Blessing, W.W. (2011). SR59230A, a beta-3 adrenoceptor antagonist, inhibits ultradian brown adipose tissue thermogenesis and interrupts associated episodic brain and body heating. *Am. J. Physiol. Regul. Integr. Comp. Physiol.* 301, R987-94.

Oscari, L.B., and Holloszy, J.O. (1969). Effects of weight changes produced by exercise, food restriction, or overeating on body composition. *J. Clin. Invest.* 48, 2124–2128.

Parati, G., and Esler, M. (2012). The human sympathetic nervous system: its relevance in hypertension and heart failure. *Eur. Heart J.* 33, 1058–1066.

Passino, M.A., Adams, R.A., Sikorski, S.L., and Akassoglou, K. (2007). Regulation of hepatic stellate cell differentiation by the neurotrophin receptor p75NTR. *Science* 315, 1853–1856.

Patterson, M., Bloom, S.R., and Gardiner, J. V. (2011). Ghrelin and appetite control in humans—Potential application in the treatment of obesity. *Peptides* 32, 2290–2294.

Peeraully, M.R., Jenkins, J.R., and Trayhurn, P. (2004). NGF gene expression and secretion in white adipose tissue: regulation in 3T3-L1 adipocytes by hormones and inflammatory cytokines. *Am. J. Physiol. Endocrinol. Metab.* 287, E331-9.

Penn, D.M., Jordan, L.C., Kelso, E.W., Davenport, J.E., and Harris, R.B.S. (2006). Effects of central or peripheral leptin administration on norepinephrine turnover in defined fat depots. *Am. J. Physiol. Regul. Integr. Comp. Physiol.* 291, R1613-21.

Pierucci, D., Cicconi, S., Bonini, P., Ferrelli, F., Pastore, D., Matteucci, C., Marselli, L., Marchetti, P., Ris, F., Halban, P., et al. (2001). NGF-withdrawal induces apoptosis in pancreatic beta cells in vitro. *Diabetologia* 44, 1281–1295.

- Rahmouni, K., Correia, M.L.G., Haynes, W.G., and Mark, A.L. (2005). Obesity-associated hypertension: new insights into mechanisms. *Hypertension* 45, 9–14.
- Raile, K., Klammt, J., Garten, A., Laue, S., Blüher, M., Kralisch, S., Klötting, N., and Kiess, W. (2006). Glucose regulates expression of the nerve growth factor (NGF) receptors TrkA and p75NTR in rat islets and INS-1E β -cells. *Regul. Pept.* 135, 30–38.
- Reaven, G.M. (2011). Insulin Resistance: the Link Between Obesity and Cardiovascular Disease. *Med. Clin. North Am.* 95, 875–892.
- Romanov, R.A., Zeisel, A., Bakker, J., Girach, F., Hellysaz, A., Tomer, R., Alpár, A., Mulder, J., Clotman, F., Keimpema, E., et al. (2017). Molecular interrogation of hypothalamic organization reveals distinct dopamine neuronal subtypes. *Nat. Neurosci.* 20, 176–188.
- Rosenbaum, M., and Leibel, R.L. (2014). 20 years of leptin: role of leptin in energy homeostasis in humans. *J. Endocrinol.* 223, T83-96.
- Rössner, S., Taylor, C.L., Byington, R.P., and Furberg, C.D. (1990). Long term propranolol treatment and changes in body weight after myocardial infarction. *BMJ* 300, 902–903.
- Russell, C.D., Petersen, R.N., Rao, S.P., Ricci, M.R., Prasad, A., Zhang, Y., Brodin, R.E., and Fried, S.K. (1998). Leptin expression in adipose tissue from obese humans: depot-specific regulation by insulin and dexamethasone. *Am. J. Physiol.* 275, E507-15.
- Ryu, V., Garretson, J.T., Liu, Y., Vaughan, C.H., and Bartness, T.J. (2015). Brown Adipose Tissue Has Sympathetic-Sensory Feedback Circuits. *J. Neurosci.* 35, 2181–2190.
- Sachs, B.D., Baillie, G.S., McCall, J.R., Passino, M.A., Schachtrup, C., Wallace, D.A.,

- Dunlop, A.J., MacKenzie, K.F., Klussmann, E., Lynch, M.J., et al. (2007). p75 neurotrophin receptor regulates tissue fibrosis through inhibition of plasminogen activation via a PDE4/cAMP/PKA pathway. *J. Cell Biol.* *177*, 1119–1132.
- Schachtrup, C., Ryu, J.K., Mammadzada, K., Khan, A.S., Carlton, P.M., Perez, A., Christian, F., Le Moan, N., Vagena, E., Baeza-Raja, B., et al. (2015). Nuclear pore complex remodeling by p75NTR cleavage controls TGF- β signaling and astrocyte functions. *Nat. Neurosci.* *18*, 1077–1080.
- Schwartz, J.H., Young, J.B., and Landsberg, L. (1983). Effect of dietary fat on sympathetic nervous system activity in the rat. *J. Clin. Invest.* *72*, 361–370.
- Sharma, A.M., Pischon, T., Hardt, S., Kunz, I., and Luft, F.C. (2001). Hypothesis: - Adrenergic Receptor Blockers and Weight Gain : A Systematic Analysis. *Hypertension* *37*, 250–254.
- Sharma, N., Deppmann, C.D., Harrington, A.W., St. Hillaire, C., Chen, Z.Y., Lee, F.S., and Ginty, D.D. (2010). Long-Distance Control of Synapse Assembly by Target-Derived NGF. *Neuron* *67*, 422–434.
- Shin, H., Ma, Y., Chanturiya, T., Cao, Q., Wang, Y., Kadegowda, A.K.G., Jackson, R., Rumore, D., Xue, B., Shi, H., et al. (2017). Lipolysis in Brown Adipocytes Is Not Essential for Cold-Induced Thermogenesis in Mice. *Cell Metab.* *26*, 764–777.e5.
- Sipe, L.M., Yang, C., Ephrem, J., Garren, E., Hirsh, J., and Deppmann, C.D. (2017). Differential sympathetic outflow to adipose depots is required for visceral fat loss in response to calorie restriction. *Nutr. Diabetes* *7*, e260.
- Smith, S.R., and Zachwieja, J.J. (1999). Visceral adipose tissue: a critical review of intervention strategies. *Int. J. Obes. Relat. Metab. Disord.* *23*, 329–335.

- Song, C.K., Jackson, R.M., Harris, R.B.S., Richard, D., and Bartness, T.J. (2005). Melanocortin-4 receptor mRNA is expressed in sympathetic nervous system outflow neurons to white adipose tissue. *Am. J. Physiol. Integr. Comp. Physiol.* *289*, R1467–R1476.
- Stefanidis, A., Wiedmann, N.M., Adler, E.S., and Oldfield, B.J. (2014). Hypothalamic control of adipose tissue. *Best Pract. Res. Clin. Endocrinol. Metab.* *28*, 685–701.
- Tchernof, A., Després, J.-P., Consolation, E., Abate, N., Garg, A., Peshock, R., Stray-Gundersen, J., Grundy, S., Adiels, M., Taskinen, M., et al. (2013). Pathophysiology of human visceral obesity: an update. *Physiol. Rev.* *93*, 359–404.
- Tchkonina, T., Thomou, T., Zhu, Y., Karagiannides, I., Pothoulakis, C., Jensen, M.D., and Kirkland, J.L. (2013). Mechanisms and Metabolic Implications of Regional Differences among Fat Depots. *Cell Metab.* *17*, 644–656.
- Tentolouris, N., Liatis, S., and Katsilambros, N. (2006). Sympathetic system activity in obesity and metabolic syndrome. *Ann. N. Y. Acad. Sci.* *1083*, 129–152.
- Vaanholt, L.M., Mitchell, S.E., Sinclair, R.E., and Speakman, J.R. (2015). Mice that are resistant to diet-induced weight loss have greater food anticipatory activity and altered melanocortin-3 receptor (MC3R) and dopamine receptor 2 (D2) gene expression. *Horm. Behav.* *73*, 83–93.
- Vaughan, C.H., Zarebidaki, E., Ehlen, J.C., and Bartness, T.J. (2014). Analysis and measurement of the sympathetic and sensory innervation of white and brown adipose tissue. *Methods Enzymol.* *537*, 199–225.
- Verdery, R.B., and Walford, R.L. (1998). Changes in plasma lipids and lipoproteins in humans during a 2-year period of dietary restriction in Biosphere 2. *Arch. Intern. Med.*

158, 900–906.

Vollenweider, P., Tappy, L., Randin, D., Schneiter, P., Jéquier, E., Nicod, P., and Scherrer, U. (1993). Differential effects of hyperinsulinemia and carbohydrate metabolism on sympathetic nerve activity and muscle blood flow in humans. *J. Clin. Invest.* 92, 147–154.

Wajchenberg, B.L. (2000). Subcutaneous and Visceral Adipose Tissue: Their Relation to the Metabolic Syndrome. *Endocr. Rev.* 21, 697–738.

Weyer, C., Gautier, J.F., and Danforth, E. (1999). Development of beta 3-adrenoceptor agonists for the treatment of obesity and diabetes--an update. *Diabetes Metab.* 25, 11–21.

Yang, M.U., and Van Itallie, T.B. (1976). Composition of weight lost during short-term weight reduction. Metabolic responses of obese subjects to starvation and low-calorie ketogenic and nonketogenic diets. *J. Clin. Invest.* 58, 722–730.

Yoon, S.O., Casaccia-Bonnel, P., Carter, B., and Chao, M. V. (1998). Competitive Signaling Between TrkA and p75 Nerve Growth Factor Receptors Determines Cell Survival. *J. Neurosci.* 18, 3273–3281.

Young, J.B., and Landsberg, L. (1977). Stimulation of the sympathetic nervous system during sucrose feeding. *Nature* 269, 615–617.

Young, H.M., Cane, K.N., and Anderson, C.R. (2011). Development of the autonomic nervous system: a comparative view. *Auton. Neurosci.* 165, 10–27.

Young, J.B., Saville, E., Rothwell, N.J., Stock, M.J., and Landsberg, L. (1982). Effect of diet and cold exposure on norepinephrine turnover in brown adipose tissue of the rat. *J. Clin. Invest.* 69, 1061–1071.

Youngstrom, T.G., and Bartness, T.J. (1995). Catecholaminergic innervation of white

adipose tissue in Siberian hamsters. *Am. J. Physiol.* 268, R744-51.

Zeng, W., Pirzgalska, R.M., Pereira, M.M.A., Kubasova, N., Barateiro, A., Seixas, E.,

Lu, Y.H., Kozlova, A., Voss, H., Martins, G.G., et al. (2015). Sympathetic Neuro-adipose

Connections Mediate Leptin-Driven Lipolysis. *Cell* 163, 84–94.